A Vector Approach to Size and Shape Comparisons among Zooids in Cheilostome Bryozoans

Alan H. Cheetham
and Douglas M. Lorenz

ISSUED

JUL 8 1976

ABSTRACT

Cheetham, Alan H., and Douglas M. Lorenz. A Vector Approach to Size and Shape Comparisons among Zooids in Cheilostome Bryozoans. *Smithsonian Contributions to Paleobiology*, number 29, 55 pages, 37 figures, 19 tables, 1976.— Although zooid size and shape have long been used in comparative studies of cheilostome bryozoans, procedures for measuring these properties have been little investigated. Predominantly intussusceptive growth of buds suggests a method of comparing zooid outlines based on (1) correspondence of principal growth direction (proximal-distal axis) and (2) size and shape properties expressing differential growth about this axis.

Vector properties of a wide variety of autozooidal outlines (in frontal view) were studied by principal components. Size (area within the outline) accounts for more than one-third of the variation and tends to vary less within colonies than shape, even in severely disturbed budding patterns. The portion of shape independent of size is divisible into three components. Each of the first two components accounts for about one-fourth of the total variation, the third for less than five percent. One shape component is associated with asymmetry of outline, as measured both by departure of the mean vector direction from the proximal-distal axis and by inequality of vector lengths on either side of the axis. The amount of asymmetry is small, can be either antisymmetry or fluctuating asymmetry, and varies greatly within colonies apparently with microenvironmental effects on budding patterns. The second shape component is associated with elongation (concentration of vector lengths near the mean growth direction) and distal inflation (proportion of area distal to the midpoint of the proximal-distal axis). These two variables seem less affected by microenvironment than is asymmetry. The third component accounts for only the small part of variation in elongation and distal inflation that is not positively correlated. Variation in this component suggests that distal inflation is slightly more sensitive to microenvironment than is elongation. Estimates of intrapopulation variation in one fossil species suggest that size and that part of elongation varying in opposition to distal inflation are sufficiently consistent within single populations, under the same conditions of ontogeny, astogeny, and polymorphism, to form a basis for taxonomic discrimination. Within the range of colony means for each of these two properties among the variety of outlines examined, at least three and possibly four potentially taxonomically distinct intervals can be recognized. The number of measurements per colony needed to detect differences between these intervals is surprisingly small.

Contents

A Vector Approach to Size and Shape Comparisons among Zooids in Cheilostome Bryozoans

Alan H. Cheetham

and Douglas M. Lorenz

Introduction

Many groups of colonial invertebrates, including the cheilostome bryozoans, commonly display a greater complexity of morphologic variability than do most groups of solitary animals. Such complex variation is useful in evolutionary biology, for it provides a wide array of phenotypes in which many microevolutionary processes may be expressed which are not detectable in populations of solitary animals. On the other hand, such complexity has been a major problem in cheilostome taxonomy (Stach, 1935), for there have proved to be few characters sufficiently invariant that their taxonomic utility can be easily determined.

In order to cope with the problem of complex variation, cheilostome taxonomists are in the process of reevaluating the entire taxonomic structure of their group. One important result of this reexamination has been the realization that single characters sufficiently diagnostic to provide a consistent basis for classification are unlikely to be found. Indeed, many characters vary even within colonies among zooids of the same ontogenetic, astogenetic, and polymorphic state. Consequently, some taxonomists now consider a polythetic ap-

Alan H. Cheetham, Department of Paleobiology, National Museum of Natural History, Smithsonian Institution, Washington, D.C. 20560. Douglas M. Lorenz, Department of Geology, University of California, Los Angeles, California 90024.

proach to cheilostome classification not only desirable, but indispensable in order to make progress toward taxonomic stability.

In contrast to monothetic classification systems, for which single taxonomic characters are relatively invariant within taxa and distinctly different between taxa, polythetic systems require consideration of the patterns of variation and covariation among all available, potentially useful characters. Redundancy, or statistical covariation among polythetic characters, is particularly troublesome because it tends to mask independent genetically controlled variation. From a theoretical standpoint, reducing observed phenotypic covariation by removing undesirable environmentally correlated and genetically redundant effects should emphasize independent genetically controlled components of the phenotype and permit improved estimates of true genetic similarities and differences. Therefore resolution of independent variance components should improve the phylogenetic fidelity of the resulting classification.

Variation and covariation in observed quantitative characters can be estimated directly from measurements. Once the observed covariation has been eliminated and the total variation resolved into a number of statistically independent components, the proportions of each component attributable to sources of variation within colonies, between colonies, and between populations can be estimated. Under certain not-too-restrictive conditions, hy-

potheses of statistical difference between colonies and/or populations can be tested for each independent component.

For each component, such an analysis provides an estimate of the minimum independent differences by which taxa can be distinguished. Each of these differences can be used to recognize two or more intervals, or variable states, of the corresponding component. The set of components for which such variable states can be recognized then serves as a basis for classification. But in contrast to a monothetic system, not all taxa can be expected to have different states of each component, nor can all taxa having the same state of a given component be expected to have like states for each of the other components. It is the entire set of independent taxonomic components which serves to distinguish among taxa in a polythetic classification.

Statistical analysis also provides an estimate of the number of zooids per colony and the number of colonies per population that must be measured to detect the minimum taxonomic difference in states of a character with a given degree of confidence. These numbers are obviously important in the allocation of resources in a taxonomic study.

Precise estimation of taxonomically significant states of variable characters requires precise measurement and analysis. Once such states have been estimated with a high degree of confidence, they commonly can be sufficiently distinguished in the study of additional taxa by more approximate, perhaps even qualitative methods. The recognition in the present study of four or five size classes of cheilostome autozooids, for example, does not demand precise measurement and analysis, but precision was necessary to establish that differences of this magnitude and no smaller are highly likely to reflect taxonomic differences. For less quantifiable characters, more approximate methods must be used throughout, but under guidelines provided by the analysis of quantitative characters. The methods used here thus should be applicable, at least in principle, to a wide variety of morphologic characters in cheilostomes, as well as answering the question of taxonomic usefulness of quantitative characters themselves.

Size and shape of autozooids in cheilostomes are examples of variable characters, the taxonomic significance of which has been controversial. In past studies, measurements of "standard" dimensions

(e.g., length, width) and qualitative comparisons of zooid outlines with idealized shapes (e.g., rectangle, hexagon, pear-shape) commonly have been employed. The question of how size and shape can be expressed in mutually independent series of linearly arranged numerical states by which taxa can be compared and contrasted has been little investigated.

For a few cheilostome species, principal components analysis has been used on sets of standard dimensions to extract independent components ("characters") which, although mathematical abstractions, usually can be interpreted as "size" and "shape" factors. Studies employing this method (Cheetham, 1968a; 1973; Malmgren, 1970) suggest that there is considerable redundancy among the autozooid dimensions commonly measured. The particular dimensions which are redundant or which are associated with "size" or "shape" components, however, differed among the species studied. Principal components analysis of standard dimensions can be expected to indicate whether all of the dimensions measured need have been included, but it is possible that other dimensions, not measured, should have been included for adequate characterization. For example, if zooids differ only in size, any one of a number of linear dimensions may be sufficient to distinguish between them. For zooids of different shapes, length and width, or length-width ratios, etc., may be insufficient for distinguishing them.

In addition to possible redundancy and insufficiency, standard dimensions suffer from another drawback. Each dimension is at least implicitly, sometimes explicitly, assumed to measure the distance between corresponding morphologic points (h-points of Sneath, 1967) on different zooids and therefore to express the same morphologic property, no matter how different in shape the zooids may be. In the same polymorph in closely related species, there are probably many such points recognizable on the zooid outline. For zooids of very different shapes in widely divergent species, there may be few such points. Ideally, morphologic correspondence should be based on growth properties in addition to simple geometric similarity.

Recent advances in understanding the mode of growth of cheilostome autozooids and in applying multivariate analytical techniques to the study of size and shape now make it possible to try new

approaches to the evaluation of these characters with a minimum of assumptions of morphologic correspondence and maximum expectation for adequate characterization. As in past studies of autozooid size and shape in cheilostomes, we have attempted to analyze the frontal outline (Figures 1–3), but the approach explored here should apply to other orientations as well.

Fourier series analysis provides a characterization of shape that avoids problems of sufficiency and redundancy and involves no assumption of morphologic correspondence except for an initial orientation (Ehrlich and Weinberg, 1970). This method was employed by Anstey and Delmet (1972, 1973) to characterize cross-sectional shapes of zooecia in some trepostome bryozoans by computing the contributions of successively more intricate geometric figures to the shape analyzed. Geometric and biologic interpretations were then attached to these contributions by comparing them with those for ellipses, equilateral pentagons, equilateral hexagons, etc. (Anstey and Delmet, 1973: 1955).

In this paper we explore a slightly different approach to characterizing autozooid outlines, following the suggestion of D'Arcy Thompson (1942: 1044) to " . . . look on the outline . . . as a vector-diagram of its own growth." In particular, we attempt to analyze the frontal outline of cheilostome autozooids with respect to relative growth about a principal (proximal-distal) axis. We employ this approach to examine differences in autozooid size and shape both within and among colonies in a variety of genera with a wide range of autozooid morphotypes. Some polymorphic and ontogenetically and astogenetically differing autozooids have been included in the analysis for comparison, but for the most part we have concentrated on the ordinary, fully formed autozooids in primary zones of astogenetic repetition, the size and shape of which have figured most prominently in past discussions of taxonomic significance. Our results indicate that the highly significant independent taxonomic aspects of size and shape can be separated from those aspects that are too highly modified by the environment to have much taxonomic potential, and that this can be done by measurement of surprisingly few antozooids in surprisingly few colonies with a high degree of confidence. This suggests that these important taxonomic characters

should be amenable to more approximate characterization without an unacceptable risk of losing or obscuring important taxonomic information. Before approximate methods are applied to all variable morphologic characters in cheilostomes, however, more of them should be subjected to similar statistical analysis.

Growth of Zooid Outline

Viewed frontally, zooids in cheilostome bryozoans are generally outlined at some or all ontogenetic stages by cuticular boundaries marking the junctions of their frontal wall with their vertical walls. Zooids thus outlined originate as hollow, bladderlike buds, which grow by swelling (intussusception) of their membranous exterior walls (Figures 1, 2; Silén, 1944a; Lutaud, 1961; Banta,

1969). This mode of growth prevails even in species in which one bud is partitioned to form multiple zooids (Silén, 1944b; Lutaud, 1961; Håkansson, 1973) or multiple buds fuse to form one zooid (Silén, 1944b; Banta, 1969; Gordon, 1971). (Silén, 1944b, and Banta, 1969, considered lateral communication organs, present in most species investigated, to be tiny buds which have fused with the main bud; the contribution of communication organs to the zooid outline, however, is assumed to be of minor consequence.) In addition to exterior walls, a fully formed zooid has interior walls grown from exterior walls to cut off the zooidal cavity from those of neighboring zooids in the same budding series (Silén, 1944a, 1944b; Banta, 1969). Interior walls may comprise no more than pore plates forming parts of communication organs (Silén, 1944b) and thus not contribute significantly to zooid outlines, or these walls may comprise extensive partitions between zooidal cavities with a corresponding reduction in the extent of exterior walls. Even in species having all their vertical zooid walls grown as interior walls, the vertical walls reach and are attached to outer cuticles which define the zooid outline in frontal view, and upgrowth of vertical walls is preceded in these species by intussusceptive growth of a bladderlike bud having approximately the shape of the fully developed zooidal unit (Håkansson, 1973). Intussusceptive growth thus appears to be the primary factor conditioning cheilostome zooid outlines.

According to Thompson (1942:346–363), intussusceptive growth of membranes, whether on organisms or colloids, leads to curved boundaries, which tend to assume a spherical shape. Flattening or embayment of boundaries results from interference with the expanding membrane, localized changes in internal pressure, or the solidification to a rigid state of parts of the membrane as other parts of it continue to expand (Thompson, 1942: 346). Walls at the frontal surface of a cheilostome zooid are largely exposed, partly or wholly uncalcified, and more or less swollen and bubblelike. Basal walls are pressed against the substrate in encrusting growth or against those of other zooids in most forms of erect growth; they are commonly completely calcified and generally flattened. Vertical walls are calcified and vary in curvature. Calcification generally proceeds close behind the growth of the bud, except for transverse walls in species hav-
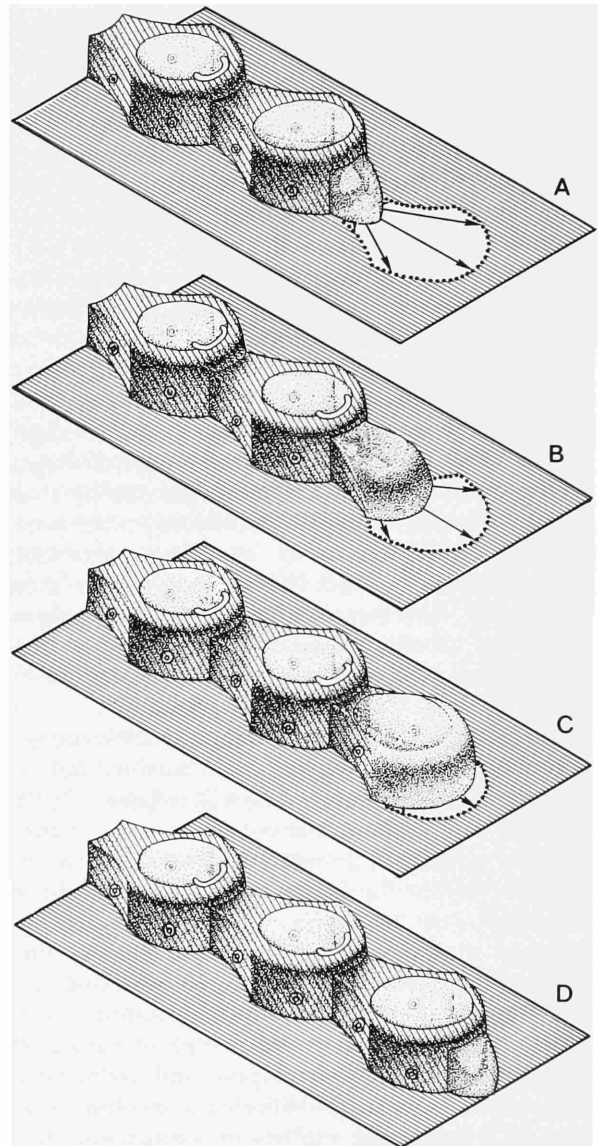
FIGURE 1.—Idealized diagram to illustrate predominantly intussusceptive growth in a hypothetical anascan cheilostome. An autozooid budded at the distal end of one lineal series from a multiserial colony is shown from just after budding (A) to just before completion of its walls (D). (Growth directions are indicated by arrows on basal projection of completed zooid outline.)

ing multizooidal buds (giant buds of Lutaud, 1961). The shape of the vertical walls and therefore to a large extent the shape of the zooid in frontal view appear to depend upon the direction of expansion of the bud, the influence of the
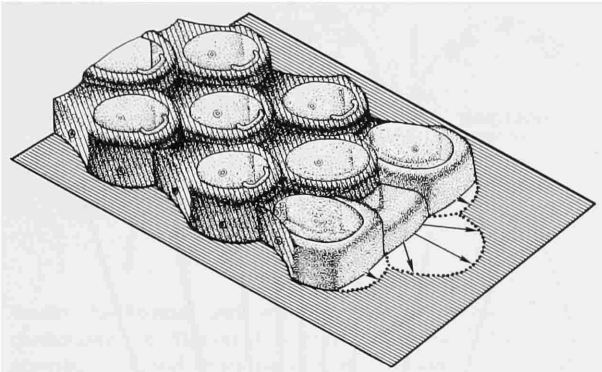
FIGURE 2.—Idealized diagram of three adjacent lineal series of hypothetical cheilostome shown in Figure 1. Buds in adjacent lineal series form a coordinated growing edge, along which more than one ontogenetic stage is represented because of typical quincuncial arrangement of zooids.

growth of adjoining zooids, and external interference.

The type of budding most commonly described in cheilostomes results from intussusception at the distal end of a lineal series of zooids (Figure 1; primogenial budding of Banta, 1972). A bud grows principally on a proximal-distal axis, but a variable

FIGURE 3.—Frontal view of outlines of autozooids near growing edge (A) of hypothetical cheilostome shown in Figure 2. Note changing relationships between growth directions of shaded zooid and those lateral to it as growing edge advanced from position A to position B. (DLZ=distolateral zooid; PLZ=proximolateral zooid.)

proportion of growth usually also takes more lateral directions, in accordance with the influence of adjoining lineal series (Figures 2, 3), external interference, and internal control. The directions in which, and distances to which, a bud expanded to produce the zooid outline determine a set of vectors characterizing the size and shape of the zooid. It must be emphasized that the different lengths of these vectors do not in most cases represent different growth rates but rather may be more or less proportional to growth duration. The distal portion of a zooid normally continues to expand after walls bounding more proximal portions of the outline have calcified and stopped growth. The greater lengths of the vectors intersecting the distal margin reflect the continued expansion.

Zooids budded in other directions are also common in some cheilostomes, generally in addition to those formed by distal budding. Their characterization by the vector representation used here would involve the same arbitrary initial orientation as application of the terms "distal" and "proximal" to the description of their morphology (Banta, 1972).

A Vector Diagram of Zooid Outline

The proximal margin of a cheilostome zooid normally is colinear with the distal margin of the preceding zooid. Since budding is initiated somewhere along this margin, all growth in the distal zooid must originate there and if the zooid outline is to be geometrically represented as a " . . . vector diagram of its own growth" (Thompson, 1942), so also must a system of vectors. In some simple cheilostomes having pyriform zooids with very narrow proximal margins consisting of little more than points (Figure 28, specimen 28; Silén, 1944a, figs. 5, 6; Thomas and Larwood, 1960, figs. 1, 4; Pohowsky, 1973, pl. 1: figs. 1–3, 5, 6), the placement of this vector origin is unambiguous. In many other cheilostomes zooids have wider proximal margins, but although the detailed directions of early growth in such forms clearly are complex, overall zooid growth can be represented to a close approximation by placing the vector origin at a point on the proximal margin midway between the proximolateral walls of the fully formed bud (Figure 3). Hence the proximal part of the outline is represented by vectors which, although not parallel
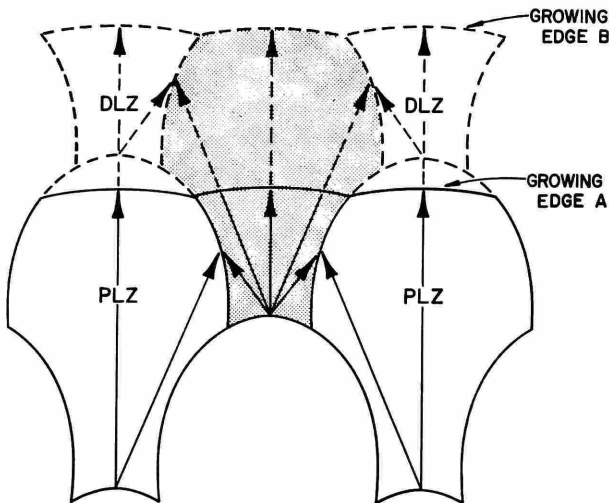
to actual early growth directions, nevertheless accurately reflect zooid size and shape.

The vector whose tip falls on the vector origin of the next successive zooid, or on the midpoint of the combined proximal margins of twinned zooids where lineal series bifurcate, is called the "Proximal-Distal Axis." Its azimuth is termed the "Principal Growth Direction" and is defined to be the direction from which the remaining vector arguments are measured. By this definition, it is apparent that the vector origin ("point of budding") is the only point of morphological correspondence that need be assumed for this measurement system.

To avoid directional bias in size-shape measurements, vector azimuths should be symmetrically distributed about the principal growth direction (Figure 4). Maintaining a constant angle between all adjacent vectors immediately suggests itself as the simplest scheme of azimuth spacing and would be appropriate if zooid frontal outlines tended to be semicircular. Most shapes we have encountered, however, are longer than they are wide, and spacing vectors at equal angles would emphasize the proximolateral margins at the expense of the more distal portions of the outline. In addition, the proximolateral margins are highly sensitive to unsystematic irregularities in budding pattern and early growth direction (Figures 5, 6), at least partly because newly budded zooids are often crowded by more fully developed, laterally adjacent zooids (Figure 3). To deemphasize these irregularities, vectors measuring outline geometry on or near the distal margin should be more closely spaced than those in the proximal part of the outline. We have more or less arbitrarily chosen a roughly geometric rate of increase in azimuth spacing with the vectors distributed symmetrically about the principal growth direction (Figure 4).

A complete vector representation of a cheilostome zooidal outline can be constructed as follows (Figures 4, 33):

1. Determine vector origins on proximal margins of both the zooid to be measured and the next succeeding zooid in lineal series.

2. Connect these points by a vector to form the proximal-distal axis.

3. Construct remaining vectors at geometrically increasing azimuths distributed symmetrically about the principal growth direction (azimuth of the proximal-distal axis). Vectors terminate at inter-
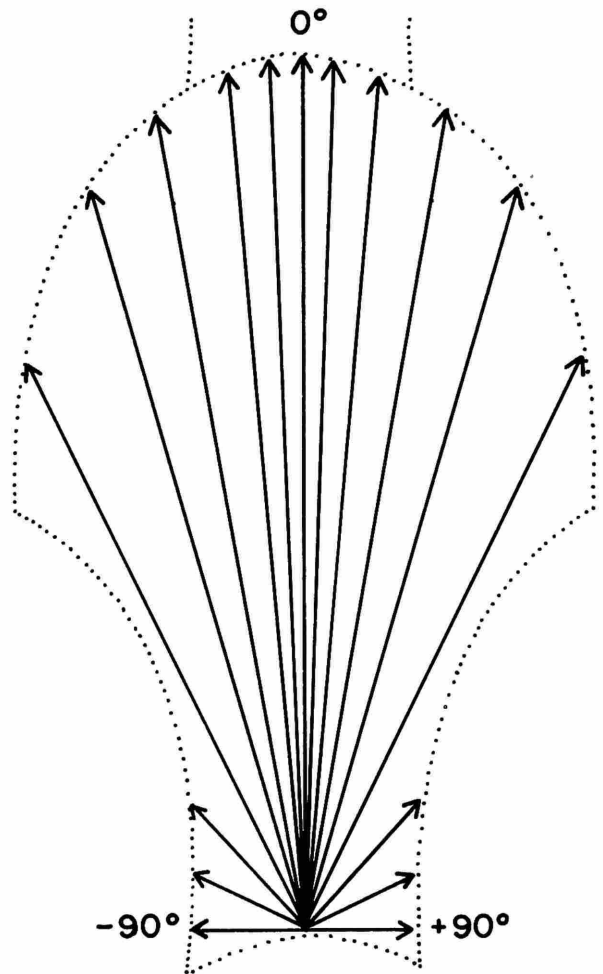
FIGURE 4.—Frontal outline of autozooid of hypothetical cheilostome in Figures 1–3 showing spacing of reference directions for vector representation ($0°$, $±2°$, $±5°$, $±10°$, $±16°$, $±26°$. $±42°$, $±64°$, $±90°$).

section with zooid margin (intersection farthest from the vector origin in cases where vector intersects margin more than once).

4. Connect vector termini with straight-line segments.

The resulting polygon is the approximation of true frontal outline that is used in further computations.

The precision with which a particular vector system represents the zooid outline depends on the number of vectors employed, the complexity of the outline to be measured, and the curvature of the
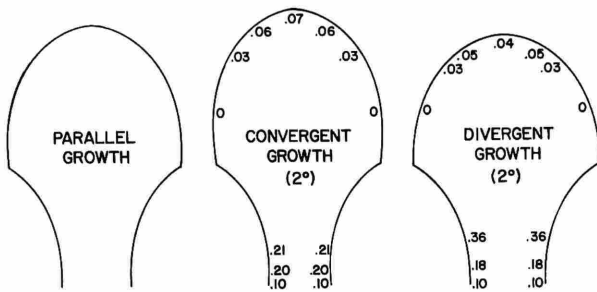
FIGURE 5.—Frontal outlines of autozooid of hypothetical cheilostome in Figures 1–3 under different conditions of growth, i.e., lineal series parallel, or converging or diverging at small angles. Area within outlines has been held constant. (Proportional changes in vector lengths in different parts of the outline are indicated.)

proximal margin. Spacing at angular intervals that are too great to detect significant irregularities in the outline will introduce serious errors in the estimates of various size-shape factors such as area, asymmetry, and distal inflation (see page 10). Reentrants along the lateral margins can result in overestimated areas (Figure 7). And because portions of the proximolateral margin proximal to the 90° vector (Figure 4) are ignored, areas of zooidal outlines with highly concave proximal margins will be slightly underestimated.

To estimate the error introduced in our estimates of zooidal area (as an example) by using the vector system of measurement described above, the area enclosed within the outline was measured by a different method and compared with that calculated from the vector measurements (see Appendix A). We obtained this independent measurement by counting (at × 100 magnification) the number of 0.01 mm squares contained within the entire outline. (The average-sized zooidal outline encloses about 1850 such squares.) For the 129 autozooecia studied in the initial analysis, the area calculated from vectors is correlated at 0.999 with that obtained by counts (Figure 7). Differences between the two estimates were greater than the empirically determined limits of precision of the counting method in only 30 of the 129 outlines. We conclude that for the range of shapes studied, the error introduced by using the vector system of measurement is of minor consequence. For zooids having long, narrow, irregular caudae or proximal extensions (e.g., some species of *Hippothoa;* see

Harmer, 1957, pl. 73: figs. 25, 27) the error can be much greater, but such shapes are not common and can be treated individually as they occur.

Quantitative Measures of Outline Geometry

In the vector representation of zooidal growth, only a single point, the vector origin, and direction, the principal growth direction, are assumed to correspond morphologically among different zooids. Vectors from different zooids that might be considered geometrically analogous because they fall in the same positions relative to their respective principal growth directions are expressly *not* considered to correspond and hence are not compared directly. It is only the entire set of vectors which is assumed to express properties of growth that are comparable from zooid to zooid. Geometric properties of these vector sets which reflect various intuitive aspects of outline size and shape are defined in this section and treated as measured characters in the subsequent taxonomic analyses. Measurement precision is discussed in the following section (Study Methods)

A measure of size is required both as a geometric property of autozooidal outline and as a reference with which to standardize size-independent shape variation. The area contained within the zooidal outline is certainly the most direct measure of the total amount of growth and can be computed trigonometrically from the vector measurements (see Appendix A for computational details). In order to preserve dimensional consistency with the various measures of shape, we have converted this area estimate into an equivalent linear metric, the radius of a semicircle with the same area, which we have denoted ra. In the 129 autozooecia studied initially, ra ranges from 0.18 to 0.57 mm, with a mean of approximately 0.35 mm. An alternative measure of size that might be used is the arithmetic mean of the vector lengths, but in a random sample of 11 from the 129 autozooecia, its correlation with the estimated area obtained by counting squares (see above) was only 0.918, suggesting that this measure would yield less precise estimates of area than ra.

In addition to the single estimate of size, ra, we have defined six vector statistics reflecting various aspects of what can be considered outline shape. Four of these shape measures have proved useful
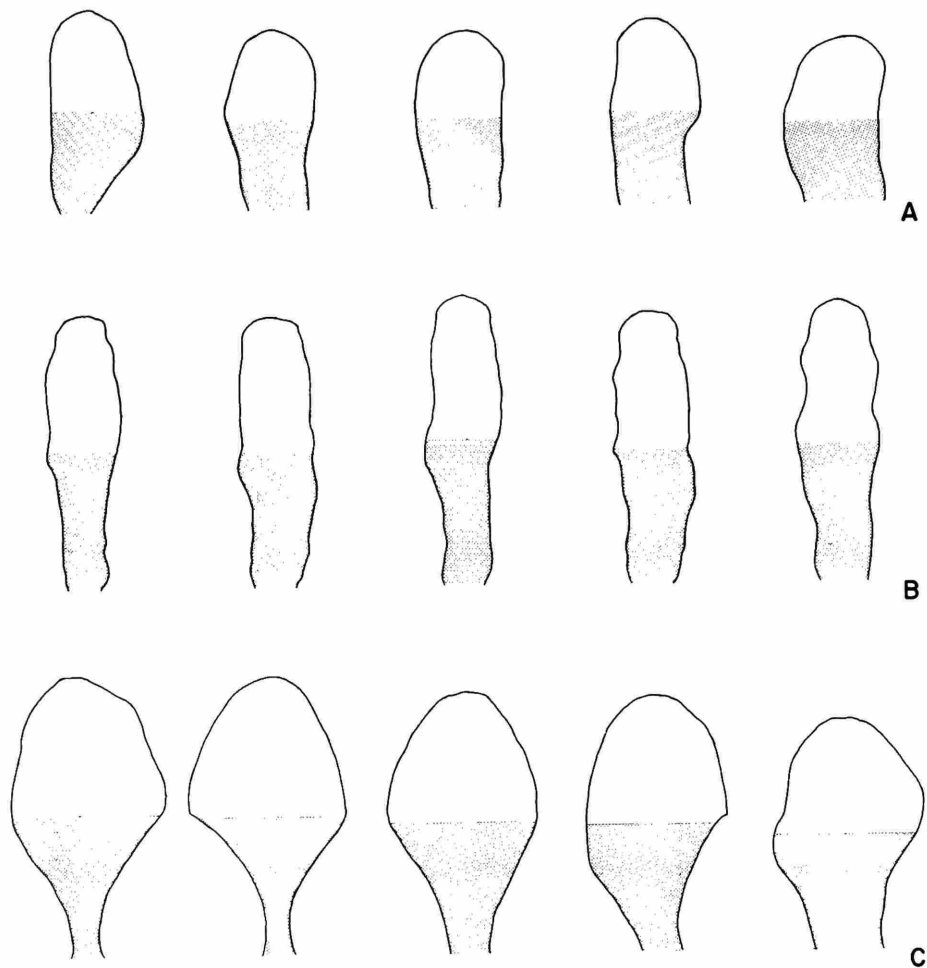
FIGURE 6.—Variation within each of three cheilostome colonies in the halves of autozooecial outlines proximal and distal to the midpoint of the axis: *a, Electrina lamellosa* d'Orbigny (Appendix B, Id. no. 17); *b, Houzeauina parallela* (Reuss) (Appendix B, Id. no. 24); *c, Tretosina arcifera* Canu and Bassler (Appendix B, Id. no. 27).

in the taxonomic analyses; the other two are redundant. The three conceptual aspects of shape which were most useful are elongation, asymmetry, and distal inflation.

Elongation can be visualized as the tendency of zooidal growth to be concentrated in a "preferred" direction. In the cheilostomes we studied, this direction lies near, but does not coincide with the principal growth direction. Elongation can be measured by the standard coefficient of vector concentration (Appendix A), herein denoted ρ. Theoretically ρ ranges from 0 to 1, corresponding to single straight lines representing growth in op-

posing or a single direction, respectively. But for the zooid shapes encountered, its range is 0.86 to 0.96, which roughly corresponds to shapes ranging from semicircles (0.77) to straight lines (1.0). The arithmetic mean of ρ for all 129 outlines studied is 0.91.

Asymmetry is also related to the "preferred" direction of growth. It reflects the departure of this direction from the principal growth direction, and is measured herein using two vector statistics. The tangent of the vector mean azimuth, $\tan \bar{\theta}$, has intuitive appeal in that it is theoretically closely related to ρ (Appendix A). In addition, its value is
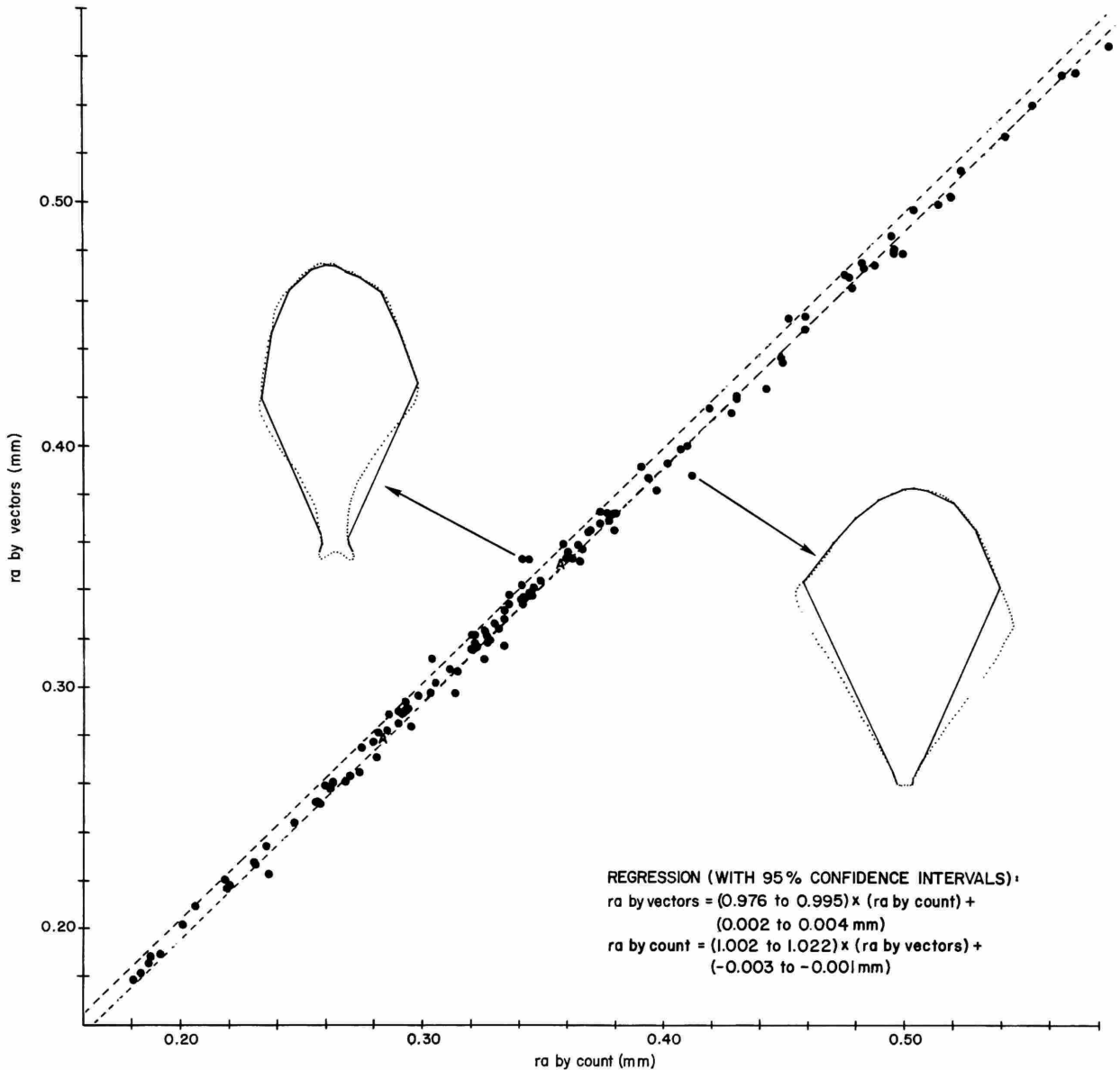
FIGURE 7.—Comparison of area enclosed by autozooecial outline (expressed as radius of equivalent semicircle, ra) determined by vector representation and by direct measurement (counts). The coefficient of correlation between the two methods is 0.999. Dots are 129 autozooecia measured in 32 zoarial fragments (Appendix B, specimens used in principal components analysis). (Dashed lines are limits of precision (empirically determined) of the counting method. Actual outlines (dotted lines) and vector representations (solid lines) are shown for the two zooecia that yielded the extremes of difference between the two methods.)

signed and hence distinguishes between "left" and "right" asymmetrical outlines. Unfortunately, tan $\bar{\theta}$ is much more sensitive to slight variations in outline width along the proximolateral margins than to variations of similar magnitude along the distal margin. Consequently, a second measure of asymmetry was devised to reflect variation in vector magnitudes rather than just their width compo-

nents. This measure, denoted a, is a weighted root-mean-square of proportional differences between the lengths of pairs of vectors at equal angular intervals on either side of the proximal-distal axis (Appendix A). Although it is more sensitive than $tan\ \bar{\theta}$ to departures from symmetry in the distal portion of the outline, a has the disadvantage that it is always positive and hence cannot convey directional information. Because these two measures of asymmetry convey complementary information, both were included in the analyses. Neither a nor $tan\ \bar{\theta}$ reflect large departures from symmetry in the outlines studied (maximum $\bar{\theta} = 4.06°$).

Finally, the term "distal inflation" refers to the relative concentrations of lateral growth components in the distal and proximal parts of the zooidal outline. Its measure, di, is defined as the proportional area that is distal to the midpoint of the proximal-distal axis (Appendix A). Zooid shapes examined range from distinctly proximally inflated ($di = 0.38$) to distinctly distally inflated ($di = 0.64$); the average of 129 autozooecia lies at about $di = 0.5$.

In addition to these five measures of size and shape, we initially considered two others, which later proved to be redundant. The length of the mean vector ($\bar{r}$) is obviously related to the "preferred" direction of growth, but is also highly correlated with size. The maximum vector length ($rmax$), which has been used as a measure of zooid length in some previous studies, also has high correlations with both size and shape variables. For this reason, and because its use would require an

assumption of morphologic correspondence in addition to the vector origin, it was dropped from consideration very early in the analyses and is not treated further.

Means and standard deviations of all size and shape measures except $rmax$ are given in Appendix B for each of the 32 cheilostome zoaria studied.

Study Methods

Thirty-two colonies representing 30 species (Appendix B) were selected for the initial analyses to give a wide range of autozooidal shapes and sizes. Most specimens studied are type-specimens of type-species and thus represent, for the most part, different genera. On each specimen, an attempt was made to measure outlines of five autozooids, a number which subsequent analysis indicated to be adequate for recognizing minimum taxonomic differences (Table 18). A total of 129 autozooecia were included in the initial analyses, the results of which are described in the next section (Comparison of Outlines).

Vector lengths were measured from projections of frontal outlines from × 50 or × 75 photographs onto the semistarburst pattern (Figure 4) at a standard magnification of × 100. A precision of measurement of 0.01 mm (to which all vector lengths used in the analyses were recorded) was estimated from separate trials of projecting, orienting, and measuring the same and separate photographic outlines of the same zooecium (Table 1). Replicate measurements from the sep-

TABLE 1.—Precision of measurement of 17 vectors of same autozooecial outline with three measurement techniques (standard deviation calculated as square root of weighted average variance)

Method of measurement	Standard deviation (mm)
Projection from photograph to semistarburst pattern	
Separate measurements, same projection...............................	0.00097
Separate projections, same photograph, same orientation................	0.00146*
Separate orientations, same photograph................................	0.00306
Separate photographs, same zooecium..................................	0.00449
Projection of camera lucida image to semistarburst......................	0.01113
Direct measurement with rotating stage, ocular micrometer................	0.00792**

* two replications only; all others three   **excludes deviations in measurement of angles

arate photographic projections were more consistent than either replicate measurements made with an ocular micrometer directly from the specimen on a rotating mechanical stage or replicate measurements made from camera lucida outlines projected onto the semistarburst pattern (Table 1).

The size and shape coefficients ra, ρ, $tan\ \bar{\theta}$, a, di, and $\bar{r}$ were computed from the measured vector lengths and the a priori determined vector directions using a program (VECSTAT) written by one of us (DML). The program includes principal components analysis of the correlations among the vector coefficients and computes normalized coordinates for each zooecium in eigenvector space. Procedures in which variables and components are standardized were used throughout because of the differences in units of the vector coefficients.

Principal component axes were subjected to two separate orthogonal rotations to measure the relationships among certain vector coefficients. Both rotations were made in 4-component space, in which well more than 90 percent of the total variation and of that in each vector coefficient is accounted for (Tables 3–5). The first axis, lying in the direction of maximum variation, was rotated to coincide approximately with the direction of the size coefficient, ra, in order to examine variation in size and to remove size effects from the analysis of variation in shape. The rotated second axis was further rotated to a position near the directions of two of the shape coefficients, ρ and di, in order to study the relationships among independent aspects of shape.

For each of the four rotated components, variation within and among the 32 colonies used in the initial analysis was compared by analysis of variance, after first determining that nonnormality of data, or of transformed data, and heterogeneity

of variances do not preclude use of this method.

Certain parts of the sample of 32 colonies used in the initial analyses were supplemented by additional material in order to examine aspects of intracolony and intrapopulation variation. Ontogenetically and astogenetically differing autozooids were measured in one colony each; dimorphic autozooids were measured in each of three conspecific colonies; and autozooids were measured in each of six colonies inferred to be from the same fossil population. Variation within each of these subsamples was studied by, first, transforming variation in the six vector coefficients to the same rotated 4-component space developed in the initial analyses and, then, performing analyses of variance (or, where data were significantly nonnormal or variances were significantly heterogeneous, substituting appropriate nonparametric methods) on each rotated component. The analyses including the additional material (a total of 51 zooecia) are described in a following section (Nature of Variation in Outlines).

Comparison of Outlines

The interrelations among the six size and shape variables calculated for the frontal outlines of 129 cheilostome autozooecia (see Appendix B), from measured vector lengths and chosen vector directions (see Appendix A), are summarized in Tables 2–6 and Figures 8–11.

Correlations between pairs of variables (Table 2) include three high values, 0.957 for ra and $\bar{r}$, 0.813 for ρ and di, and 0.724 for a and $tan\ \bar{\theta}$. Two of these highly correlated pairs comprise conceptually related variables, ra and $\bar{r}$ primarily expressing size and a and $tan\ \bar{\theta}$ primarily expressing asymmetry. The high correlation between ρ and di is

TABLE 2.—Correlation coefficients of six vector variables for 129 cheilostome autozooidal outlines (underlined values significantly different from 0 at P = 0.01; other values not significantly different from 0 at P = 0.05)

Variable	$\bar{r}$	ρ	di	a	$tan\ \bar{\theta}$
ra...............	.957	-.433	-.321	-.247	-.001
$\bar{r}$		-.171	-.130	-.132	.018
ρ			.813	.516	.080
di...............				.479	.019
a					.724

not conceptually required, and some cheilostome autozooids can differ in these two variables independently. All the shape variables except $tan\ \bar\theta$ are significantly, but not highly, correlated with size (which we have defined to be measured by ra). Although the significant size-shape correlations are all negative, the directions of the shape variables relative to size are arbitrary. For example, elongation could be redefined as squatness or distal inflation could be redefined as proximal inflation, and their resulting correlations with size would be numerically unchanged but positive rather than negative. Three of the shape variables—ρ, di, and a—are significantly, but not consistently highly intercorrelated. The remaining shape variable, tan

$\bar\theta$, is significantly correlated only with a, not with any other variable.

The rather complex pattern of intercorrelations among the six variables is resolved by principal components analysis into as few as three orthogonal components (Table 3), each of which expresses an independent linear combination of the variables. Although these three components account for almost 95 percent of the total variation in the outlines examined, they account for appreciably less of the variation in ρ and di (see communalities, Table 3). Moreover, the correlations between ra and other variables are reproduced considerably less closely in three-component space than in four-component space (see Tables 4 and 5

TABLE 3.—Normalized eigenvectors from principal components analysis of six vector variables based on correlation matrix in Table 2

Component	Eigenvector coefficients (loadings)						Eigenvalue	Prop. of variance	Cum. prop.
	ra	$\bar{r}$	ρ	di	a	$tan\ \bar\theta$			
F(1).....	.754	.590	-.811	-.750	-.724	-.335	2.777	.462	.462
F(2).....	.615	.706	.148	.172	.570	.651	1.675	.279	.742
F(3).....	-.222	-.382	-.472	-.560	.270	.643	1.218	.203	.944
F(4).....	-.058	.076	.312	-.280	-.077	.042	.192	.032	.976
F(5).....	-.015	-.008	.014	-.124	-.269	.222	.137	.023	.999
F(6).....	.044	-.040	.015	-.003	-.001	.000	.004	.001	1.000
Communality									
F(1)-F(2)..	.946	.847	.679	.593	.849	.536	−		
F(1)-F(3)..	.995	.993	.902	.906	.922	.949			
F(1)-F(4)..	.998	.998	.999	.985	.928	.951			

TABLE 4.—Factors resulting from orthogonal rotation of first three normalized eigenvectors in Table 3 so that F(1)′ approximately coincides with ra (correlations of ra with other variables in parentheses)

Factor	Factor coefficients (loadings)						Sum of squared coeff.	Prop. of variance	Cum. prop.
	ra	$\bar{r}$	ρ	di	a	$tan\ \bar\theta$			
F(1)′........	.997	.966	-.416	-.336	-.256	.005	2.280	.380	.380
		(.957)	(-.433)	(-.321)	(-.247)	(-.001)			
F(2)′........	.000	.174	.627	.608	.899	.716	2.114	.352	.732
F(3)′........	.000	-.171	-.580	-.651	.218	.661	1.273	.212	.944
Communality									
F(1)′-F(3)′..	.995	.992	.902	.906	.922	.949			

TABLE 5.—Factors resulting from orthogonal rotation of first four normalized eigenvectors in Table 3 so that F(1)' approximately coincides with *ra* and F(2)'' lies near *ρ* and *di* (correlations of *ra* with other variables in parentheses)

Factor	Factor coefficients (loadings)						Sum of squared coeff.	Prop. of variance	Cum. prop.
	ra	$\bar{r}$	*ρ*	*di*	*a*	*tan* $\bar{\theta}$			
F(1)'.......	.999	.960	-.434	-.319	-.251	.003	2.273	.379	.379
		(.957)	(-.433)	(-.321)	(-.247)	(-.001)			
F(2)''......	-.000	.244	.853	.890	.482	.039	1.813	.302	.681
F(3)''......	-.000	.002	.034	-.030	.790	.973	1.574	.262	.943
F(4)'......	.001	.133	.286	-.299	-.092	.043	.199	.033	.976
Communality									
F(1)'-F(4)'.	.998	.999	.999	.985	.928	.951	-		

and discussion of rotation below). Therefore, the first four components were employed in all further calculations, even though the fourth component accounts for a small percentage of the total variation.

The principal components axes do not lie very near the directions of any of the size or shape variables and thus have low morphologic interpretability (Table 3; Figures 8–11). The direction of greatest variation, F (1), is subequally distant from *ra*, *ρ*, *di*, and *a*, disregarding whether their directions are positive or negative. To examine independent aspects of size and shape differences among the autozooid outlines measured, it is important to separate the effect of size from those of shape while keeping each aspect of shape differences independent of the others. To improve morphologic interpretability within these guidelines, we rotated the first four component axes orthogonally so that the first axis coincides with the direction of the size variable, *ra*. As this rotation was made in the reduced space of four components, the coincidence of the rotated axis F (1)' with *ra* is approximate but close (Table 5; Figures 8–10). Although F (1)' is no longer in the direction of maximum variation defining F (1), its variance is not much less than that of F (1) (Table 5).

Rotation of F (1) to coincide approximately with *ra* placed F (2) among the shape variables as a generalized measure of shape (Figure 8, F (2)'). In order to separate aspects of shape, axes F (2)' and F (3)' were rotated again, this time in the plane which contains them both, to new positions F (2)'', lying near the directions of *ρ* and *di*, and
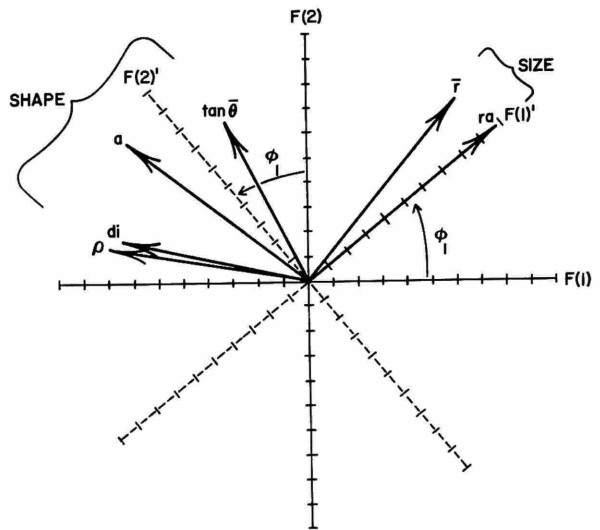
FIGURE 8.—Relation of six vector variables to first two principal components axes showing separation of size and shape. (Orthogonal rotation ($\phi_1 = 39.2°$) of F (1) to approximate coincidence with *ra* results in placement of F(2)' amid the shape variables.)

F (3)'', lying near *tan* $\bar{\theta}$ (Figure 11). This rotation preserved the orthogonal relationships among all axes, and left the positions of F (1)' and F (4)' unchanged. The new directions F (2)'' and F (3)'' have variances little different from those of components F (2) and F (3) (Table 5). Thus the two rotations produced a set of orthogonal axes with variances little different from those of the unrotated components, but lying in directions near those of size and shape variables. The transforma-

FIGURE 9.—Relation of six vector variables to principal components axes F(1) and F(3) showing separation of asymmetry from elongation and distal inflation. (Orthogonal rotation ($\phi_2 = -12.85°$) of F(1) to approximate coincidence with *ra* results in little change in position of F(3).)

FIGURE 11.—Additional orthogonal rotation ($\phi_4 = -45°$) of F(2)' (Figure 8) to new position F(2)'' near ρ and *di*. (Rotation results in displacement of F(3)' to F(3)'', which is nearer *tan $\bar\theta$* and *a*.)
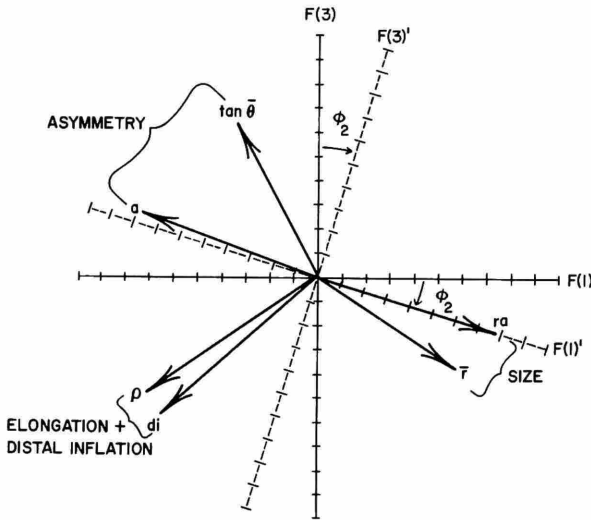

FIGURE 10.—Relation of six vector variables to principal components axes F(1) and F(4) showing partial separation of elongation and distal inflation. (Orthogonal rotation ($\phi_3 = -3.38°$) of F(1) to approximate coincidence with *ra* results in little change in position of F(4).)

tion matrix for the two rotations is shown in Table 6.

The especially high correlation between *ra* and $\bar r$ (Table 2) suggests that one or the other of these

variables could have been dropped from the principal components analysis with little or no loss of information. The principal components analysis itself takes redundancy into account, but it is interesting to compare the results of the four-component representation based on the correlation matrix with $\bar r$ dropped out to that based on all six variables and used throughout the analyses. Although the first four eigenvectors have different coefficients and different proportional eigenvalues, the cumulative proportion of their eigenvalues and their communalities for each variable are practically identical (maximum difference = 0.003). This means that a similarly orthogonally rotated four-component representation based on the five variables excluding $\bar r$ would have almost exactly the same correlations with variables and proportions of variance as the four-component representation based on all six variables.

SIZE.—Among the 129 autozooecia included in the initial analyses, almost 40 percent of the total variation in outlines is in the direction of the rotated first principal component, F (1)', which was made to coincide approximately with *ra*, the size variable. The size variation in outlines is greater than that in any single aspect of shape but less than that in all aspects of shape combined.

The plot of F (1)' against F (2)' (Figure 12)

TABLE 6.—Transformation matrix of direction cosines used to rotate first
four components in Table 3 to factors in Table 5

Rotated factors	Unrotated components			
	F(1)	F(2)	F(3)	F(4)
F(1)'..........	.7542	.6152	-.2220	-.0590
F(2)"..........	-.5688	.4486	-.6894	0
F(3)"..........	-.3250	.6474	.6894	0
F(4)'..........	.0446	.0364	-.0131	.9983

shows within-colony variation polygons to be appreciably more elongated parallel to the shape axis (F (2)') than parallel to the size axis (F (1)'). This suggests that differences between colonies (most of which belong to different species and genera in this sample) are better expressed by size than by shape. However, the shape axis, F (2)', is a composite of the several shape variables, and the within-colony variation in any one shape variable can be considerably less than that in F (2)'. The separate aspects of shape variation are examined in the following sections.

The plot of F (1)' against F (2)' also provides an opportunity to show graphically the relative "distortion" of the rotated four-component representation, i.e., the differences between the values of a variable and those of the component which has been rotated to coincide approximately with it. As a very high percentage of the total variation and of the variation in each variable (97.6 percent of total; 92.8 to 99.9 percent of that in each variable; see Table 5) is accounted for, the distortion can be expected to be small. This is also suggested by the almost perfect correlation (0.999; see Table 5) between variable ra and its representation in four-component space, F (1)'. Even with a lower percentage of the total variation accounted for (see Rohlf, 1972), one could expect the zooecia to be arranged in the direction of F (1)' in their actual rank order with respect to ra. In Figure 13, the actual values of ra for the 129 zooecia used in the initial analyses have been plotted at their positions ordinated in the F (1)', F (2)' plane, and lines of equal values of ra have been interpolated between points. With no distortion, the lines of equal ra would be parallel and evenly spaced. The distor-

tion of ra by the four-component representation is obvious, especially for zooecia of approximately mean size and mean shape (center of Figure 13), for which it can amount to 0.6 standardized unit (= 0.05 mm). For colony means, however, the distortion should be less (central limit theorem), and is indicated graphically (Figure 14) to be less than 0.2 standardized unit (< 0.017 mm).

ASYMMETRY.—The two orthogonal rotations, F (3) to F (3)' (Figure 9) and F (3)' to F (3)" (Figure 11), placed the third axis near the directions of $\tan \bar{\theta}$ and a as a measure of asymmetry which is independent of size and other aspects of shape. Thus expressed, asymmetry accounts for about one-fourth of the total variation in outlines among the 129 autozooecia included in the initial analyses. As the absolute value of $\tan \bar{\theta}$ was used in the calculation of F (3)", this axis measures the amount but not the direction (handedness) of asymmetry.

The amount of asymmetry, as indicated by a and by the absolute value of $\tan \bar{\theta}$, is small for all zooecia examined (Table 7). The maximum observed value of $\tan \bar{\theta}$ corresponds to an angle of about 4°. The plot of F (3)" against F (2)" (Figure 15) further suggests that asymmetry accounts for most of the high within-colony variation in shape.

The nature of the asymmetry exhibited by the 129 autozooecia examined is suggested by the signed values of $\tan \bar{\theta}$ (Table 7). Of the three kinds of asymmetry distinguished by Van Valen (1962), that deriving from the systematic prevalence of one side over the other (directional asymmetry) appears not to be important except possibly in localized regions of colonies, such as in a branch with a diverging budding direction (e.g., Figure
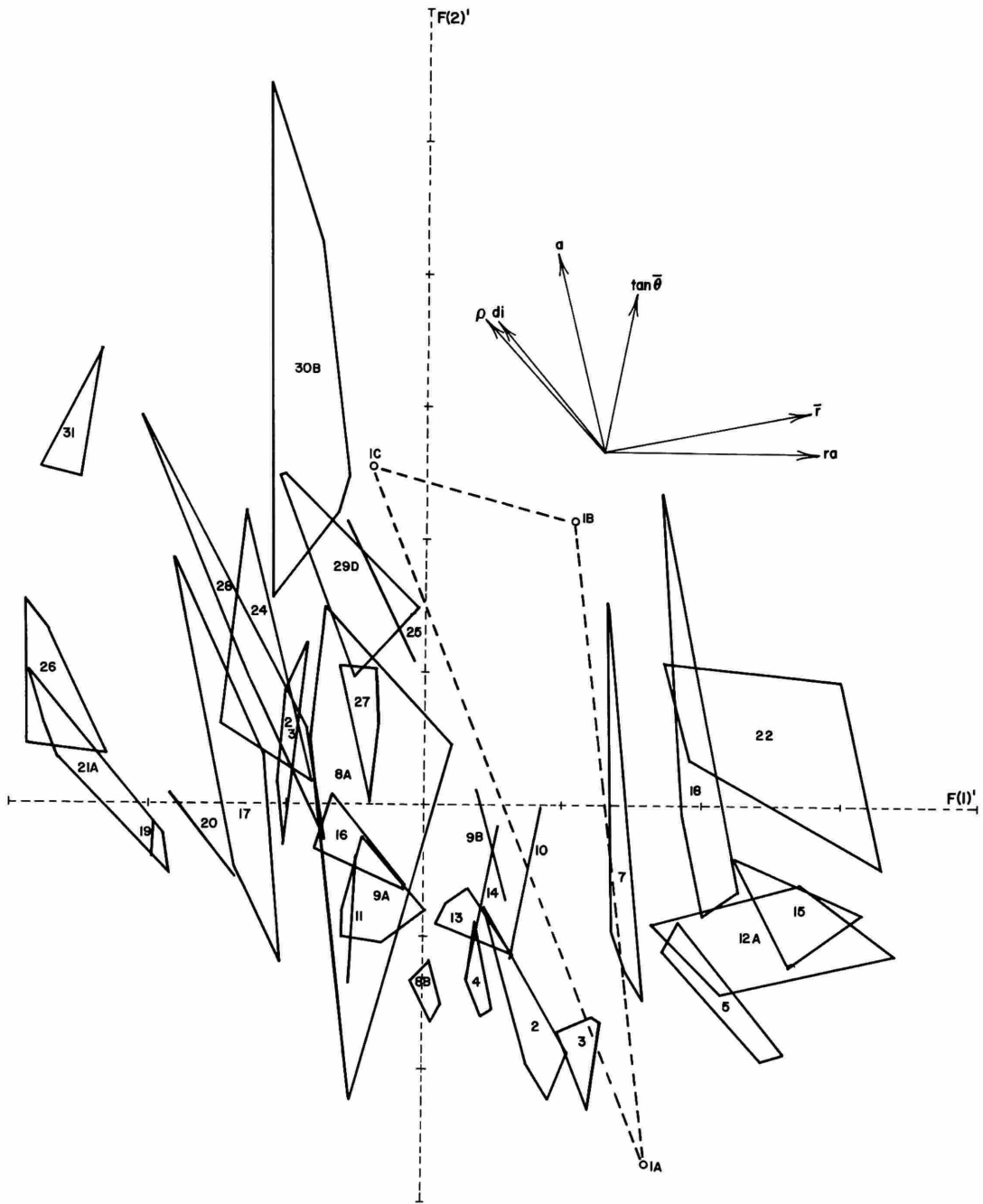
FIGURE 12.—Variation in 129 autozooecial outlines in 32 zoarial fragments for first two rotated principal components, F(1)′ (size) and F(2)′ (overall shape). (Scatter polygons are numbered as in Appendix B. Directions of vector variables are indicated by arrows arranged as in Figure 8. Colony 1 (dashed polygon) exhibits astogenetic variation in shape. F(1)′ and F(2)′ scales are in standardized units normalized to their respective factor variances (Table 4). One unit on F(1)′ is approximately equivalent to 0.06 mm of *ra*, with smaller zooecia lying to the left and the center at the grand mean of the 129 zooecia. The variables related to F(2)′ are dimensionless.)
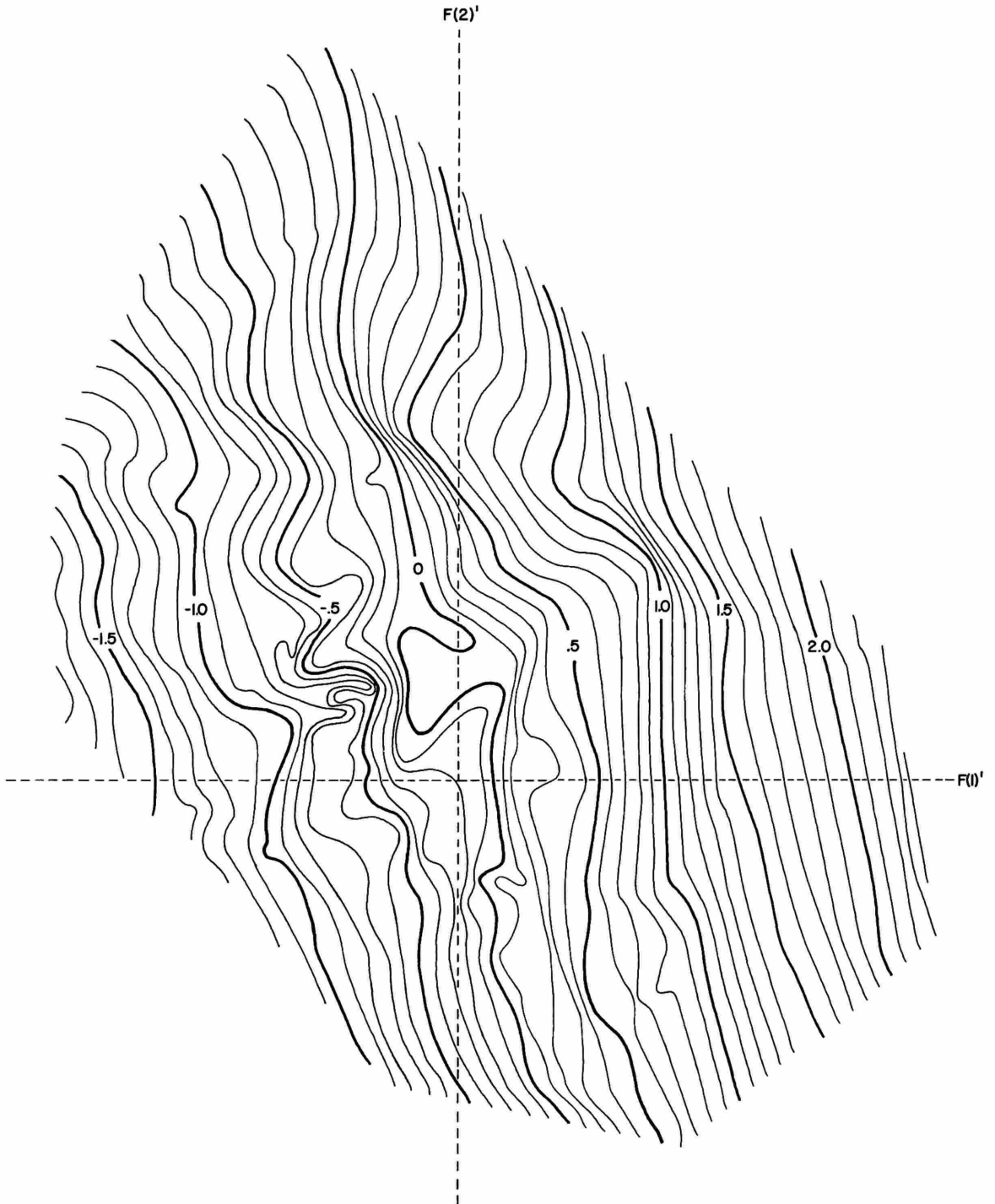
FIGURE 13.—Lines of equal values of *ra* for the 129 autozooecial outlines of Figure 12 at their positions ordinated by the rotated four principal component representation. (Units of *ra* are standardized, but not normalized, one unit equivalent to approximately 0.09 mm.)
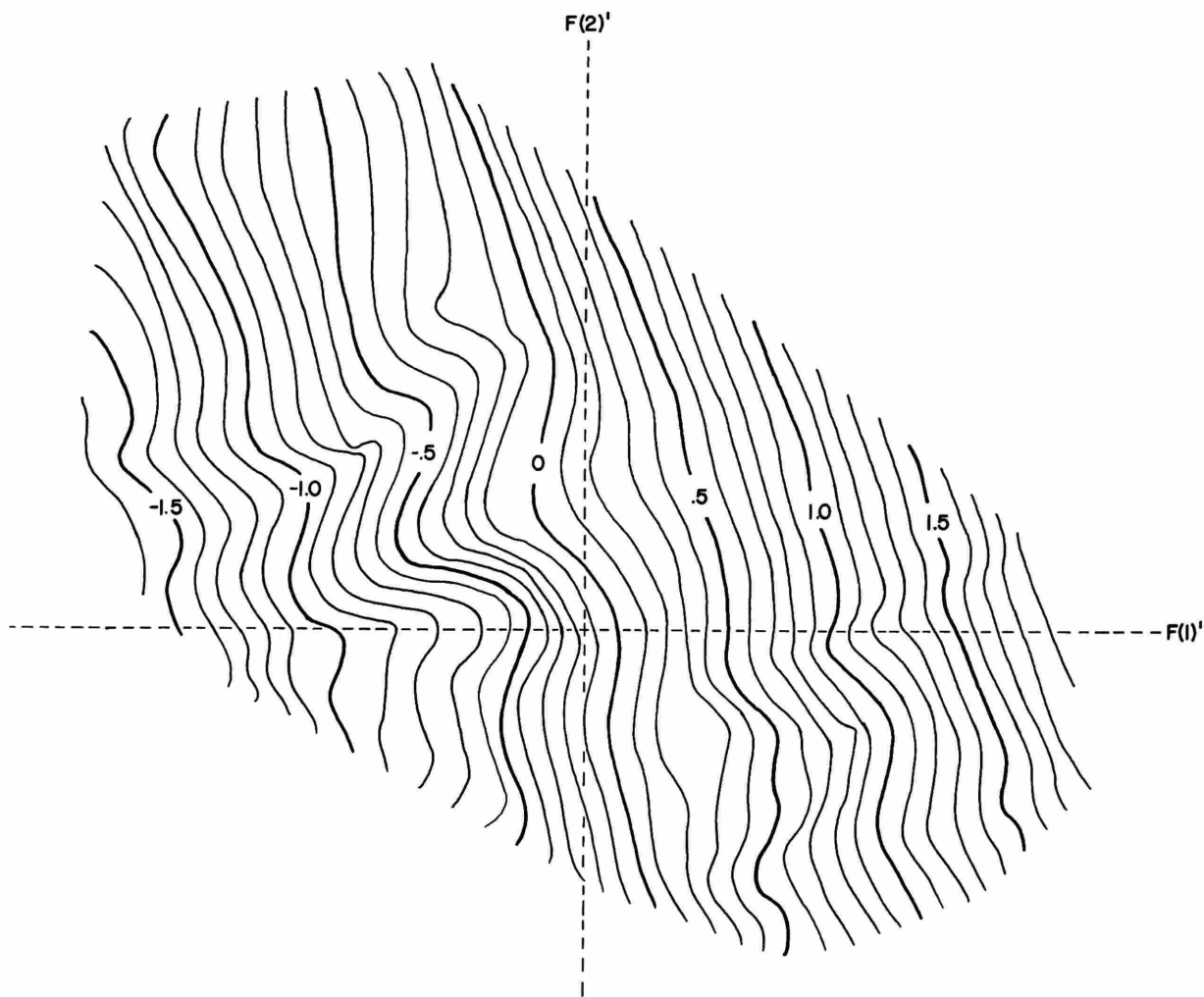
FIGURE 14.—Lines of equal values of *ra* for 31 of the within-colony means of Figure 12 (omitting colony 1). (Representation is as in Figure 13.)

TABLE 7.—Comparison of asymmetry statistics *(tan $\bar{\theta}$)*, using absolute and signed values, for 105 zooecial outlines in 22 zoarial fragments

Statistic	Signed value	Absolute value
Range, pooled data............	-0.040 to 0.071	0.000 to 0.071
Proportion + values...........	0.52	--
Range, colony means...........	-0.010 to 0.032	0.004 to 0.041
Proportion + values...........	0.64	--
Pooled mean...................	0.003	0.014
Range, colony variance........	0.00002 to 0.0018	0.00001 to 0.0008
Pooled variance...............	0.0004	0.0002

24, D). Although the data tend to have more positive than negative values of $tan\ \bar{\theta}$ (i.e., to be slightly "right-handed"), the pooled mean is not significantly different from zero ($P > 0.05$). In addition, none of the individual zoarial fragments studied have means significantly different from zero ($P > 0.05$). (The slight apparent directional asymmetry was removed from further calculations by standardization as described in "Study Methods.") Antisymmetry, that is, the tendency to be asymmetrical but "right" or "left" with about equal frequency, is suggested in zoarial fragments having near-zero means and high variances. The most obvious example is furnished by *Thalamoporella biperforata* (Figure 23, A; mean, 0.0008; variance, 0.0018). All such examples appear related to arrangement of asymmetrical zooids in more or less bilaterally symmetrical budding patterns. Most of the asymmetry in outlines appears to be fluctuating asymmetry, that is, the generally small, subequally "right" and "left" departures from a general tendency toward bilateral symmetry. This is suggested by the near-zero means and low variances for most of the zoarial fragments studied. Fluctuating asymmetry has been taken as a measure of "developmental noise" (Van Valen, 1962), and in the zooecial outlines examined it seems ascribable chiefly to microenvironment.

It must be emphasized that the asymmetry examined here is that of the outline only. Asymmetry of other zooidal structures, such as placement of the orifice or orientation of adventitious avicularia (see Cheetham, 1973), can be exactly reversed in handedness and different in amount from that displayed by the outline.

ELONGATION AND DISTAL INFLATION.—The rotated second axis F (2)″ (Figure 11; Table 5), accounting for almost one-third of the total variation in outlines, represents the size-independent, positively correlated portion of the variation in ρ and di.

The plot of F (2)″ against F (3)″ (Figures 15, 16) suggests that elongation and distal inflation are generally less variable within colonies than is asymmetry. Although there is only a weak correlation between asymmetry and the other two shape variables, Figure 15 further suggests that departures from symmetry can be greater in more elongate and distally inflated outlines. This is to be expected because the greater inequality of vector lengths in different parts of elongate or distally inflated outlines can emphasize inequalities on either side of the proximal-distal axis. Both squat, proximally inflated and elongate, distally inflated outlines, however, vary from nearly symmetrical to distinctly asymmetrical.

Most of the remaining size-independent variation in ρ and di is associated with the rotated fourth axis F (4)′ (Figure 10; Table 5), which accounts for only a small part of the total variation in outlines. The variation of ρ and di on F (4)′, unlike that on F (2)″, is not correlated.

Almost all of the size-independent variation in ρ and di is thus expressed in the plot of F (2)″ against F (4)′ (Figure 17). That part of the variation in ρ that is independent of di, as well as of size, is expressed at right angles to the direction of di in that plot (Figure 17a). Conversely, size- and ρ-independent variation in di is expressed at right angles to the direction of ρ (Figure 17b). Observed ranges of outlines within colonies measured in those directions suggest that part of ρ is less variable within colonies than the corresponding part of di. This suggests that, even though ρ and di are strongly correlated among the outlines examined, these two variates in part measure different aspects of shape and that ρ may be slightly more important in characterizing the shapes of zooids within a colony.

The principal variations in elongation and distal inflation are summarized on Figure 18. Ten zoarial fragments from which autozooecial outlines were measured for the foregoing analysis are arranged approximately as in Figure 17 with respect to the F (2)″ and F (4)′ axes. With differences in size and asymmetry disregarded, these ten groups of autozooecia illustrate shape variation as a whole. It can be noted that the mean shape of the 129 outlines (Figure 18, specimen 18) is similar to that of the hypothetical cheilostome shown in Figures 1–4.

VARIATION AMONG AND WITHIN COLONIES.—Relations between variation among colonies and that within colonies for the four orthogonally rotated axes (factors of Table 5) are suggested by the ranges of variation plotted in Figures 12, 15, 16, and 17. These relations were further examined by single-classification analysis of variance (Tables 8, 9). One zoarial fragment, *Tetraplaria simata* (1A-C), was excluded because of obvious astogenetic heterogeneity in autozooecial outlines. Con-

FIGURE 15.—Means of 31 of the 32 zoarial fragments of Figure 12 for rotated principal components F(2)″ and F(3)″. Individual values are shown for specimen 1. (For colonies in which three to five zooecia were measured, 95 percent confidence intervals for F(3)″ are indicated by horizontal lines. Directions of vector variables are shown by arrows arranged as in Figure 11. Dotted line marks empirically determined position of perfectly symmetrical shapes, the value of asymmetry increasing to the right. F(2)″ and F(3)″ scales are in standardized units normalized to their respective factor variances (Table 5). The variables associated with these two components are dimensionless. Portions of confidence intervals for specimens 7 and 28 extending to left of symmetry line are hypothetical.)

sistent deviations from normality or significant heterogeneity (Fmax test, Sokal and Rohlf, 1969) of within-colony variances, which would have made questionable the application of analysis of variance to this problem, were not found for factors (F (1)′, F (2)″, or F (4)′.

For F (3)″, the plot of colony means and their con-

fidence intervals (Figure 15) suggests a positive correlation between means and variances. This is not surprising because the measures a and absolute value of $tan\ \bar{\theta}$, on which F (3)″ is primarily based, permit high variances only with large means. Low variances are possible with either large or small means, but the predominance of fluctuating asym-
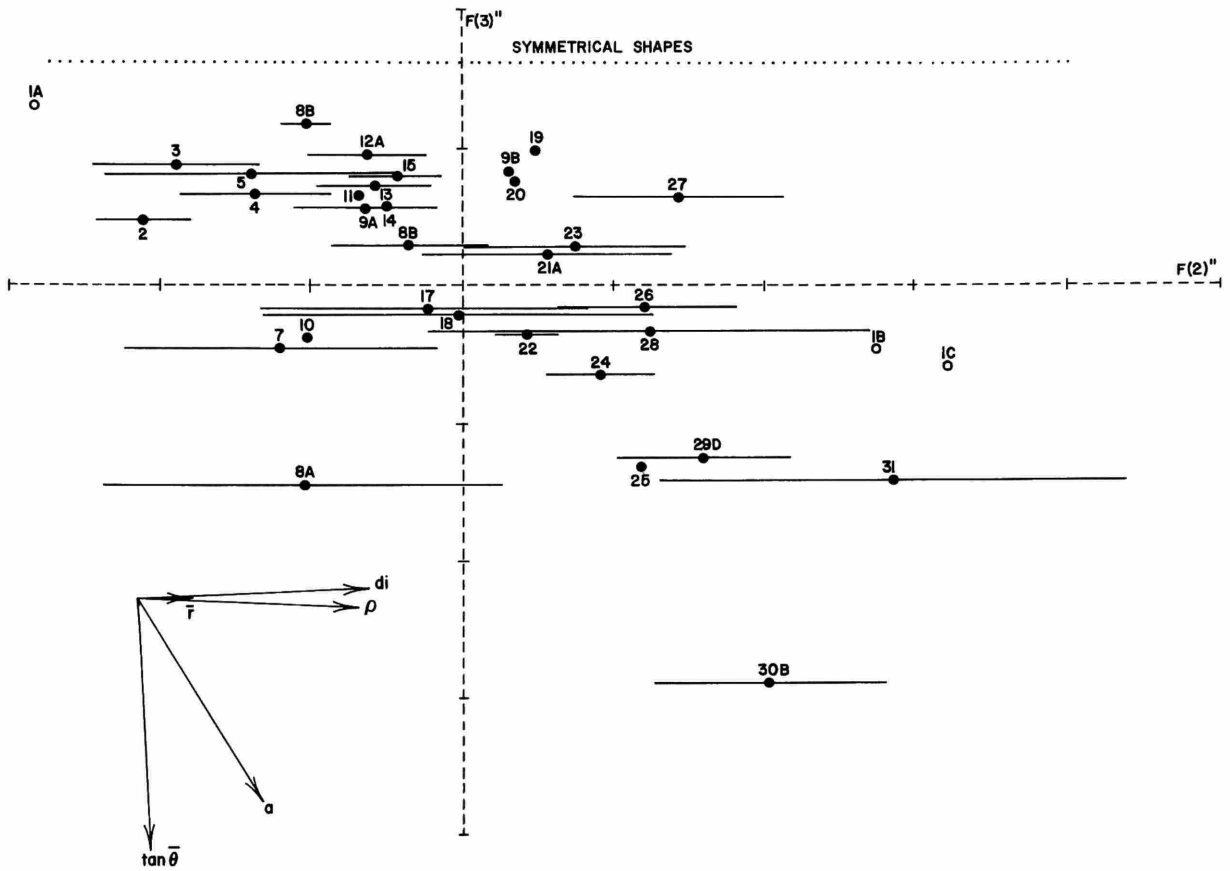
FIGURE 16.—Same plot as Figure 15 but turned so that 95 percent confidence intervals for means of F(2)″ are indicated by horizontal lines. (The values of elongation and distal inflation increase to the right, with the grand mean for the 129 outlines at the intersection of the F(2)″ and F(3)″ axes.)

metry in the data, as discussed above, results in association of low variances almost entirely with small means. To reduce this apparent departure from normality, the appropriate logarithmic transformation (Sokal and Rohlf, 1969) was used on F (3)″. Within-colony variances are not significantly heterogeneous, so analysis of variance was performed on log (F (3)″). For comparison, an analysis of variance was made on the untransformed data, with practically identical results.

For all four factors, the among-colonies component of variance is highly significant, indicating that all factors are potentially important in distinguishing autozooecial outlines in different colonies. Even though each factor expresses highly significant differences among colonies (Table 8), the relative importance of the four factors appears

to differ appreciably, not only with regard to their portion of the total variance as revealed by the foregoing principal components analysis, but also with regard to the portion of each attributable to among-colonies differences over and above within-colony variation (Table 9).

The importance of size is further emphasized by the extremely high proportion of the variance in F (1)′ that is attributed to the among-colonies variance component. The distinction between a high among-colonies and a low within-colony variance is demonstrated by the wide gap between their 95 percent confidence intervals.

Because of possible distortion of within-colony variances introduced by the rotated principal components representation (see page 15), another analysis of variance was made directly on values of
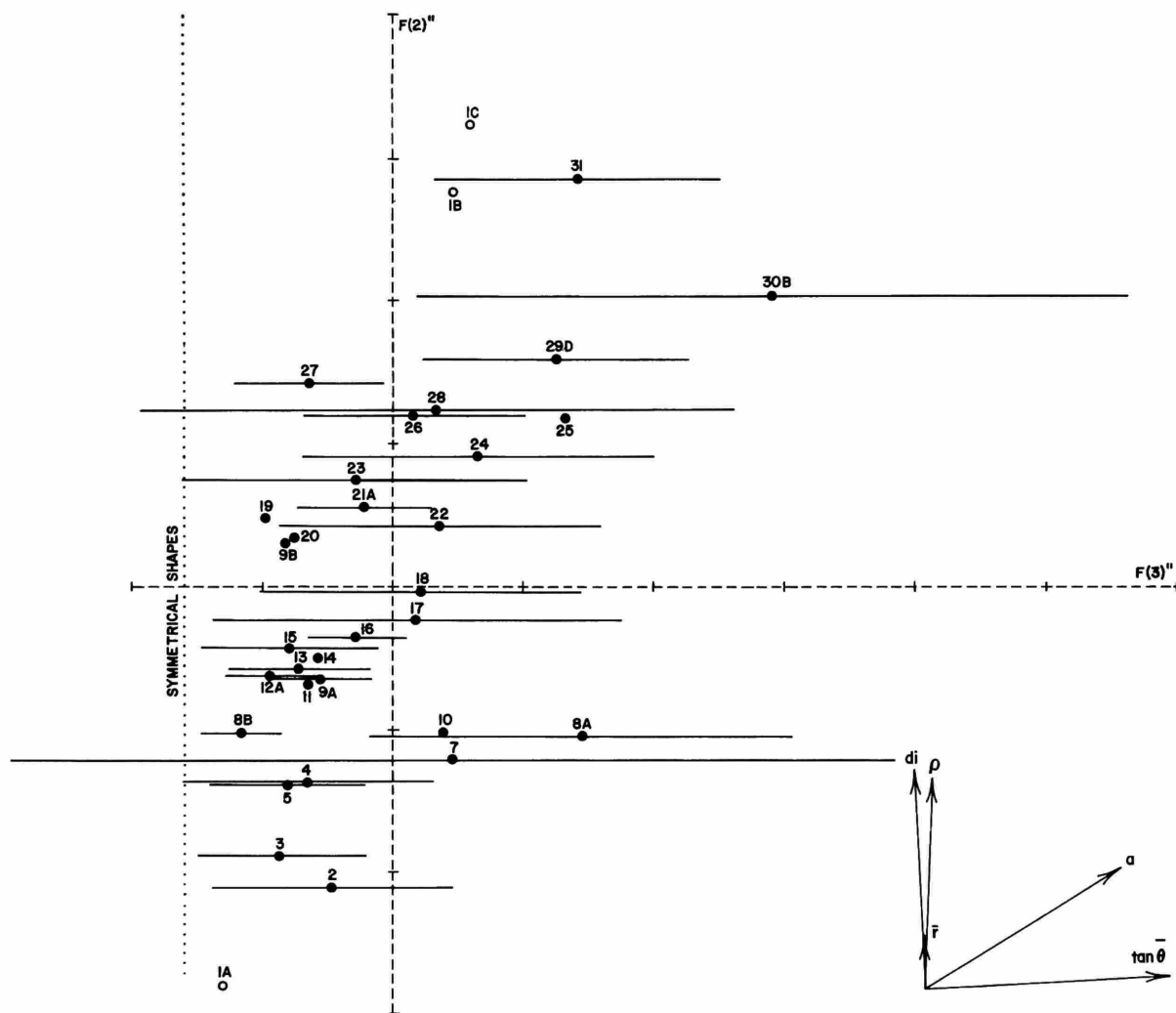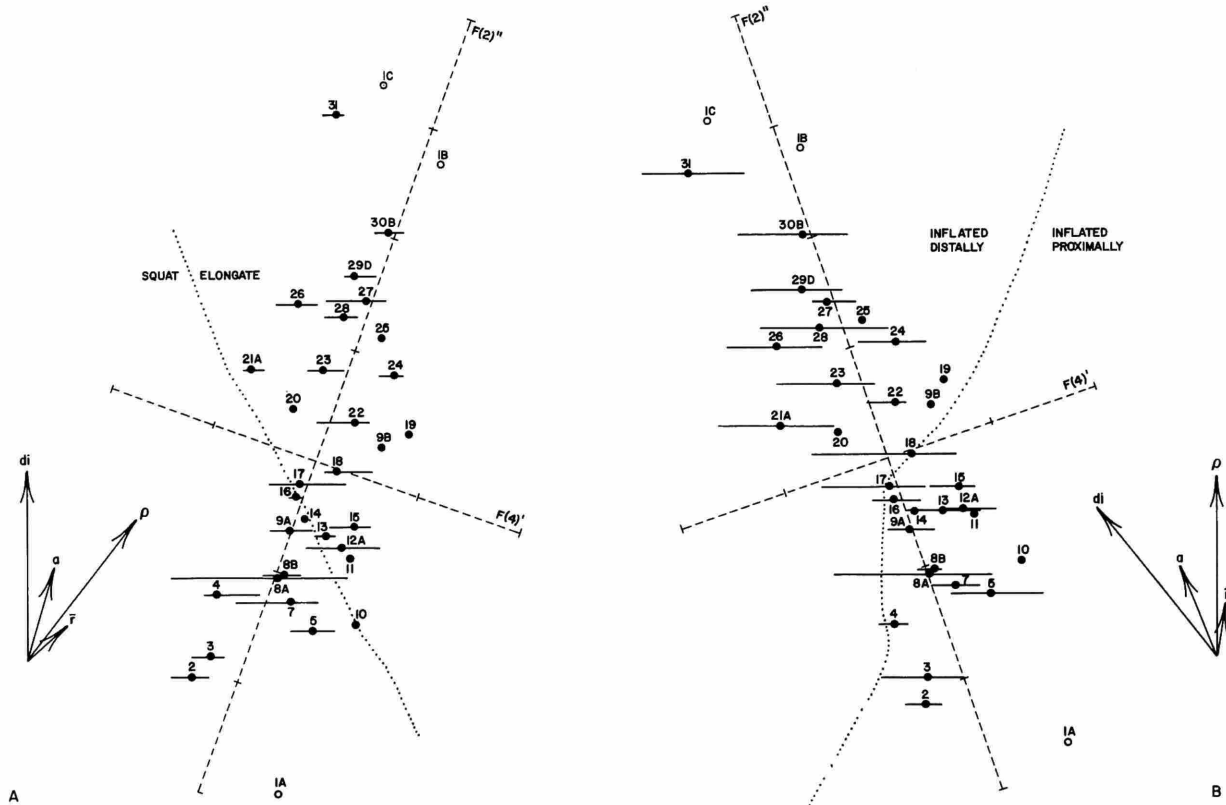
FIGURE 17.—Means of 31 of the 32 zoarial fragments of Figure 12 for rotated principal components $F(2)''$ and $F(4)'$: *a*, plot turned to allow observed range in each zoarial fragment in which three to five zooecia were measured to be represented by horizontal line perpendicular to the direction of *di* (dotted line separates shapes having values of ρ greater than about 0.90 (elongate) from those with values less than about 0.90 (squat)); *b*, plot turned to allow observed variation ranges in zoarial fragments to be represented by horizontal lines perpendicular to the direction of ρ (dotted line separates shapes with values of *di* greater than about 0.50 (distally inflated) from those with values less than about 0.50 (proximally inflated)). (Individual values are shown for specimen 1. Directions of vector variables are shown by arrows. Scales are in standardized units normalized to factor variances (Table 5). The variables associated with the components except $\bar{r}$, are dimensionless.)

ra. The proportions of variance within and among colonies are virtually the same as those obtained for $F(1)'$ (Tables 8, 9).

Elongation and distal inflation, as measured by $F(2)''$ and $F(4)'$, also show high among-colonies variance components, although not so proportionally high as that associated with size. The gap between 95 percent confidence intervals for among-colonies and within-colony variances in $F(2)''$ is small, and the intervals for variances in $F(4)'$ partly overlap. The importance of these two as-

pects of shape in distinguishing outlines in different colonies thus seems to be slightly less than that of size.

Asymmetry, as measured by $F(3)''$, is the only one of the four factors for which the within-colony variance component is larger than that among colonies (Table 9). The 95 percent confidence interval for within-colony variance, however, is completely overlapped by that for among-colonies variance, making interpretation of the relationship more uncertain than that in other factors.
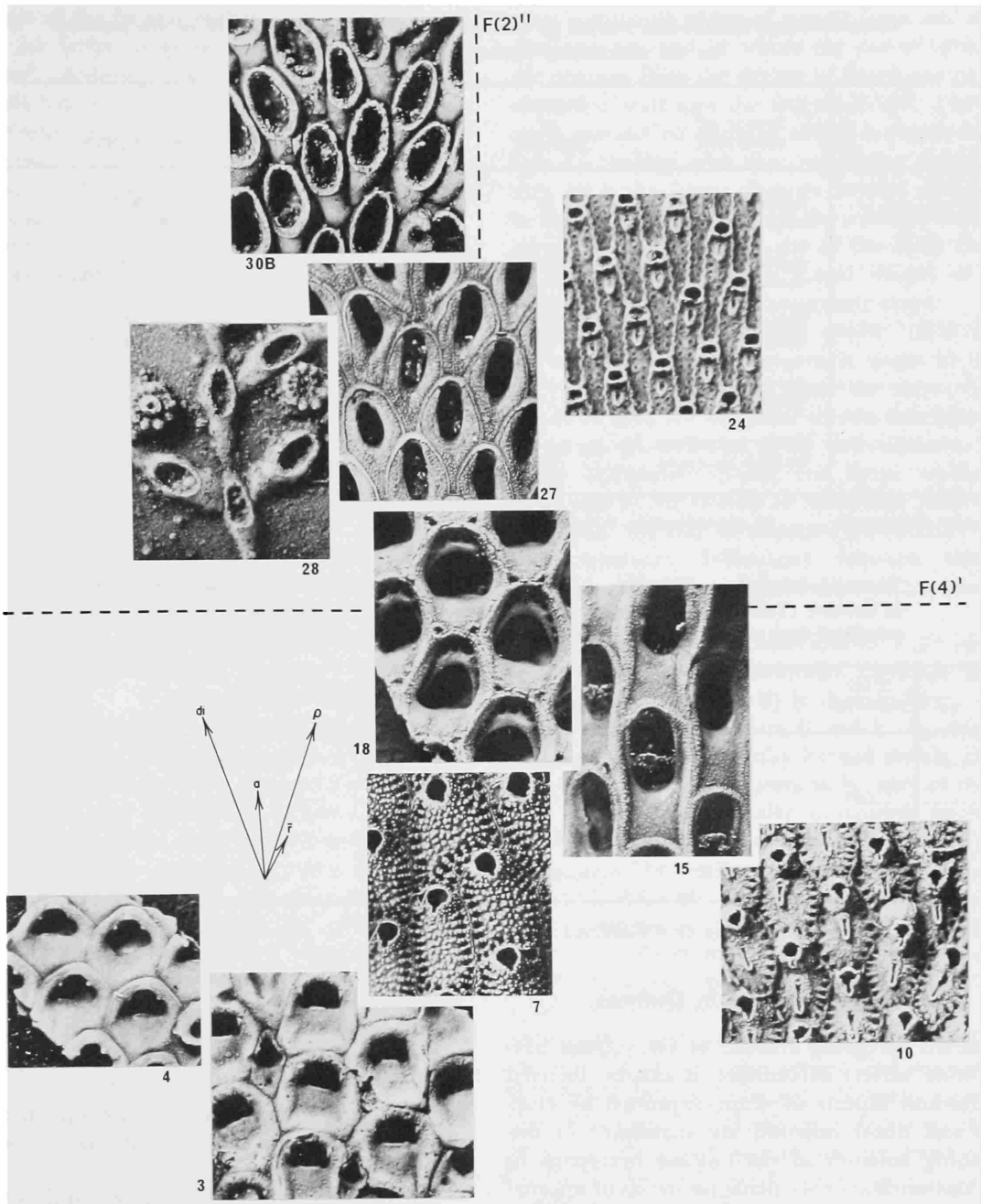
FIGURE 18.—General variation in shapes of autozooecia, independent of size and asymmetry, in 10 of the 32 zoarial fragments on which principal components analysis was based. Directions of vector variables are indicated by arrows. Frontal views (× 25) are arranged approximately as in Figure 17 with respect to F(2)″ and F(4)′ axes, and are numbered as in Appendix B: 30B, *Wilbertopora mutabilis* Cheetham; 28, *Pyripora texana* Thomas and Larwood; 27, *Tretosina arcifera* Canu and Bassler; 24, *Houzeauina parallela* (Reuss); 18, *Antropora? oculifera* (Canu and Bassler); 15, *Ogivalia elegans* (d'Orbigny); 10, *Schismoporella schizogaster* (Reuss); 7, *Metrarabdotos unguiculatum pacificum* (Osburn); 4, *Floridina* sp. 1: Cheetham and Håkansson; 3, *Entomaria spinifera* (Canu).

TABLE 8.—Single-classification analysis of variance in factors (Table 5) and in ra (in brackets) for 126 autozooecial outlines measured in 31 colonies

Factor	Source of variation	Degrees of freedom	Sum of squares	Mean square	F ratio
F(1)'.............	Among colonies	30	274.110	9.137	74.893**
	Within colonies	95	11.624	0.122	
[ra]..............	Among colonies	[30]	[119.782]	[3.993]	[81.818**]
	Within colonies	[95]	[4.636]	[0.049]	
F(2)".............	Among colonies	30	175.710	5.857	18.833**
	Within colonies	95	29.472	0.311	
F(3)"*............	Among colonies	30	9.018	0.301	3.471**
	Within colonies	95	8.228	0.086	
F(4)'.............	Among colonies	30	19.791	0.660	14.348**
	Within colonies	95	4.505	0.046	

* log transformation   ** significant, P < 0.001

TABLE 9.—Components of variance in factors (Table 5) estimated by single-classification analysis of variance (Table 8) of 126 autozooecial outlines in 31 colonies (confidence intervals of variance calculated from subsample of 17 colonies in each of which five outlines were measured)

Factor	Total variance	Among colonies		Within colonies		Proportions	
		Variance	95% conf. int.	Variance	95% conf. int.	Among	Within
F(1)'.......	2.347	2.225	0.971–4.207	0.122	0.092–0.180	0.948*	0.052*
F(2)".......	1.680	1.369	0.684–3.119	0.311	0.237–0.462	0.815	0.185
F(3)"**.....	1.643	0.729	0.411–2.344	0.914	0.636–1.239	0.379	0.621
F(4)'.......	0.199	0.153	0.050–0.242	0.046	0.036–0.071	0.761	0.239

* proportions from anova of variable ra   0.952 and 0.048, respectively   ** partitioned from log transformation

Nature of Variation in Outlines

From the foregoing analysis of autozooecia having a wide variety of outlines, it can be inferred that size and aspects of shape expressed by elongation and distal inflation are significant in distinguishing colonies of cheilostome bryozoans in which measurements are made on zooids of approximately the same ontogenetic, astogenetic, and polymorphic condition. How are these distinctions likely to be affected by measuring zooids belonging to different asexual generations in a zone of astogenetic change or to different autozooidal polymorphs, or by measuring zooids at different ontogenetic stages, unlikely though that may be in many cheilostomes? And are these distinctions as evident if the variation among colonies belonging to the same population is taken into consideration? To explore these questions, we enlarged parts of the sample used in the foregoing analysis to estimate intracolony and intrapopulation variation in factors F (1)'–F (4)' in some of the species examined in this study.

To evaluate factors F (1)'–F (4)', it is of course necessary to distinguish zooids ontogenetically, astogenetically, or polymorphically by means of morphologic criteria separate from those being evaluated. These criteria enable one to recognize the ancestrula and the growing edge of the colony and the sequences of morphologically differing zooids from each, and to distinguish among polymorphs. Differences in the factors expressing size

and shape of the frontal outline can then be tested against the series or groups of autozooids so distinguished. Although the examples studied here were selected for the distinctiveness with which they exhibit criteria on which to identify their ontogenetic, astogenetic, and polymorphic states, variation in factors $F(1)'$–$F(4)'$ cannot be precisely assigned to each possible source of intracolony variation. A difference in size or shape between two zooids which are obviously in different ontogenetic stages or which obviously belong to different asexual generations in a zone of astogenetic change can, and probably generally does, also reflect, less obviously, difference in microenvironmental conditions. The evaluation of ontogenetic, astogenetic, and polymorphic differences in $F(1)'$–$F(4)'$ could well yield new and possibly more precise criteria for recognizing these kinds of intracolony variation, but its purpose here was rather to compare these kinds of variation with potential taxonomic differences. How much will the unlikely eventuality of overlooking ontogenetic, astogenetic, and polymorphic heterogeneity in the material at hand obscure possible taxonomic distinctions?

The vector properties obtained for these enlarged subsamples were transformed to the same set of rotated axes as in the foregoing analysis to hold constant the previously inferred relationships among variables. For each subsample, plots were made of $F(1)'$ against $F(2)'$ (size vs. overall shape), $F(2)''$ against $F(3)''$ (elongation + distal inflation vs. asymmetry), and $F(2)''$ against $F(4)'$ (elongation vs. distal inflation). Among-colonies and within-colony components of variation were examined through analysis of variance, or, with contraindication of normality or homogeneity of within-colony variances, with nonparametric analogues.

ONTOGENETIC VARIATION.—Although the size and shape of an autozooidal bud change obviously during growth to the complete zooid, the pattern of change in size and the various aspects of shape can be expected to vary, and the stages at which there is no further change can be expected to differ for different aspects of the outline. To illustrate ontogenetic changes in factors $F(1)'$–$F(4)'$, we selected a specimen of *Metrarabdotos unguiculatum* Canu and Bassler (Figure 19) in which the shapes of buds at the growing edge appear similar to those

most commonly observed among fossil and modern cheilostomes, and in which the ontogenetic stages are obvious from the degree of development of the transverse wall and the frontal shield. The distalmost, uncalcified margins of the buds are missing, but, by analogy with observed living forms, probably lay a very short distance beyond and parallel to the preserved margins of the calcified walls. The shapes of the calcified parts of the buds thus can be expected to represent actual shapes of whole buds at slightly earlier ontogenetic stages.

The five zooecia measured (Figure 19, A–E) represent a sequence of ontogenetic stages at increasing distances proximally from the growing edge. These zooecia are members of two contiguous lineal series (A–C–E and B–D) and alternate in position. Differences in size and shape within each series and in the two series combined (Figures 18, 20; Table 10) can be expected to follow comparable sequences. Differences between these sequences are small and generally can be attributed to microenvironment.

From zooecium A to zooecium D, $F(1)'$ increases progressively, but not uniformly. Zooecium D (and possibly also zooecium B) is slightly larger for its ontogenetic stage than are C and E. As zooecia D and E both represent fully formed zooids, the difference in their size appears to be part of the general, microenvironmentally controlled fluctuation to be expected throughout the zone of astogenetic repetition. The similar difference between zooecia B and C, although these two represent slightly different ontogenetic stages, suggests that microenvironmental effects may have been similar within lineal series, but different between series. It also seems possible that the development of the transverse wall, which began to grow in zooid C at a stage just later than that represented by zooecium B, affected the size difference. Initially, growth of the transverse wall would have decreased the size of the zooid by partitioning off the distal part of the bud. With continued growth of this wall obliquely upward (stages represented by zooecia C to D), size would again have increased until, once the wall was fully developed (stages represented by zooecia D and E), there was no further increase in size.

For the most part, changes in $F(2)''$ parallel those in $F(1)'$, i.e., as buds became larger, they also became generally more elongate and distally in-
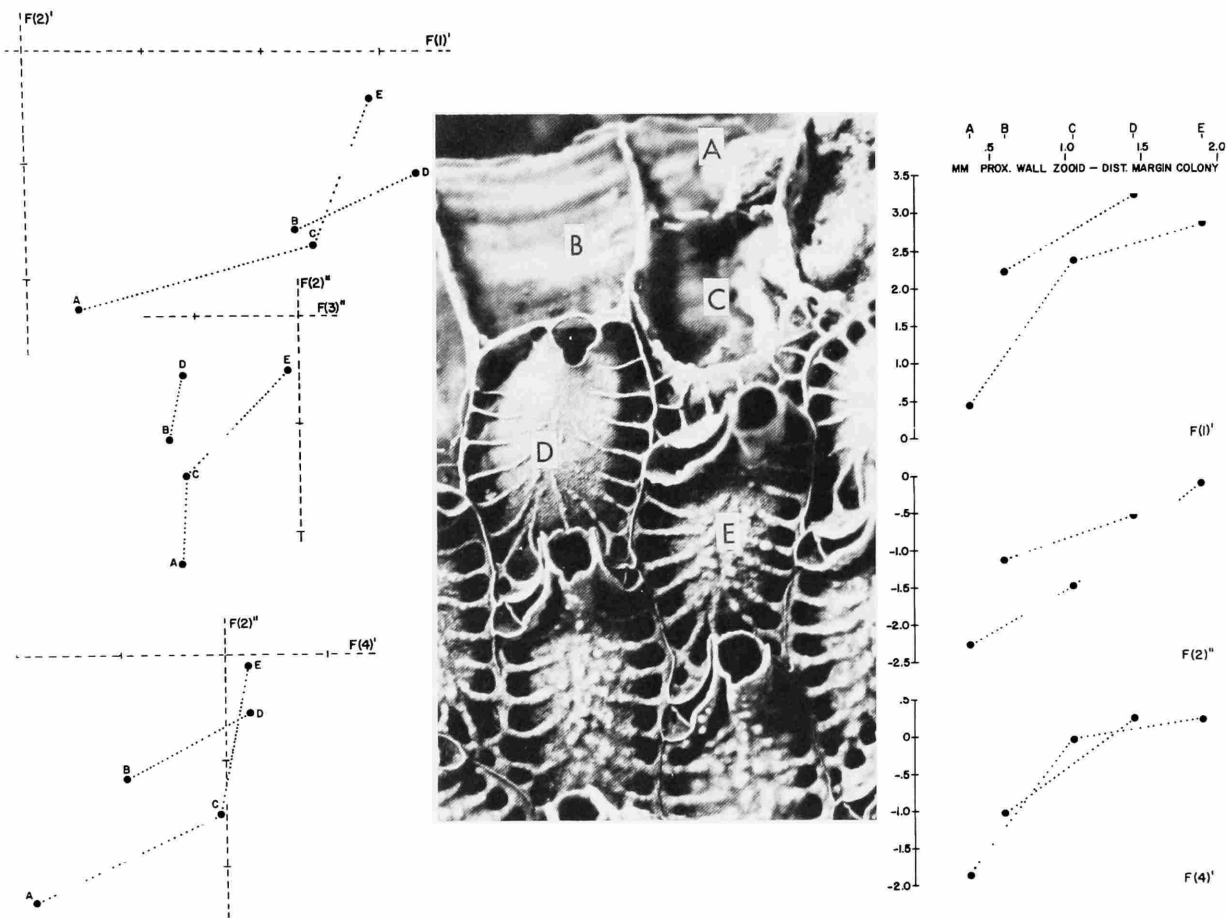
FIGURE 19.—Variation in size and shape of autozooecial outlines near growing edge of colony of *Metrarabdotos unguiculatum* Canu and Bassler (Appendix B, Id. no. 6). (Frontal view × 40.)

TABLE 10.—Changes in factors (Table 5) with increasing distance (in mm) from proximal wall of zooid to growing edge of colony for five autozooecial outlines in *Metrarabodotos unguiculatum* Canu and Bassler, Recent, Brazil, expressed as proportions of greatest difference measured

Factor	0.37 – 0.59	0.59 1.05	1.05 1.45	1.45 1.90
F(1)'....	+ 0.637	+ 0.054	+ 0.309	0.137
F(2)"....	+ 0.526	0.160	+ 0.432	+ 0.202
F(3)"....	0.173	+ 0.221	0.018	+ 0.798
F(4)'....	+ 0.401	+ 0.463	+ 0.136	0.000

flated. However, the rate of increase is reversed (Figure 20) near the middle of the sequence, resulting in a decrease in F (2)" between zooecia B and C, presumably as a result of the introduction of the transverse wall and of microenvironmental factors. One increase in F (2)" apparently not reflected by an increase in size is that between the proximal zooecia (D and E). This appears related
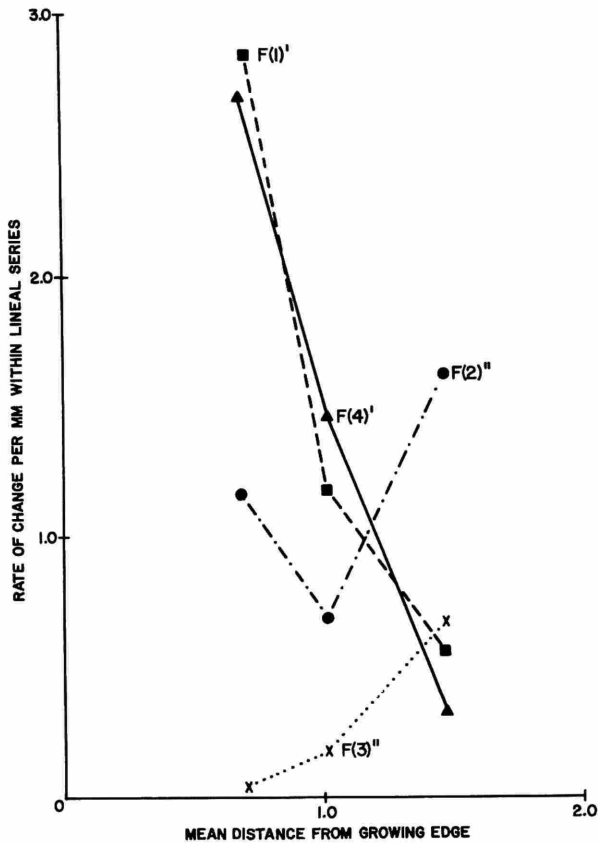
FIGURE 20.—Rates of change, in standardized units, in F(1)′ to F(4)′ between ontogenetic stages within lineal series represented by zooecia A to E of Figure 19. (Rate of change is the difference between contiguous zooids within series divided by the mean of their distance from growing edge (Table 10).)

to development of the peristome and avicularian rostrum which project slightly beyond the transverse wall.

Changes in F (3)″ from zooecium A to zooecium D appear to be minor fluctuations related to microenvironment. That between zooecium D and zooecium E, however, is larger and seems to have resulted from development of the peristome and avicularium, accentuating the slight initial asymmetry. The amount of asymmetry in fully developed zooecia is variable but generally low.

The uniformly progressive increase in F (4)′ from zooecium A to zooecium D seems to reflect that part of the gradient of increasing elongation least affected by microenvironmental "noise," although the rate of change within series is close to

that for F (1)′ (Figure 20). F (4)′ thus appears to be potentially the best indicator of ontogenetic change among the characters examined. In the plot of F (2)″ against F (4)′, most of the change is near the direction of ρ and approximately perpendicular to that of di.

In summary, the largest ontogenetic changes inferred for M. unguiculatum (Figure 20) are size increases, generally obvious and rapidly decelerating but slightly complicated by microenvironmental "noise," and variations in shape, expressed by that part of elongation contrasted with distal inflation and which are also large and rapidly decelerating; these form the smoothest gradient and reach the most characteristic completed state. Changes in asymmetry are small, the most important increase occurring late in ontogeny during development of the peristome and avicularium.

These ontogenetic changes were inferred from zooids within two and one-half to three lengths of the growing margin. In other colonies of this species, this interval can be observed to differ in length, probably under environmental as well as genetic control, but the pattern of changes is otherwise similar.

ASTOGENETIC VARIATION.—Astogenetic differences in size and shape of autozooids are generally less obvious than ontogenetic changes in these characters. In primary zones of astogenetic change a common pattern in cheilostomes is a general increase in average size for a variable number of asexual generations from the ancestrula. The astogenetic increase in size is generally accompanied by an increase in morphologic complexity, commonly including the introduction of polymorphism (Abbott, 1973). In Wilbertopora mutabilis Cheetham, the first five asexually produced generations of zooids have previously been recognized as belonging to the primary zone of astogenetic change, chiefly from the dimensions of the zooecia, although the first appearance of ovicelled zooecia in a colony coincides with the beginning of repetition of nonovicelled zooecial morphology. To illustrate astogenetic changes in factors F (1)′–F (4)′, we selected a specimen in which the ancestrula and the asexual generations succeeding it are readily identifiable and measured nonovicelled zooecia in the first seven generations (Figure 21, I–VII). The ancestrula was excluded from measurement because its growth directions cannot be expected to
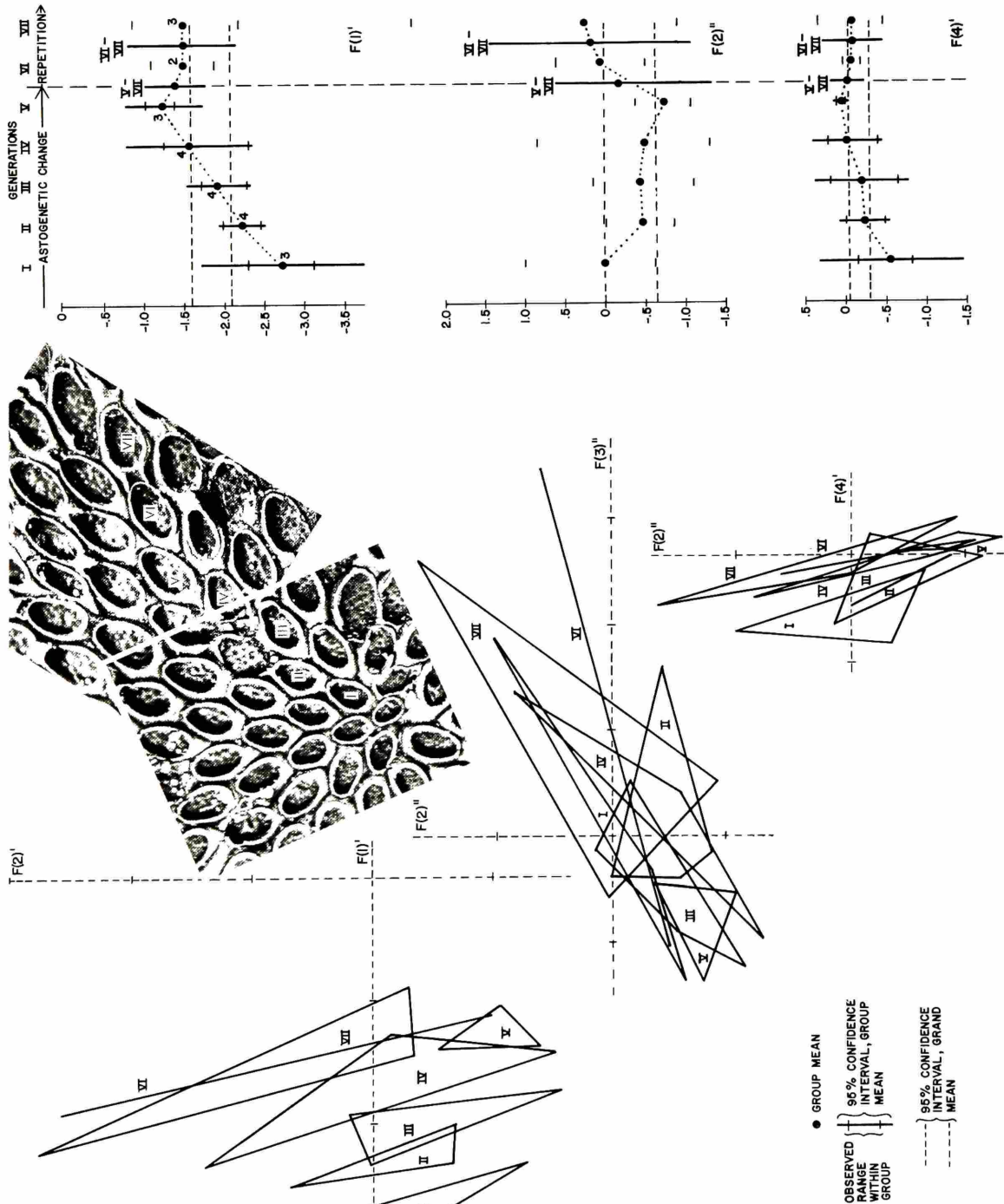
FIGURE 21.—Variation in size and shape of autozooecial outlines in first seven asexual generations in colony of *Wilbertopora mutabilis* Cheetham (Appendix B, Id. no. 30A). (Frontal view × 25.)

have conformed to those of the vector representation.

The plots of factors F (1)' to F (4)' for the seven generations examined (Figure 21) suggest an astogenetic gradient of increasing size and slightly increasing elongation from generation I to generation V, with generation VI forming the first repetition of size and shape, although with a wide range of variation. The great variability of size and particularly of shape within generations further suggests a high level of microenvironmental "noise" complicating the astogenetic pattern.

The high within-generation variability of this colony of *W. mutabilis* is indicated by the fact that fully one-half the within-generation variances exceed the 95 percent confidence intervals for within-colony variances for the general sample of cheilostomes (Table 9). Another one-third fall within the confidence intervals. Because this heterogeneity of within-generation variances is significant for all factors (Fmax test; Sokal and Rohlf, 1969), we have examined differences between generations entirely with nonparametric tests (Table 11). With the exception of F (1)', we found no significant differences, even though the pattern of changes of within-generation means in F (4)' is similar to that in F (1)' (Figure 21).

For F (1)', the uniformly progressive increase of within-generation means from generation I to generation V (Figure 21) is reflected in a significant overall difference between generations (Table 11). In no case, however, is the increase from one generation to that immediately succeeding it significant. Instead, significant increases skip one or two generations. After generation IV, no differences are significant.

In summary, the obvious astogenetic gradient in the colony of *W. mutabilis* is an increase in mean size distributed over the first five asexual generations, with no significant changes in shape. Variation within generations precludes significant size differences between contiguous generations.

POLYMORPHISM.—In addition to the obvious qualitative differences between polymorphic autozooids (e.g., presence or absence of ovicells), size and shape of autozooidal outlines can be expected to show discontinuous, but less obvious differences in correlation with qualitative characters. A well-

TABLE 11.—Variation in factors (Table 5) for 23 autozooecial outlines in first seven asexual generations of *Wilbertopora mutabilis* Cheetham, holotype, Albian, Ft. Worth Limestone, Krum, Texas (differences among all generations tested by Kruskal-Wallis method, those between successive generations by Mann-Whitney U-test)

Factor	*Variance*		*Differences between generations*						
	Total	Within generation	Generation	II	III	IV	V	VI	VII
F(1)'............	0.341	0.169	I	ns	*	**	**	**	**
		0.035	II		ns	ns	*	*	*
		0.064	III			ns	*	*	*
		0.244	IV				ns	ns	ns
		0.038	V					ns	ns
		0.298	VI						ns
		0.439	VII						
F(2)"............	0.555	0.121	(all differences ns)						
		1.710							
F(3)"............	1.715	0.264	(all differences ns)						
		10.404							
F(4)'............	0.095	0.001	(all differences ns)						
		0.168							

* significant, P < 0.05   ** significant, P < 0.01   ns not significant

known example is *Steganoporella magnilabris* (Busk), in which autozooids are dimorphic, one set (a-zooids) having opercula with the main sclerite inverted U- or V-shaped and the zooecium with a thin oral arch and a narrow postoral shelf, and the other set (b-zooids) having opercula with an inverted Y-shaped main sclerite, augmented opercular musculature, and the zooecium with a thickened oral arch and a broad postoral shelf (Harmer, 1900; Cook, 1964). The b-zooids in this species are reportedly usually larger than the a-zooids, although specimens have been described in which some a-zooids are longer than b-zooids (Cook, 1964).

To examine size and shape of outlines in dimorphic autozooids, we chose three modern colonies of *S. magnilabris* from Puerto Rico (Figure 22, A–C). In each colony, a- and b-zooids are distinguished by their opercula, oral arches, and postoral shelves. In two colonies (Figure 22, A, B), the budding pattern is regular; in the third (Figure 22, C), it had apparently been disrupted by breakage and subsequent regenerative budding. Morphologic differences between zooids in colony C on the one hand and colonies A and B on the other can thus be expected to relate in part to the environmental causes of budding pattern disruption, although such morphologic differences can include the genetic differences between colonies as well.

The plots of F (1)′ to F (4)′ for the three colonies (Figure 22) suggest that b-zooids are generally larger, more elongate, and more inflated distally than a-zooids, and that there is no systematic difference in the highly variable asymmetry of both dimorphs. For the two colonies having regular budding patterns, no overlap was observed between a- and b-zooids for F (1)′ or F (4)′, but overlap is considerable in F (2)″. Colony C, however, complicates these relationships so that the dimorphs, considered in all three colonies, overlap in all four factors. This seems to suggest that the function of dimorphism in this species was not related to space filling.

The variation in size and shape of each dimorph is quite large, and a considerable portion appears to be a morphologic effect of the disruption of the regular budding pattern. In the two colonies showing regular patterns, less than one-fourth of the within-dimorph, within-colony variances exceed

the 95 percent confidence intervals for within-colony variances for the general sample of cheilostomes (Table 9). In colony C, on the other hand, fully three-fourths of the variances exceed these intervals. The heterogeneity of variances in *S. magnilabris* is significant (Fmax test; Sokal and Rohlf, 1969) for F (3)″ and F (4)′, but not for F (1)′ and F (2)″. In keeping with these results, we examined the differences between dimorphs and among colonies with two different sets of tests (Tables 12, 13).

For F (1)′, the difference by which b-zooecia on the average exceed a-zooecia is significant. Differences between dimorphs are in the same direction and of about the same magnitude in all colonies, as indicated by the insignificant interaction between colonies and dimorphs (Table 12). Differences among colonies, however, are also significant, and for the zooecia measured account for most of the within-dimorph variance. Tests on colony means (Student-Newman-Keuls test, Sokal and Rohlf, 1969) reveal significant difference between colony C and the other colonies for b-zooecia but not for a-zooecia. Differences between colonies A and B are not significant. This suggests that variation in size associated with difference in budding pattern is accommodated principally by the b-zooids.

The only shape factor in which the difference between dimorphs is unequivocally significant is F (4)′. Differences among colonies are not significant, suggesting that this factor is less sensitive to disruption of the budding pattern than is size.

The difference between dimorphs in F (2)″, although barely significant, is not strong enough to yield a significant overall among-groups difference (Table 12). The difference between dimorphs in F (3)″ is not significant. For F (2)″, among-colonies variance is small and insignificant. That of F (3)″, however, is highly significant and again appears related to the difference in budding pattern and to have been felt more strongly by b-zooids.

In summary, a- and b-zooecia in the three colonies of *S. magnilabris* differ significantly but overlap in size and shape. On the average, b-zooecia exceed a-zooecia in size and in that part of elongation contrasted with distal inflation. Size and shape, especially asymmetry, of both dimorphs are highly variable in the colony in which the budding pattern is disrupted, and the b-zooids seem to have
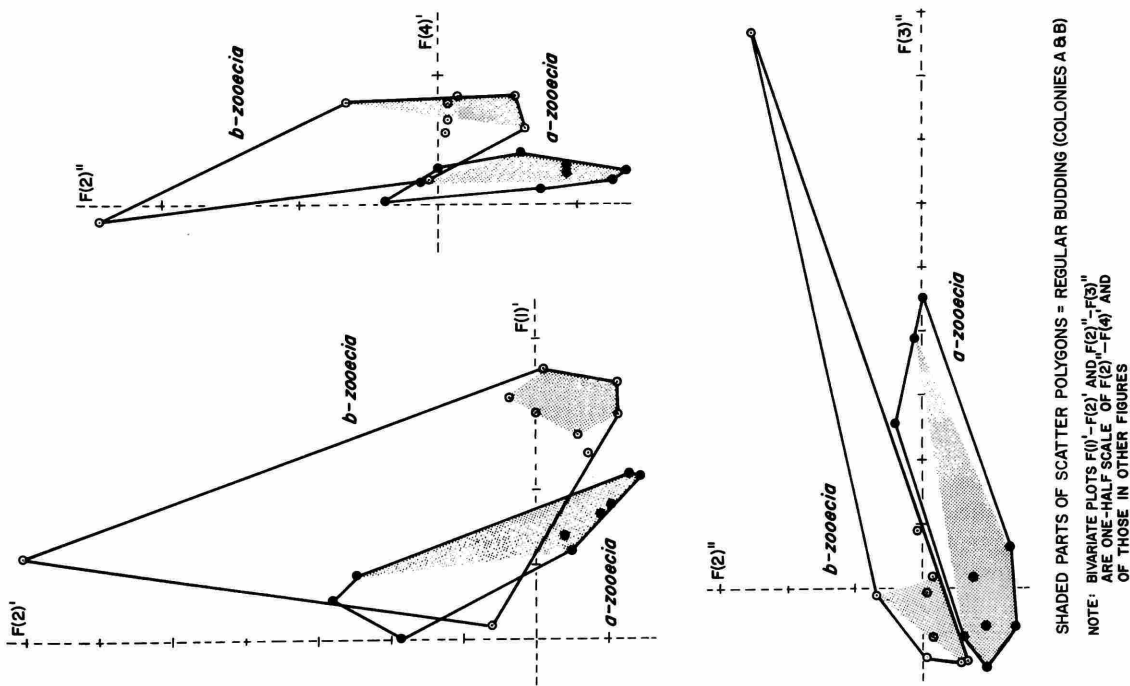
FIGURE 22.—Variation in size and shape of autozooecial outlines in three colonies of *Steganoporella magnilabris* (Busk) (Appendix B, Id. no. 12A–C). (Frontal views × 25; symbols, other than for a- and b-zooecia, as in Figure 21.)

TABLE 12.—Two-way (dimorphs vs. colonies) analysis of variance in factors F (1)′ and F (2)″ (Table 5) for 18 autozooecial outlines in *Steganoporella magnilabris* (Busk), three a-zooecia and and three b-zooecia measured in each of three colonies, Recent, Puerto Rico

Factor	Source of variation	Degrees of freedom	Sum of squares	Mean square	F ratio
F(1)′.......	Between dimorphs	1	6.682	6.682	15.610**
	Among colonies	2	8.574	4.287	10.015**
	Interaction	2	1.218	0.609	1.422 ns
	Within dimorphs,within colonies	12	5.137	0.428	
F(2)″.......	Between dimorphs	1	2.632	2.632	4.833*
	Among colonies	2	3.038	1.519	2.789 ns
	Interaction	2	0.361	0.180	0.330 ns
	Within dimorphs, within colonies	12	6.535	0.545	

* significant, P < 0.05, but overall anova not significant   ** significant, P < 0.01   ns not significant

TABLE 13.—Summary of variation in all factors (Table 5) for 18 autozooecial outlines in *Steganoporella magnilabris,* three a-zooecia and three b-zooecia in each of three colonies (variance components for F(1)′ and F(2)″ based on two way analysis of variance (Table 12); variation in F(3)″ and F(4)′ tested by Kruskal-Wallis method)

Factor	Difference between dimorphs	Variance within dimorphs			
		Variance	Among-colonies proportion	Within-colony proportion	Interaction proportion
F(1)′.......	**	1.124	0.572	0.381	0.047
F(2)″.......	+	0.707	0.230	0.770	0.000

Factor	Difference between dimorphs	Mean variance within dimorphs	Difference between colonies
F(3)″.......	ns	7.159	**
F(4)′.......	*	0.047	ns

* significant, P < 0.05   ** significant, P < 0.01   ns not significant   + see Table 12

been more sensitive to this disturbance than the a-zooids.

MICROENVIRONMENTAL VARIATION.—In all the foregoing examples, outlines of autozooecia measured within the same zoarial fragment and inferred to be in the same condition of ontogeny, astogeny, and polymorphism were found to vary in size and in all aspects of shape. This variation is ascribed to microenvironment (Boardman et al., 1970) on the assumption of genetic uniformity throughout a colony.

Microenvironmental variation, as measured by

within-colony variances, is itself variable among the specimens and characters examined. Two colonies can show different amounts of microenvironmental variation because of differences in the sets of microenvironmental conditions each experienced and/or differences in the latitudes of phenotypic variation permitted by each genotype. These sources (compare with the "nongenetic (microenvironmental)" effect and "nongenetic-genetic" interaction term of Farmer and Rowell, 1973) apply to differences between colonies, whereas variations within a colony all must have
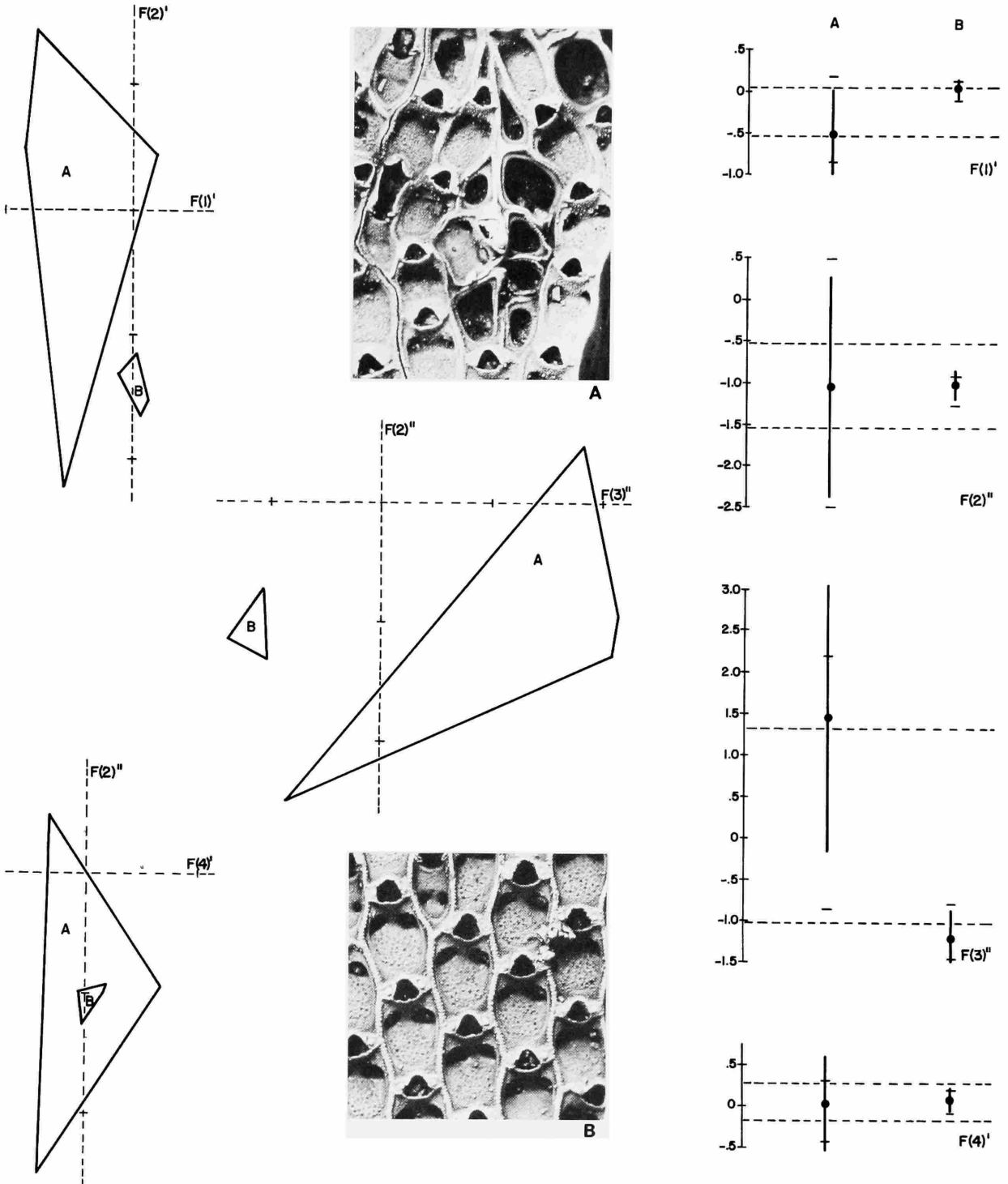
FIGURE 23.—Variation in size and shape of autozooecial outlines in two zoarial fragments of *Thalamoporella biperforata* Canu and Bassler (Appendix B, Id. no. 8A–B). (Frontal views × 25; symbols as in Figure 21.)

resulted from the different microenvironmental conditions experienced by that colony, if its zooids are genetically uniform. It is thus possible to state that the microenvironmental variation in one colony is greater than that in another, whether the sets of microenvironmental conditions under which the two colony variances developed were different or the same. In some cases at least, it is further possible to infer that the sets of microenvironmental conditions encountered by different colonies differed in one or more factors such as crowding, substrate irregularity, injury, etc. (Abbott, 1973). Then, the difference between colony variances, and that between colony means, is very likely to reflect further environmental modification as well as the genetic difference in latitudes of phenotypic variation permitted by different genotypes.

Comparison of two zoarial fragments of *Thalamoporella biperforata* Canu and Bassler from the same Miocene locality suggests the relative effects of environmental modification of size and the three aspects of shape expressed by factors $F(1)'$ to $F(4)'$. In one specimen (Figure 23, A), an irregular budding pattern apparently resulted from crowding of several divergent lineal series into fewer, convergent ones. In the other (Figure 23, B), the regular budding pattern indicates absence of crowding.

Differences in the amount of variation in size and all aspects of shape are immediately suggested in the plots of $F(1)'$ to $F(4)'$, and their significance is substantiated by Fmax test (Table 14; Sokal and Rohlf, 1969). The differences between the values of the factors in the two specimens, however, are not significant, except for $F(3)''$. Thus, the inferred difference in the sets of microenvironmental conditions which acted on the colonies represented by these specimens is significantly reflected in size, elongation, and distal inflation of autozooecial outlines by modification of the amount of variation, but not of the within-colony mean. For $F(3)''$, modification of the mean as well as the variance was expected from the interdependence of these two parameters as noted above.

INTRAPOPULATION VARIATION.—To estimate the variability of size and shape of autozooecial outlines in a fossil population, we selected six zoarial fragments of *Coscinopleura angusta* Berthelsen (Figure 24, A–F) from a single mound in the Danian of southern Sweden. (Evidence suggesting that sediments in this mound incorporate bryozoans and other biotic remains approximately where the organisms grew has been summarized by Cheetham, 1971.) Measurements on these specimens were restricted to nonovicelled autozooecia, and generational differences were not apparent in any of the specimens studied. Although ontogenetic differences are evident between zoarial fragments in the thickness of the cryptocyst (Figure 24, A, D, and E vs. B, C, and F), we did not discern an ontogenetic gradient for the autozooecial outlines measured, either within or between specimens. (Zoarial fragment A, Figure 24, includes at its distal end a preserved growing edge, at which occur several zooecia with partly formed cryptocysts. These zooecia were not included in this examination of autozooecial shape.)

The plots of factors $F(1)'$ to $F(4)'$ for the six zoarial fragments (Figure 24) suggest a greater

TABLE 14.—Comparison of variation in factors (Table 5) for five autozooecial outlines measured in each of two colonies of *Thalamoporella biperforata* Canu and Bassler, Miocene, Cercado de Mao, Dominican Republic (colony A = budding pattern disturbed; colony B = budding pattern regular)

Factor	Within-colony variances		Fmax test between variances	Mann-Whitney U-test between colonies
	Colony A	Colony B		
$F(1)'$...	0.164	0.008	*	ns
$F(2)''$...	1.130	0.020	**	ns
$F(3)''$...	1.689	0.064	*	*
$F(4)'$...	0.210	0.014	*	ns

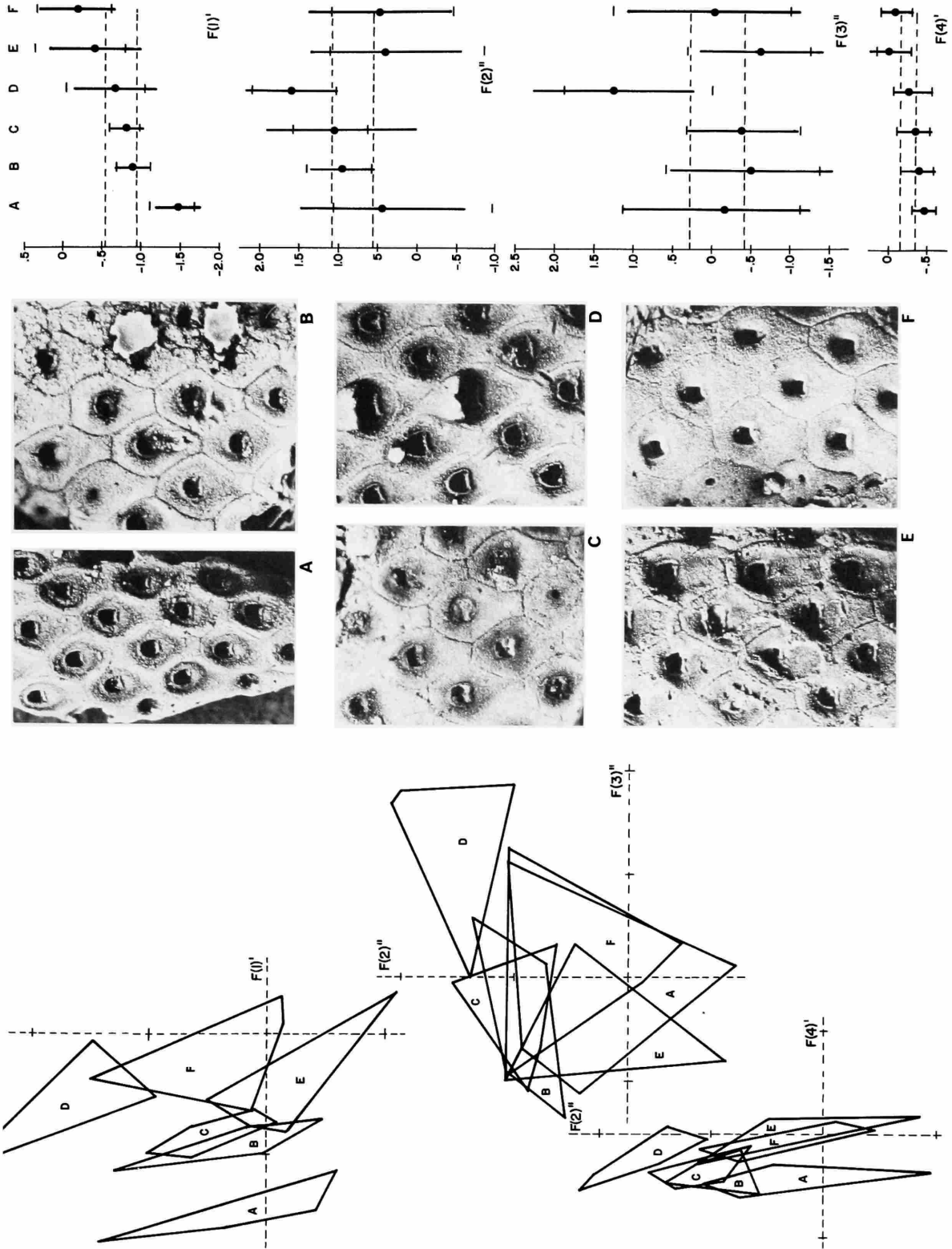* significant, $P < 0.05$ ** significant, $P < 0.01$ ns not significant

FIGURE 24.—Variation in size and shape of autozooecial outlines in six zoarial fragments of *Coscinopleura angusta* Berthelsen (Appendix B, Id. no. 29A–F). (Forntal views × 25: symbols as in Figure 21.)

variability of shape than of size both within colonies and for the group of zoarial fragments as a whole. In keeping with the results from the foregoing principal components analysis, most of the shape variation is accounted for by asymmetry.

The within-colony variances in this sample are entirely consistent with those of the wide range of species previously examined, as a comparison of their 95 percent confidence intervals (confirmed by F-tests) in Tables 9, 16, and 17 reveals. In the absence of significant heterogeneity of within-colony variances (Fmax test; Sokal and Rohlf, 1969), we examined variation in all factors with analysis of variance. Log transformation was used for $F(3)''$ in which plots against rankits (Sokal and Rohlf, 1969) suggested a consistent skewness to the right, in keeping with the expected non-normality of the asymmetry measures used, as dis-

cussed above. A lesser suggestion of right skewness in the plot against rankits for $F(1)'$ was not substantiated by the Kolmogorov-Smirnov test (Sokal and Rohlf, 1969). Therefore we used no further transformation on this factor.

Although all factors but $F(3)''$ yielded significant among-colonies differences (Table 15), $F(1)'$ is the only one which yielded a higher proportion of among-colonies than within-colonies variance (Table 16). It might then be expected that several of the specimens have significantly different mean values of $F(1)'$. Student-Newman-Keuls tests (Sokal and Rohlf, 1969) yielded few significant differences among the six means, however. Specimen A has significantly smaller autozooecia than all other specimens, although the difference between the mean of this specimen and the grand mean for the sample (Figure 24) is a small part of the total

TABLE 15.—Single-classification analysis of variance in factors (Table 5) for 30 autozooecial outlines in *Coscinopleura angusta* Berthelsen, Danian, Limhamn, Sweden, five autozooecia measured in each of six colonies.

Factor	Source of variation	Degrees of freedom	Sum of squares	Mean square	F ratio
$F(1)'$..............	Among colonies	5	4.850	0.970	9.062**
	Within colonies	24	2.569	0.107	
$F(2)''$..............	Among colonies	5	5.490	1.098	2.932*
	Within colonies	24	8.987	0.374	
$F(3)''+$.............	Among colonies	5	1.094	0.219	2.281 ns
	Within colonies	24	2.301	0.096	
$F(4)'$..............	Among colonies	5	0.821	0.164	4.977**
	Within colonies	24	0.791	0.033	

* significant, P < 0.05   ** significant, P < 0.01   ns not significant   + log transformation

TABLE 16.—Components of variance in factors (Table 5) estimated by single-classification analysis of variance (Table 15) of 30 autozooecial outlines in *Coscinopleura angusta*

Factor	Total variance	Among colonies		Within colonies		Proportions	
		Variance	95% conf. int.	Variance	95% conf. int.	Among	Within
$F(1)'$........	0.280	0.173	0.047-1.145	0.107	0.064-0.156	0.617	0.383
$F(2)''$........	0.519	0.145	0 -1.024	0.374	0.223-0.702	0.279	0.721
$F(3)''*$.......	0.949	0.354	0.038-2.720	0.595	0.354-1.116	0.204	0.796
$F(4)'$........	0.059	0.026	0.005-0.189	0.033	0.020-0.062	0.446	0.554

* partitioned from log transformation

range in mean size for all cheilostomes examined (Figure 28). The one other significant difference between within-colony means does not change the generally overlapping relationship among the other five specimens, i.e., most of the zoarial fragments do not differ appreciably in mean size of autozooecial outlines.

Although among-colonies variation in both F (2)″ and F (4)′ is significant, none of the six zoarial fragments examined differs in these factors from all others. In F (2)″, there are no significant differences among the six zoarial fragments.

In F (3)″, zoarial fragment D is significantly more asymmetrical than any of the others, which do not differ significantly among themselves. The overall difference among all six zoarial fragments is not significant, as noted previously. The high asymmetry of zoarial fragment D appears to be related to the general obliquity of budding direction (Figure 24, D).

In summary, the six specimens of *C. angusta* studied suggest that intrapopulation variation among colonies in size and shape of autozooecial outlines is small, although significant for all properties but asymmetry. The low within-colony variation in size and the part of elongation contrasted with distal inflation makes these two properties appear particularly significant for characterizing population morphology as a basis for taxonomic interpretation.

Taxonomic Implications of Properties of Outline

The variation of autozooecial outlines in the wide range of cheilostomes examined greatly exceeds that in the sample of *Coscinopleura angusta* for size and all aspects of shape (Figure 25). Among-colonies variances for all factors except F (3)″ are significantly less in *C. angusta* than in the multispecies sample (Table 17). All factors, with the possible exception of asymmetry, then, seem potentially useful as bases for taxonomic interpretation of cheilostome morphology. Differences in the proportions of within-colony variance (primarily microenvironmental "noise") among zooids inferred to be in the same condition of ontogeny, astogeny, and polymorphism affect the efficiency of the four factors to different degrees. Ontogeny, astogeny, and polymorphism can further affect taxonomic interpretations if their effects

are not separable from those of microenvironment, although in most cases these kinds of variation should be easily recognizable. Some assessment of these factors in taxonomic discrimination of cheilostomes can be inferred from the foregoing analyses.

SUMMARY OF CHARACTERS.—From estimates of intrapopulation variation in *Coscinopleura angusta,* whose within-colony component is close to that for most of the wide range of cheilostomes examined (see above), the average minimum recognizable taxonomic difference can be calculated for size and each aspect of shape (Table 18). We have based this calculation on the interpretation of the 75 percent rule of Mayr et al. (1953), assuming normal distributions within populations. (Contraindication of normality for F (3)″ discussed above precludes use of the value calculated for this factor for any purpose but comparison with the other factors.)

From the average minimum recognizable taxonomic difference so calculated, it is further possible to calculate the minimum number of measurements needed to detect a difference this small (Sokal and Rohlf, 1969). Calculations were made for the number of zooecia per colony needed to distinguish between two colonies and the number of colonies per population needed to distinguish between two populations (Table 18). Although graphic comparison shows the minimum taxonomic difference for every factor to be exceeded by
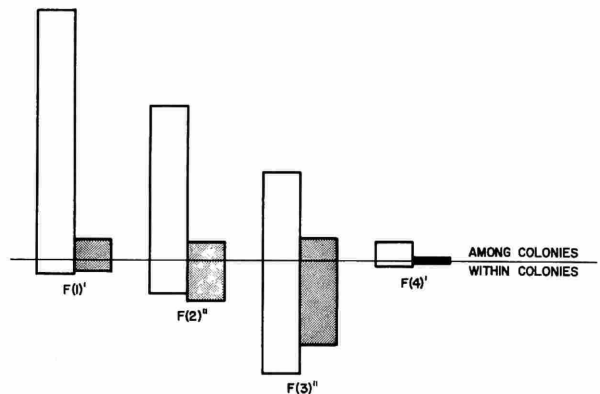

FIGURE 25.—Comparison of proportional differences in variances of F(1)′ to F(4)′ within and among colonies in 31 zoarial fragments of a wide range of cheilostome species (unshaded) and in six zoarial fragments of *Coscinopleura angusta* Berthelsen (shaded).

TABLE 17.—Comparison of variance (F-test) of 31 colonies in multispecies sample (Table 9) with those of six colonies of *Coscinopleura angusta* (Table 16)

Factor	Among-colonies variance			Within-colony variance		
	Multispp.	*C. angusta*	*Diff.*	*Multispp.*	*C. angusta*	*Diff.*
F(1)'..	2.225	0.173	**	0.122	0.107	ns
F(2)"..	1.369	0.145	**	0.311	0.374	ns
F(3)"..	0.729	0.354	ns	0.914	0.595	ns
F(4)'..	0.153	0.026	*	0.046	0.033	ns

* significant, P < 0.05   ** significant, P < 0.01   ns not significant

the expected range of variation within a colony (Figure 26), it is noteworthy that the numbers of measurements needed to detect these differences are quite small and on the average about the same as used in this study.

Because of their small within-colony variances, F(1)' (size) and F(4)' (part of elongation contrasted with distal inflation) appear to express potentially taxonomically important characters that can be distinguished with the greatest efficiency, i.e., in the greatest number of intervals with the fewest measurements per colony.

The relationships between the intervals of minimum taxonomic difference and the effects of ontogeny, astogeny, and polymorphism also appear to differ for size and the three aspects of shape (Figure 27). The maximum difference in each factor

except F(3)" with distance from the growing edge of the colony in *Metrarabdotos unguiculatum* is, in general, greater than the minimum taxonomic difference. The maximum difference between generation means in the zone of astogenetic change in *Wilbertopora mutabilis* barely exceeds the minimum taxonomic difference for F(1)' and is not significant for other factors. Finally, the average difference between dimorphic autozooids in *Steganoporella magnilabris* is less than the minimum taxonomic difference for F(1)' and F(4)', and not significant for other factors; moreover, with disruption of the budding pattern, size and shape of the more specialized set of autozooids are more obviously affected, leaving the ordinary autozooids relatively unmodified. These relationships suggest that ontogenetic differences can be expected to

TABLE 18.—Intervals of minimum taxonomic difference recognizable in observed ranges of colony means and minimum numbers of zooecia per colony and of colonies per population to detect that difference with 95 percent certainty (factors as in Table 5; observed ranges and taxonomic differences in standardized units; millimeter equivalents for F(1)' in parentheses; calculations based on within-colony estimates from Table 9 and within-population estimates from Table 16)

Factor	Observed range of within-colony means	Minimum taxonomic difference *	No. intervals distinguished within observed range	Minimum no. of replications needed to detect min. diff.	
				No. zooecia/colony	No. colonies/population
F(1)'........	6.057	1.354	4.5	3	4
	(0.36)	(0.08)			
F(2)"........	4.941	1.846	2.7	4	3
F(3)"........	4.064	2.493**	1.6	6	3
F(4)'........	2.021	0.622	3.3	5	3

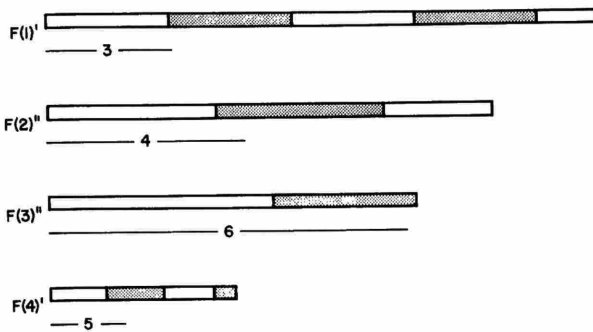* 2.56 times estimated average standard deviation of population   ** condition of normality not met

FIGURE 26.—Comparison of distribution of variation in F(1)′ to F(4)′ in all specimens studied (Appendix B). (Horizontal bars are observed ranges of within-colony means divided into intervals representing minimum recognizable taxonomic difference (see Table 18). Horizontal lines are average 95 percent ranges of variation within colonies, with minimum numbers of measurements per colony needed to detect average difference between intervals (Table 18).)
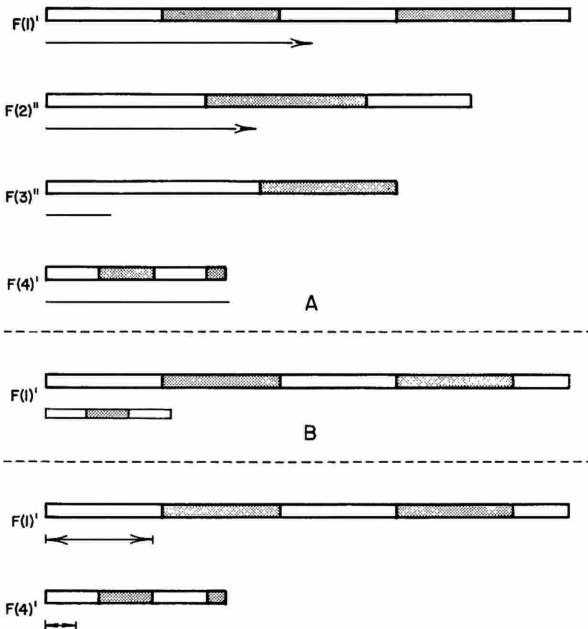

FIGURE 27.—Comparison of distribution of variation in all specimens studied (shown by horizontal bars as in Figure 26) to that in selected specimens illustrating within-colony sources of variation: *a,* maximum observed difference between zooecia at growing edge and more proximal ones in colony of *Metrarabdotos unguiculatum* (Figure 20); *b,* average difference between means of successive asexual generations in primary zone of astogenetic change in colony of *Wilbertopora mutabilis* (Figure 21); differences in factors other than F(1)′ not significant; *c,* average difference between means of a- and b-zooecia in three colonies of *Steganoporella magnilabris* (Figure 22); differences in F(2)″ and F(3)″ not significant.

have the most pronounced effects on F(1)′ and F(4)′, the two factors with the greatest inferred taxonomic potential. It is thus very important to make every effort to recognize ontogenetic differences, and this is generally easy to do from the development of frontal structures, etc. Because of their magnitude, ontogenetic differences in F(1)′ and F(4)′ can be expected to be obvious, and, because of the manner of growth of the outline, these differences can be expected to lose their significance for autozooidal outlines not in the vicinity of the growing edge of the colony. Astogeny and autozooidal polymorphism in the examples studied seem to be of generally smaller magnitude, about on the same order as the microenvironmental "noise" expected within colonies (95 percent ranges of variation, Figure 26) and thus not very important as possible sources of confusion with taxonomic differences.

For F(1)′, it is possible to compare the average minimum recognizable taxonomic difference with the precision with which the within-colony mean can be estimated. The principal source of "error" (Table 19) is the confidence interval for the mean, which is about three times as large as the next most important source, the distortion of the principal components representation. These two sources of "error" of course are not unique to the methods of measurement and characterization of the outline employed here. The distortion due to the vector representation and the error of measurement together are less than the principal components distortion and much less than the confidence interval for the mean. The cumulative effect of all of these sources of "error" at a maximum is about the same in magnitude as the minimum taxonomic difference. On the average, the "error" would not be expected to mask important taxonomic distinctions in size. There is no reason to believe that "error" in the important shape variables would differ in kind from that in size.

PRELIMINARY EVALUATION OF CHARACTERS WITHIN TAXA.—The taxonomic significance of size and shape of autozooid outlines in cheilostomes ultimately depends on how consistent these characters are among colonies within taxa. Such taxa should, of course, be based on all available independent morphologic characters that are likely to reflect genetic differences correlated with patterns of distribution in time and space. The data examined

TABLE 19.—Precision of representation of mean autozooecial size within colonies through vector measurements, calculation of area, representation by factor F(1)', and calculation of colony mean

Source of variation or error	Amount (mm)
Error of measurement from photograph (twice average standard deviation from Table 1)	0.009
Maximum distortion of vector representation (mean for colony with most distorted outlines, Fig. 7)	0.006
Maximum distortion of rotated 4-component representation (from Fig. 14)	0.017
Total error and distortion	0.032
95 percent confidence interval for average colony mean (n=5)	0.052

here were not intended to suggest a classification based on autozooidal outlines but to test whether aspects of size and shape can be expected to be generally consistent within taxa. These data suggest that size and aspects of shape expressed by elongation and distal inflation are generally consistent within species and even higher taxa, although there are exceptions in some taxa.

Division of the F (1)', F (2)", and F (4)' axes into intervals of minimum taxonomic significance (Figures 28, 29) suggests that minimally overlapping groups of colonies having autozooidal outlines of similar size and shape can be recognized. To explore this possibility among the range of outlines studied, we arranged all of the specimens listed in Appendix B in a series of dendrograms (Figures 30, 31) based on different combinations of the four factors, weighted according to their total variances. It must be emphasized that these dendrograms, based as they are on characters of the autozooidal outline only, cannot be expected to reproduce an arrangement based on characters from the whole morphology. The placement in these dendrograms of specimens inferred to be conspecific or congeneric on the basis of characters from the whole morphology can suggest how important taxonomically the characters of the outline might be.

The scattered distribution of conspecific specimens in Figure 30a (note especially *Coscinopleura angusta*, 29A–F), based on all four factors, is principally the result of the high variability in asymmetry. With F (3)" removed (Figure 30b), conspecific specimens are less scattered. With only

F (1)' and F (4)' included (Figure 31b) taxonomically related specimens generally cluster close together (see especially Poricellariidae, 21, 26, 31). However, in some species (e.g., *Thalamoporella biperforata*, 8A, B) colonies seem to cluster more closely with just F (2)" and F (4)' considered (Figure 31a) than they do with F (1)' included. This suggests that, although the combination of size and the aspect of shape contrasting elongation with distal inflation yields generally consistent taxonomic groupings, some taxa are distinctly heterogeneous with respect to this combination of characters. This does not diminish the importance of these characters, however, in contrasting the combinations of states in different taxa.

Average among-colonies differences in outlines within taxa, for which this study provided preliminary data, are summarized in Figure 32. Within the species examined, most combinations of factors, except that including asymmetry (Figure 32c), tend to give small differences, below the level of minimum taxonomic difference. Either shape (*Wilbertopora mutabilis*, Figure 32a, a) or size (*Metrarabdotos unguiculatum*, Figure 32e, e), however, may exceed the level of minimum taxonomic difference within a species. (The size difference in *M. unguiculatum* has previously been interpreted as a taxonomic difference by Osburn, 1952, and Cheetham, 1968a.) The combination of F (1)' and F (4)' seems to provide the most consistent characterization of all species considered.

Within the few genera for which among-colonies differences in outline have been estimated, size
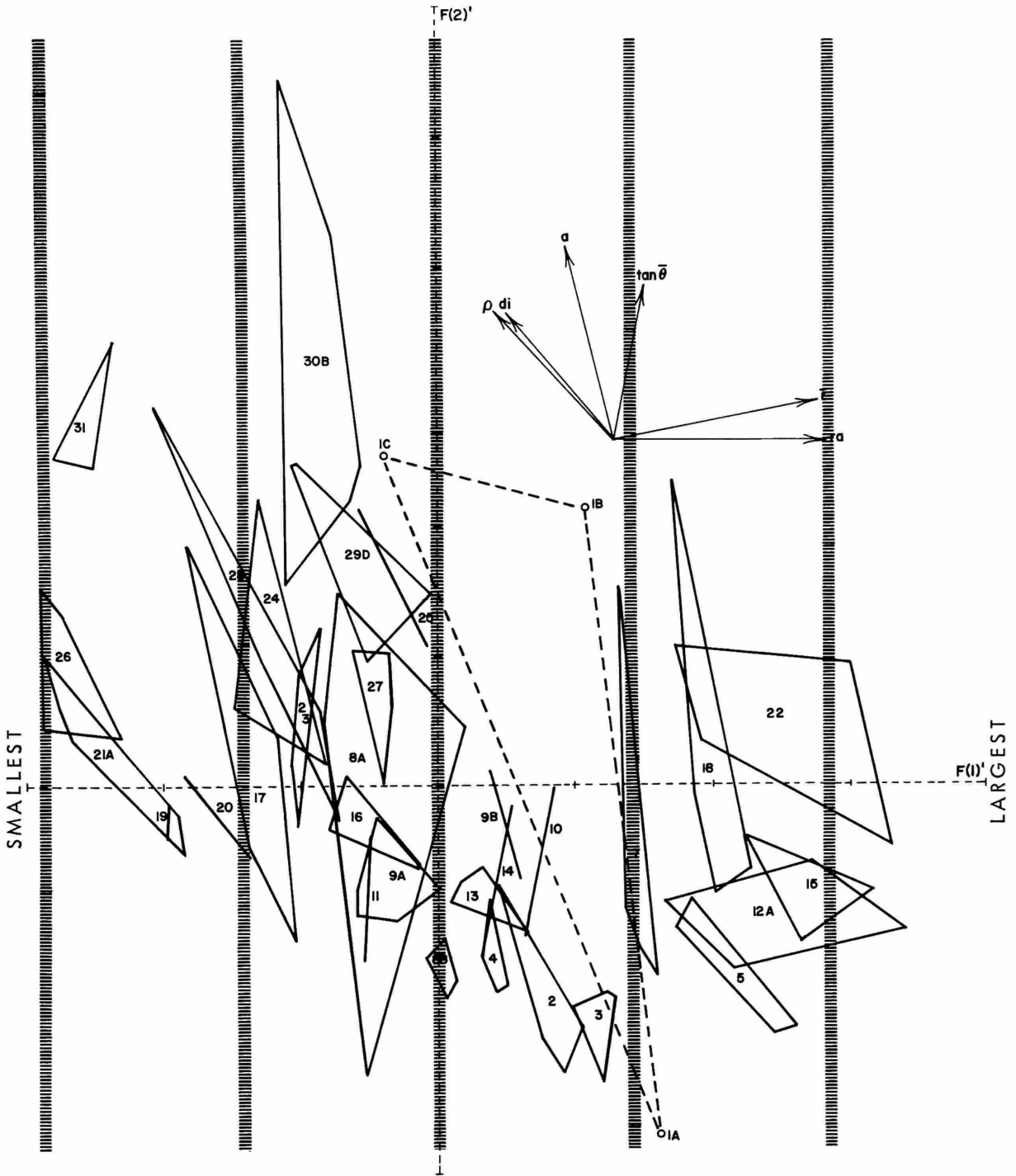
FIGURE 28.—Intervals of minimum taxonomic difference between within-colony means for F(1)′ (Figure 26) superposed on plot of F(1)′ vs. F(2)′ for 32 zoarial fragments (Figure 12).
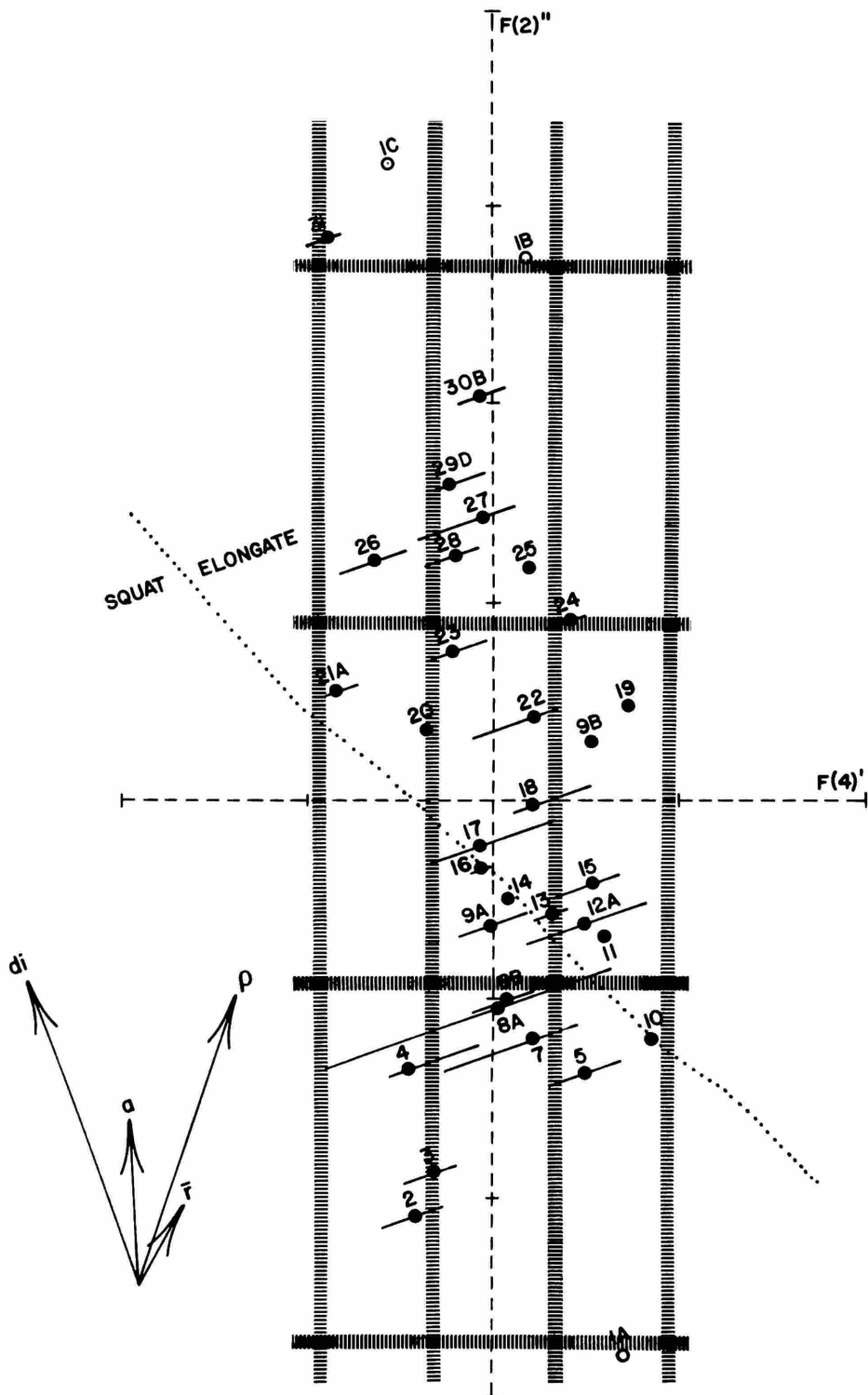
FIGURE 29.—Intervals of minimum taxonomic difference between within-colony means for F(2)″ vs. F(4)′ (Figure 26) superposed on plot of F(2)″ vs. F(4)′ for 32 zoarial fragments (Figure 17A).
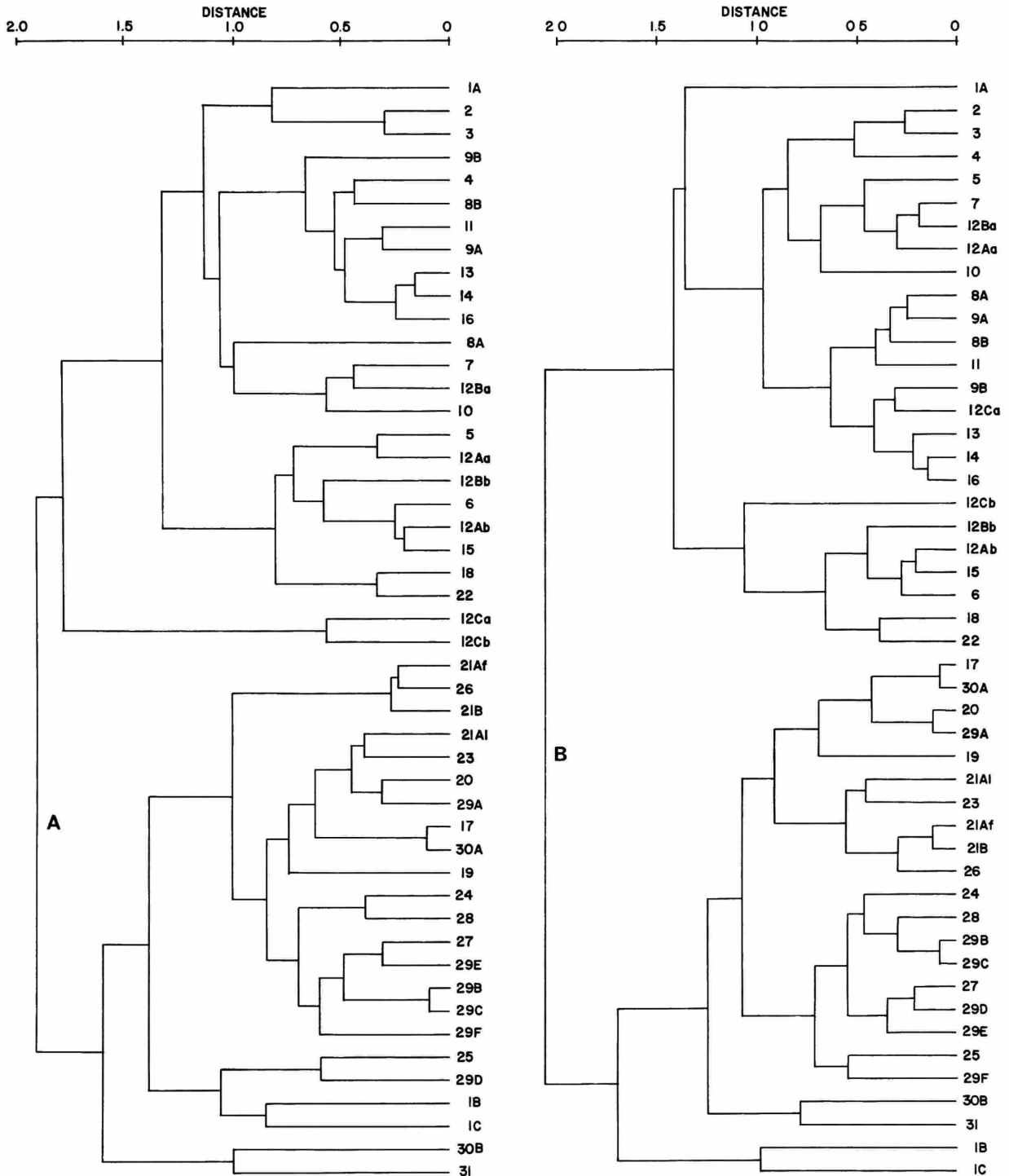
FIGURE 30.—Dendrograms of 48 groups of zooecia (Appendix B) based on factors expressing properties of autozooidal outlines: *a*, dendrogram based on all four factors, F(1)′–F(4)′; *b*, dendrogram based on factors F(1)′, F(2)″, and F(4)′. (Average taxonomic distances between colony means clustered by unweighted pair-group method using arithmetic averages, Sneath and Sokal, 1973.)
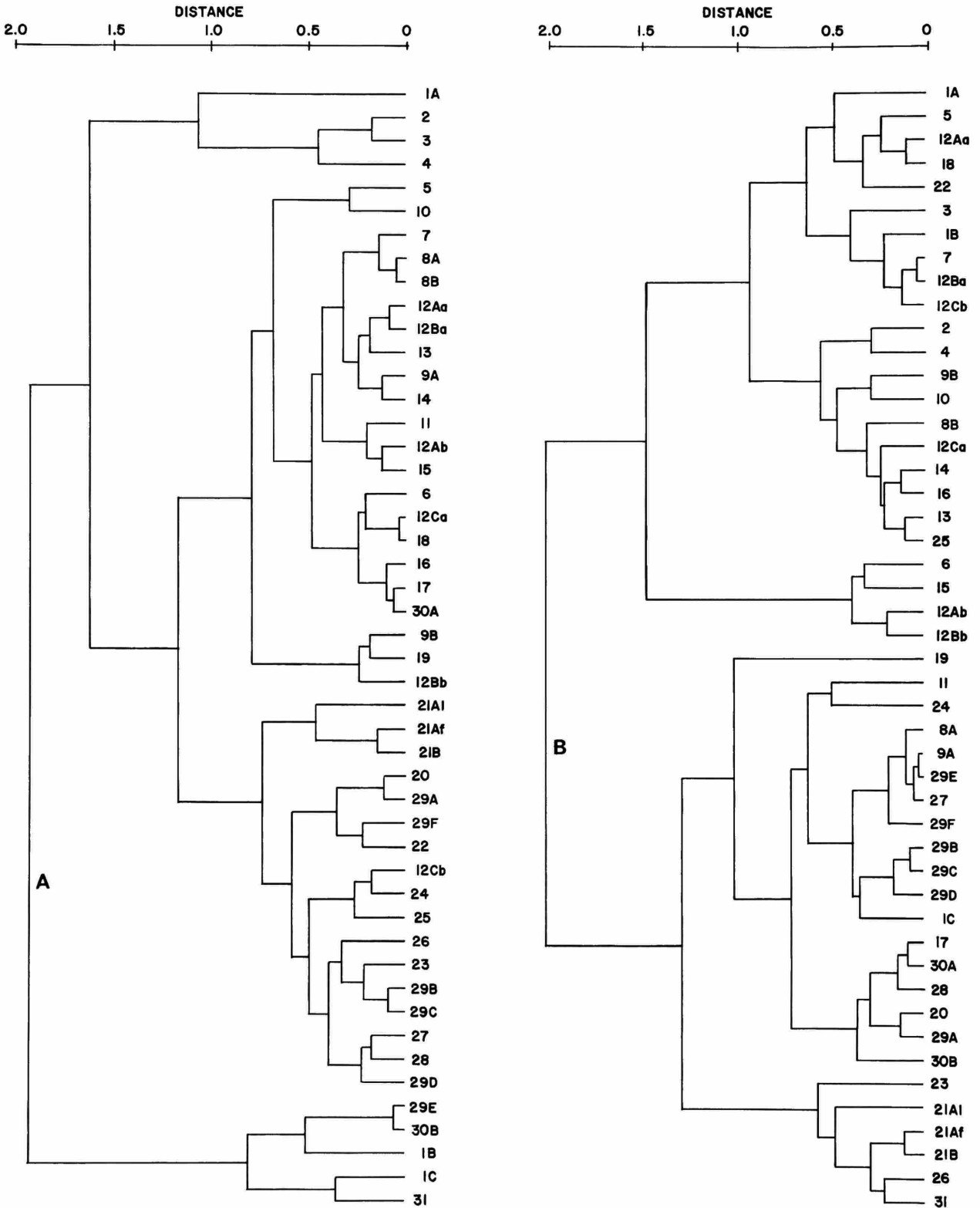
FIGURE 31.—Dendrograms of 48 groups of zooecia as in Figure 30: *a*, dendrogram based on factors F(2)″ and F(4)′; *b*, dendrogram based on factors F(1)′ and F(4)′.

(Figure 32e) apparently is less consistent than within species, but shape (Figure 32a), including F (2)″ and F (4)′, seems consistent enough to characterize taxa at this level. Within one genus, *Diplodidymia* (Figure 32, 1), and the family to which it belongs, Poricellariidae (Figure 32, i), both size and shape appear consistent enough to warrant retention as taxonomic characters at these higher levels in a polythetic classification.

Summary and Conclusions

The sizes and shapes of frontal outlines of cheilostome autozooids are so highly variable both within and among colonies of the same taxa that their use to characterize and distinguish taxa has been a matter of some controversy. However, various aspects of size and shape can be quantified, and the derived coefficients then statistically evaluated for taxonomically significant patterns of variation.

Our approach has been to try to reduce operational bias by treating the frontal outline as "a vector diagram of its own growth" (Thompson, 1942). Such a representational system of outline geometry has at least two important advantages over other measurement systems. First, it is designed to represent as closely as possible the directional components of cheilostome zooidal growth. Consequently, the vectors relate morphology directly to a functionally important biological process (growth), a desirable property of any biometric measurement. A second advantage is that the growth-vector system requires but a single pair of morphologically corresponding points (the points of budding) and

directions (the principal growth directions) between zooids. Other commonly used measurements normally assume at least two pairs of corresponding points for each measured character. Such assumptions increase the chances for both operator bias and biologically meaningless variation introduced by the measurement system itself; hence the growth-vector representation of zooidal outline al-
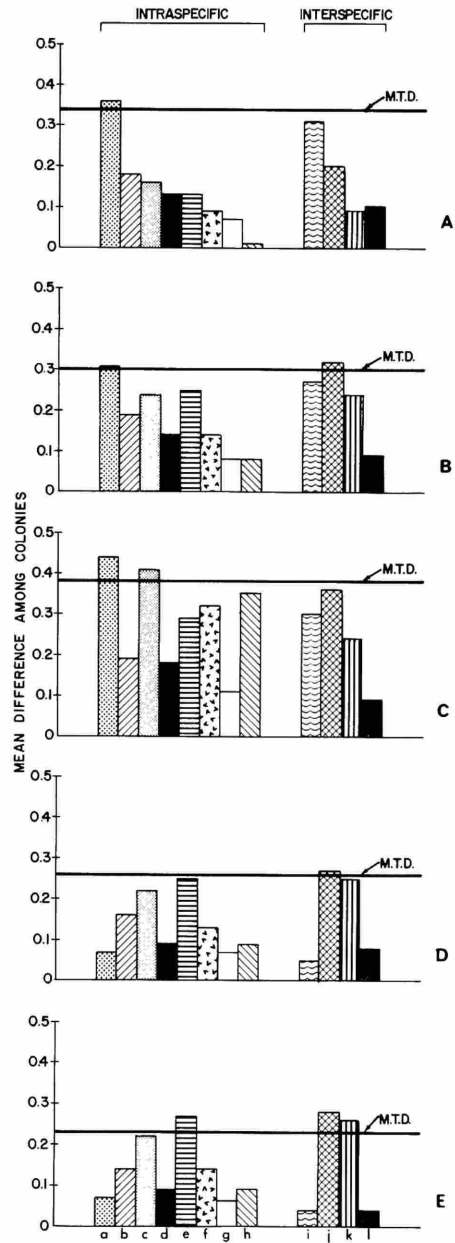
FIGURE 32.—Mean differences among colonies within taxa for various combinations of factors of autozooidal outlines: *a*, F(2)″ and F(4)′; *b*, F(1)′, F(2)″, and F(4)′; *c*, F(1)′–F(4)′; *d*, F(1)′ and F(4)′; *e*, F(1)′ alone. (Means of the average taxonomic differences, Sneath and Sokal, 1973, between colonies and the calculated minimum taxonomic difference, M.T.D., Table 18, have been normalized to the greatest observed difference among colony means for each combination of factors; bars entirely below M.T.D. level, especially where that level is low, suggest consistency of a combination of factors within a taxon. a = *Wilbertopora mutabilis* (30A, B); b = *Metrarabdotos helveticum* (9A, B); c = *Steganoporella magnilabris*, b-zooecia (12A–C); d = *Coscinopleura angusta* (29A–F); e = *Metrarabdotos unguiculatum* (6, 7); f = *Steganoporella magnilabris*, a-zooecia (12A–C); g = *Diplodidymia ratoniensis* (21A, B); h = *Thalamoporella biperforata* (8A, B); i = Poricellariidae (21, 26, 31); j = *Metrarabdotos* (6, 7, 9, 25); k = *Coscinopleura* (23, 29); l = *Diplodidymia* (21, 26).)

lows less chance for measurement error.

Size of autozooids, as measured by the area enclosed within the frontal outline, is consistent within colonies to a higher degree than previous studies based on "standard" linear dimensions (e.g., length, width) have indicated. Variation in size among comparable zooids, although not negligible, is relatively low, even in colonies with severely disturbed budding patterns. Significant differences in size can result from comparing zooids at different ontogenetic or astogenetic stages, different polymorphs, or zooids which reflect the effects of different microenvironments. Contributions from each of these sources of variation, however, can be more or less identified and accounted for prior to making taxonomic comparisons. Although differences in zooidal size among colonies within single populations are statistically significant, the range of autozooid sizes among a wide variety of cheilostome genera is so much greater that we have recognized at least four size intervals ("variable states"), each of which is larger than the observed within-population variation. These variable states have been successfully used as a basis for taxonomic distinctions among some cheilostomes. Populations differing by at least one such interval can be distinguished with a high degree of confidence by measuring as few as three zooids per colony and as few as four colonies per population, despite the appreciable within-colony and within-population variation in size.

The taxonomically significant aspects of shape, independent of size, are expressed by two derived characters. Each of these characters consists of a different linear combination of two direct measures of frontal outline shape: elongation, which is the concentration of relative growth in a "preferred" direction near the proximal-distal axis, and distal inflation, which is the proportion of relative growth concentrated in the distal half of the outline. The two derived shape characters are mutually independent and reflect two distinct patterns of covariation between elongation and distal inflation: (1) that part of their joint variation which is positively correlated, and (2) that part which is not correlated. Although the positively correlated variation in elongation and distal inflation is much greater in overall magnitude, the uncorrelated variation is much smaller within colonies. Among the cheilostomes examined, three intervals of minimum taxonomic difference can be recognized in each character, for a total of nine states when the two independent characters are considered simultaneously. Populations differing by at least one such interval are distinguishable by measuring as few as four or five zooids per colony and as few as three colonies per population. Astogenetic and polymorphic differences in these characters are relatively smaller than those in size, but ontogenetic differences are about the same magnitudes.

Asymmetry of the frontal outline (unequal relative growth on either side of the proximal-distal axis) is also independent of size and of elongation and distal inflation, but proved to have little or no taxonomic significance among the cheilostomes examined. Asymmetry is so highly variable within colonies that not even two full intervals of minimum taxonomic difference could be recognized among the wide variety of shapes studied.

The results of this study demonstrate that sensitive, taxonomically decomposable information is contained in the autozooidal outline. Statistically significant patterns of variation, both between colonies and between populations, can be recognized in zooidal size and at least two components of shape, elongation and distal inflation. Several numerically computed dendrograms using different combinations of the three independent size-shape characters group specimens in previously established taxa, although no single combination is best for all the groups studied. In general, however, dendrograms based on size and the negative component of covariation between elongation and distal inflation resemble "recognized" higher taxonomic groupings, while colonies within populations in at least some genera are more compactly clustered through the shape characters alone.

Although the frontal outline geometry of cheilostome autozooids is taxonomically important, its potential utility is masked by redundancy and nontrivial covariation among the measured characters. By empirically eliminating redundancy and extracting variance components from ontogenetic, astogenetic, and microenvironmental sources, a small set of taxonomically independent polythetic characters has been obtained. We suggest that similar procedures can profitably be applied to the problem of cheilostome taxonomy using other (hopefully larger) sets of complexly interdependent morphologic features as well.

Appendix A

Derivation of Vector Statistics

In the vectoral treatment of size and shape used herein, all statistics depend on two sets of variables: the set of vector azimuths, θ_i, which are measured as departures from the principal growth direction (pgd) and determined a priori, and the set of corresponding vector magnitudes, r_i (i's increase from left to right; Figure 33). Consequently, minor irregularities in zooid outline occurring between adjacent vector intercepts are not reflected in the statistics. However, we have found that the 17-vector system employed in the present study is sufficient to measure faithfully all but the most minor irregularities (see p. 7; Figure 7).

SIZE.—Zooid size is defined as the frontal area bounded by vertical walls. To obtain an approximation of area from the vector representation, the tips of the vectors are connected by straight lines, forming a 17-sided polygon (Figure 33). The area of a triangular wedge of this polygon (Figure 34) is easily seen to be

$$A_i = 1/2(r_i h) = 1/2(r_i r_{i+1} \sin \phi_i)$$
$$\text{where } \phi_i = |\theta_{i+1} - \theta_i|.$$

The area of the entire polygon of (n–l) segments (we have used n = 17) is thus

$$(1) \qquad A = \sum_{i=1}^{n-1} A_i = 1/2 \sum_{i=1}^{n-1} r_i r_{i+1} \sin \phi_i .$$

To allow direct comparison of size with the various measures of shape, we have transformed our measure of area to an equivalent linear metric, namely, the radius of a semicircle with equivalent inscribed polygonal area.

The area of a polygon inscribed in a semicircle of radius ra is

$$A' = 1/2 \sum_{i=1}^{n-1} ra^2 \sin \phi_i .$$

Hence, equating areas and solving for ra, our final size statistic is

$$(2) \qquad ra = \sqrt{\frac{\sum_{i=1}^{n-1} r_i r_{i+1} \sin \phi_i}{\sum_{i=1}^{n-1} \sin \phi_i}} \;, ra > 0.$$

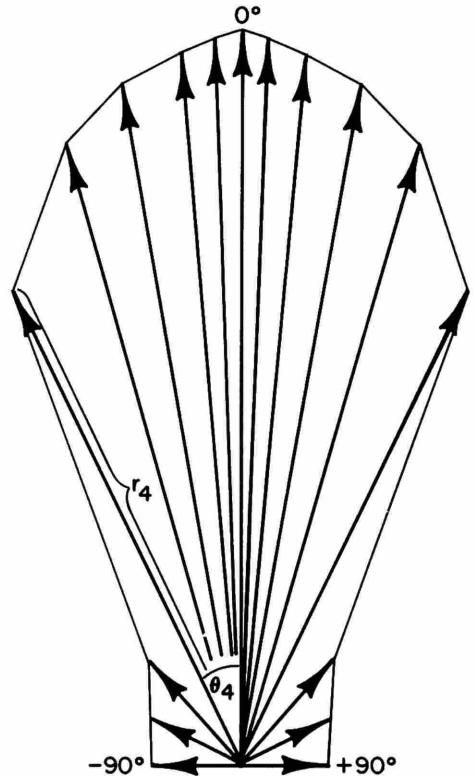FIGURE 33.—Vector representation of an ideal zooid outline (see Figure 4). (Distribution consists of 17 vectors, 8 distributed symmetrically on each side of the proximal-distal axis (0°). Azimuth (θ_i) and magnitude (r_i) indices (i) increase from left to right ($-90°$ to $+90°$). The statistic A is the area contained within the 17-sided polygon produced by connecting the tips of the vectors with straight-line segments.)
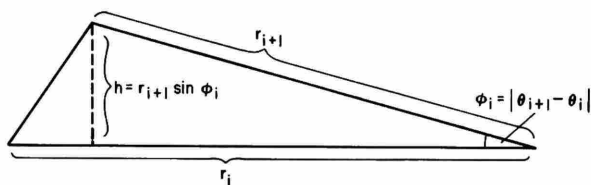
47

FIGURE 34.—Geometric relations of a single triangular wedge between two adjacent vectors in Figure 33. (The sum of areas of all such wedges is the area of the entire zooidal outline, A.)

ELONGATION.—Simple trigonometric measures of central tendency and dispersion for vector variables are well known (e.g., Batschelet, 1965:7–20) and correspond to the azimuth and magnitude, respectively, of the resultant vector obtained by graphical addition (Figure 35). For unequally weighted vector variates (r_i's not equal), the standard statistic for dispersion can be written

$$(3) \qquad \rho = \frac{\bar{l}}{\sum\limits_{i=1}^{n} r_i} = \frac{\sqrt{\left(\sum\limits_{i=1}^{n} r_i \sin \theta_i\right)^2 + \left(\sum\limits_{i=1}^{n} r_i \cos \theta_i\right)^2}}{\sum\limits_{i=1}^{n} r_i}$$

In the present application, ρ has a range from $\rho = 0$ (for two antipodal vectors of equal magnitude at $\pm 90°$) to $\rho = 1$ (for a single nonzero vector).

Assuming that vector magnitude is proportional to duration of directional growth, ρ also measures the relative distribution of growth duration over the distal margin. The statistic ρ is a useful measure of elongation in that it reflects relative concentration of vector lengths; larger values of ρ indicate longer vectors in the principal growth direction (pgd) than elsewhere (greater elongation), while smaller ρ's mean more or less equidimensional zooids (less elongation). As noted above (p. 8), cheilostome zooids normally range in shape between roughly semicircular ($\rho = 0.767$) and elongate and narrow ($\rho \simeq 1.0$).

ASYMMETRY.—Asymmetry of outline with respect to the principal growth direction implies that vector magnitudes tend to be distributed unequally on either side of the pgd. An intuitively appealing measure of this property is the tangent of the vector mean, defined as (Figure 35)

$$(4) \qquad \tan \bar{\theta} = \frac{\sum\limits_{i=1}^{n} r_i \sin \theta_i}{\sum\limits_{i=1}^{n} r_i \cos \theta_i} \qquad (-\infty < \tan \bar{\theta} < +\infty).$$

Although this statistic has the desirable property of indicating not only the amount but also the direction of deflection, the numerator of expression (4) unfortunately is sensitive to slight changes in zooidal width near the proximolateral margin. Consequently, the normally shorter vectors in the proximal region exert as much influence on $\tan \bar{\theta}$ as do longer ones near the pgd, and the statistic has proved to be relatively unstable.

A second measure of asymmetry seems to be
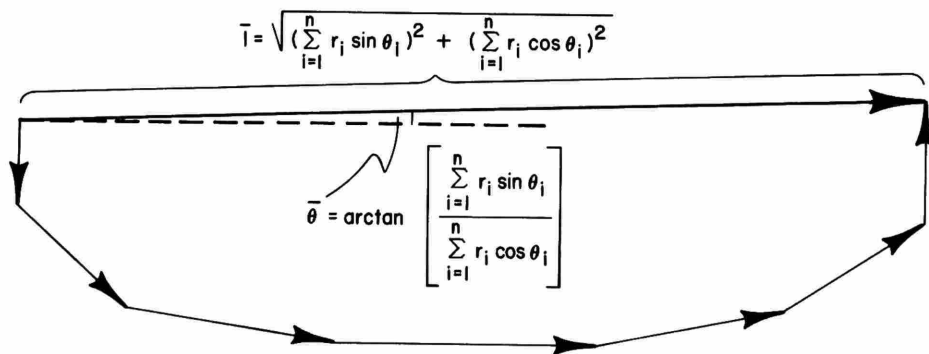

FIGURE 35.—Diagrammatic example of graphical vector addition and the equivalent trigonometric relations, where $\bar{l}$ is the magnitude of the resultant vector and $\bar{\theta}$ represents its angular deflection from the proximal-distal axis (denoted by the dashed line). (Only a 7-vector system is shown here (n = 7); we have used a 17-vector system in computing size and shape statistics.)

more robust. This statistic, denoted a, is based on a pair-wise comparison of the magnitudes of vectors deflected at the same angle $\pm \theta$ from the pgd. Asymmetry between each vector pair is defined as the ratio of the difference between their magnitudes and the sum of their magnitudes,

$$\frac{r_i - r_{n-i+1}}{r_i + r_{n-i+1}}$$

This ratio varies from 0 (if the magnitudes are equal) to ± 1 (when either magnitude is 0). The statistic a is defined as the root-mean-square of these proportions, that is

$$(5) \quad a = \sqrt{\left(\frac{2}{n-1}\right) \sum_{i=1}^{(n-1)/2} \left\{\frac{r_i - r_{n-i+1}}{r_i + r_{n-i+1}}\right\}^2}, \quad (0 < a \leq 1).$$

This statistic has the disadvantage of being unsigned and so cannot serve as a measure of directional asymmetry. However, it is somewhat less sensitive to minor variations in symmetry in the proximal part of the zooid than is $\tan \bar{\theta}$.

Both $\tan \bar{\theta}$ and a were used in the analysis of asymmetry.

DISTAL INFLATION.—Although the conceptual basis for our measure of distal inflation (denoted di) is quite simple, the analytic geometry required for its computation is somewhat tedious.

Distal inflation is defined as the proportion of the area enclosed by the distal half of the zooid (as measured along the proximal-distal axis) to the total area, or using the value for total area (A) in expression (1),

(6) $di = 1 -$ (area of proximal half of zooid/A).

The area of the proximal half of the zooid can be conveniently separated into two components, one on either side of the proximal-distal axis. Consider the region to the left of this axis and proximal to the midpoint of the axis, $r\left(\frac{n+1}{2}\right)/2$, enclosed by heavy lines in Figure 36. The area of this region can be further subdivided into the four components W, X, Y, and Z; from the geometric relations shown in Figure 36, these areas are given by

$$W = 1/2 \sum_{i=1}^{p-1} r_i r_{i+1} \sin \phi_i$$

where, as before, $\phi_i = |\theta_{i+1} - \theta_i|$,

and p is the largest index, $i < \left(\frac{n+1}{2}\right)$, satisfying the inequality $r_i \cos \theta_i < r_{\left(\frac{n+1}{2}\right)}/2$,

$$X = -1/2 \, r_p^2 \sin \theta_p \cos \theta_p,$$

$$Y = -r_p \sin \theta_p [(r_{\left(\frac{n+1}{2}\right)}/2) - r_p \cos \theta_p]$$

$$Z = - \frac{[(r_{\left(\frac{n+1}{2}\right)}/2) - r_p \cos \theta_p]^2}{2} \tan \alpha$$

where $\tan \alpha = \frac{r_{p+1} \sin \theta_{p+1} - r_p \sin \theta_p}{r_{p+1} \cos \theta_{p+1} - r_p \cos \theta_p}$.

Hence, the total area to the left of the proximal-distal axis is

$$(7) \quad \text{area}_l = W + X + Y + Z$$

$$= 1/2 \sum_{i=1}^{p-1} r_i r_{i+1} \sin \phi_i + (r_p/2)^2 \sin 2\theta_p - (r_{\left(\frac{n+1}{2}\right)}/2) r_p \sin \theta_p$$

$$- \frac{[(r_{\left(\frac{n+1}{2}\right)}/2) - r_p \cos \theta_p]^2}{2} \tan \alpha.$$

Similarly, the proximal area to the right of the proximal-distal axis is given by (Figure 37):

$$(8) \quad \text{area}_r = 1/2 \sum_{i=q}^{n-1} r_i r_{i+1} \sin \phi_i - (r_q/2)^2 \sin 2\theta_q$$

$$+ (r_{\left(\frac{n+1}{2}\right)}/2) r_q \sin \theta_q + \frac{[(r_{\left(\frac{n+1}{2}\right)}/2) - r_q \cos \theta_q]^2}{2} \tan \beta$$

where q is the smallest index, $i > \left(\frac{n+1}{2}\right)$ satisfying the inequality, $r_i \cos \theta_i < r_{\left(\frac{n+1}{2}\right)}/2$

and $\tan \beta = \frac{r_{q-1} \sin \theta_{q-1} - r_q \sin \theta_q}{r_{q-1} \cos \theta_{q-1} - r_q \cos \theta_q}$
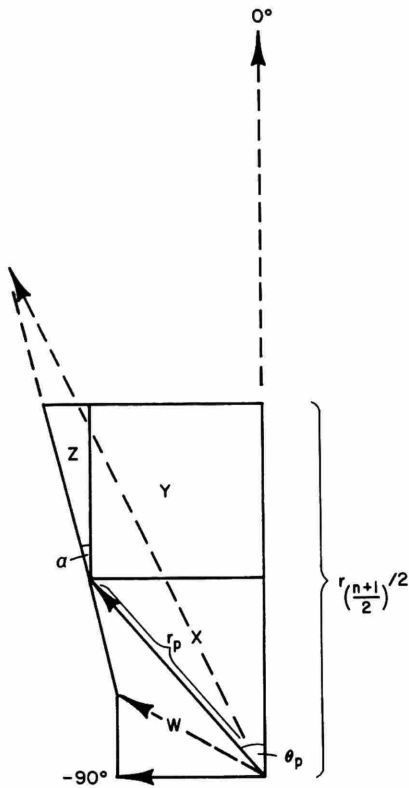
FIGURE 36.—Geometry required to compute area of the proximal half of a zooidal outline to the left of the proximal-distal axis. (Formulas for computing the areas of regions W, X, Y, Z are given in the text.)

FIGURE 37.—Geometry required to compute area of the proximal half of a zooidal outline to the right of the proximal-distal axis. (A formula for computing the area of the region W'+X'+Y'+Z' is given in the text.)

The sign changes in all but the first term of expression (8) from those in (7) result from the change in the sign of $\sin \theta$.

Finally, our expression for distal inflation is given by

(9) $di = 1 - (\text{area}_l + \text{area}_r)/A, \ (0 \leqslant di \leqslant 1)$

where, from expression (1) above,

$A = 1/2 \sum_{i=1}^{n-1} r_i r_{i+1} \sin \phi_i.$

ADDITIONAL STATISTICS.—The unweighted mean length of the resultant vector (denoted $\bar{r}$) is defined as (Figure 35)

(10) $\bar{r} = \dfrac{\bar{l}}{n} = (1/n) \sqrt{\left(\sum_{i=1}^{n} r_i \sin \theta_i\right)^2 + \left(\sum_{i=1}^{n} r_i \cos \theta_i\right)^2},$

$(\bar{r} > 0).$

This measure is obviously correlated with size, and is related to elongation (ρ) through the arithmetic mean vector length,

$\bar{r} = \left(1/n \sum_{i=1}^{n} r_i\right) \rho.$

The magnitude of the longest vector (denoted r_{max}) was included in the earlier phases of analysis, but because it confounds both size and shape and because its use imposes an additional constraint in assuming morphological correspondence between zooids in maximum growth direction, it was not considered further.

Appendix B

Summary of Data Used

Specimens studied by vector analysis are listed in order of the mean shape of autozooidal outlines as arranged in Figure 17, with the exception of the second and third zooecia in astogenetic series in *Tetraplaria simata* (1B, 1C) and of additional zoaria conspecific with those shown in Figure 17 (9B, 12B, 21C, 21B, 19B–F, 30A). Within-colony means and standard deviations of vector variables (*tan $\bar{\theta}$* is its absolute value) are for fully developed autozooecia in zones of astogenetic repetition, with dimorphic autozooecia, where present, treated separately. (Properties of each of the three zooecia of *T. simata* are given separately.) All specimens except those marked either (*) or (+) were used in both the principal components analysis and the total analysis of variance; those marked (*) were omitted from both, and those marked (+) were omitted from the anova.

Abbreviations are: a = a-zooecia; b = b-zooecia; ANS = Academy of Natural Sciences of Philadelphia; f = frontal zooecia; l = lateral zooecia; LSU = Louisiana State University Geology Museum; MNHN = Museum National d'Histoire Naturelle (Paris); n = number of zooecia measured; NHM = Naturhistorisches Museum (Vienna); USC–AHF = Allan Hancock Foundation (University of Southern California); USNM U.S. National Museum, acronym for specimens deposited in the National Museum of Natural History, Smithsonian Institution. Symbols for vector variables are explained in Appendix A.

ID. NO.	TAXON	LOCALITY	WITHIN-COLONY MEANS							WITHIN-COLONY STANDARD DEVIATIONS					
			n	ra	r̄	ρ	di	a	tan θ	ra	r̄	ρ	di	a	tan θ
1A+	*Tetraplaria simata* Cheetham, 1972	Eocene, Tertiary b, Eua, Tonga. USNM 169276, holotype	1	40.14	39.38	.8604	.3817	.0114	.0022						
1B+			1	45.49	56.29	.9598	.6093	.1049	.0144						
1C+			1	38.89	45.73	.9634	.6390	.1448	.0086	-	-	-	-	-	-
2	*Discoflustrellaria clypeiformis* d'Orbigny, 1853	Cretaceous, Senonian, Ste. Colombe (Manche), France. MNHN Paris, d'Orbigny coll. B16379, syntype	5	36.80	34.46	.8492	.4527	.0325	.0135	1.1269	1.2206	.0071	.0071	.0200	.0095
3	*Entomaria spinifera* (Canu, 1914)	Miocene, Helvetian, Touraine, France. MNHN Paris, Canu coll., syntype	5	39.82	38.05	.8542	.4606	.0283	.0072	1.1269	1.2570	.0084	.0091	.0000	.0084
4	*Floridina* sp. 1: Cheetham & Håkansson, 1972	Oligocene, ?*Sphenolithus distensus* Zone, DSDP Site 117, Rockall Plateau. USNM 171634	4	35.53	34.52	.8676	.4799	.0434	.0078	.2449	.9487	.0095	.0130	.0173	.0077
5	*Patsyella?* sp.: Cheetham, 1972	Eocene, Tertiary b, Eua, Tonga. USNM 169232	4	46.20	47.99	.8781	.4506	.0249	.0086	2.1048	1.7493	.0118	.0310	.0100	.0055
6*	*Metrarabdotos unguiculatum* Canu & Bassler,1928a, s.s.	Recent, off Bahia, Brazil, Norseman sta. 348, 49 m. (Canu & Bassler, 1928b) USNM 8571	2	54.84	57.08	.8869	.5041	.0404	.0046						
7	*Metrarabdotos unguiculatum pacificum* (Osburn, 1952)	Recent, Secas Islands, Panama, 22 m. USC, AHF-95, paratype	4	42.03	43.14	.8752	.4607	.0493	.0262	.4123	2.4860	.0205	.0276	.0490	.0281
8A	*Thalamoporella biperforata* Canu & Bassler, 1919	Miocene, Cercado de Mao, Dominican Republic. USNM 206922	5	29.07	30.75	.8851	.4533	.0914	.0349	3.0017	3.9573	.0224	.0416	.0400	.0152
8B		USNM 206923	5	32.32	34.97	.8945	.4803	.0172	.0038	.5000	1.0392	.0055	.0045	.0000	.0032
9A	*Metrarabdotos helveticum* Roger & Buge, 1947, s.s.	Miocene,Helvetian, Pont-Levoy, France. (Cheetham, 1968a) USNM 650877	5	30.06	33.51	.9006	.4898	.0434	.0090	1.4866	2.3281	.0084	.0155	.0141	.0045
9B		USNM 60540	2	36.67	44.15	.9290	.5141	.0317	.0065						
10	*Schismoporella schizogaster* (Reuss,1848)	Miocene, Leithakalk, Eisenstadt, Austria. NHM Wien, 1859.L.789, paratype	2	36.70	39.70	.8982	.4271	.0557	.0229						
11	*Microporina?* aff. *M.? polysticha* (Reuss, 1848)	Oligocene, ?*Sphenolithus distensus* Zone, DSDP Site 117, Rockall Plateau. (Cheetham & Håkansson, 1972)USNM 171640	2	28.44	33.70	.9173	.4636	.0362	.0085						
12A	*Steganoporella magnilabris* (Busk, 1854)	Recent, Johnson-Smithsonian Deep-Sea Expedition, sta. 26, north of Puerto Rico, 67-73 m. USNM 186573	3a	45.28	48.09	.8886	.4804	.0282	.0062	1.6592	1.1954	.0072	.0044	.0110	.0037
			3b	53.25	57.87	.8977	.4859	.0203	.0052	1.9771	1.9917	.0064	.0092	.0083	.0023
12B*		sta. 45, west of Puerto Rico, 37-73 m. USNM 206924	3a	43.08	43.88	.8797	.4616	.0887	.0330	3.3974	3.2991	.0109	.0061	.0833	.0242
			3b	56.00	61.88	.9063	.4986	.0487	.0177	2.0344	2.4114	.0103	.0199	.0036	.0025
12C*		sta. 68, northeast of Puerto Rico, 18 m. USNM 206925	3a	39.23	41.49	.8944	.4719	.1398	.0462	3.1151	2.7328	.0118	.0228	.0769	.0235
			3b	45.45	48.63	.9090	.5098	.1509	.0479	7.9446	8.4998	.0022	.0163	.1618	.0602
13	*Escharifora argus* d'Orbigny, 1852	Cretaceous, Senonian, Nĕhou (Manche), France. MNHN Paris, d'Orbigny coll. 7962	5	35.34	38.16	.9066	.4828	.0351	.0078	1.3711	1.3077	.0045	.0226	.0100	.0063
14	*Flustrellaria fragilis* d'Orbigny, 1853	Cretaceous, Cenomanian, LeMans (Sarthe), France. MNHN Paris, d'Orbigny coll. 6546,syntype	2	36.38	39.21	.8994	.4925	.0464	.0082						
15	*Ogivalia elegans* (d'Orbigny, 1839)	Recent, probably Falkland Islands (Îles Malouines). MNHN Paris,d'Orbigny coll. 13616, syntype	4	51.37	55.89	.8942	.4892	.0311	.0075	2.6608	2.9732	.0045	.0063	.0200	.0045
16	*Vincularia fragilis* Defrance, 1829	Eocene, Lutetian, Chaussy, France. (Canu, 1907) MNHN Paris	5	30.86	34.14	.9044	.5039	.0475	.0132	1.4000	.8832	.0089	.0232	.0100	.0032
17	*Electrina lamellosa* d'Orbigny, 1851	Recent, Noirmoutier, France. MNHN Paris, d'Orbigny coll. 13596, holotype	5	25.21	28.55	.9118	.4890	.0865	.0130	.5099	1.0630	.0161	.0148	.0755	.0118
18	*Antropora? oculifera* (Canu & Bassler, 1929)	Oligocene, ?*Sphenolithus distensus* Zone, DSDP Site 117, Rockall Plateau. (Cheetham & Håkansson, 1972) USNM 171625	5	48.19	50.63	.8972	.5049	.0662	.0180	1.1576	2.5000	.0138	.0377	.0447	.0089
19	*Rimosocella laciniosa* (Canu & Bassler, 1920)	Eocene, Jacksonian, Castle Hayne Ls., Wilmington, N.C. USNM 64013, syntype	2	21.86	27.13	.9619	.5072	.0250	.0048						
20	*Schizostomella crassa* (Canu, 1908)	Eocene, Lutetian, Cahaignes (Herouval), France. MNHN Paris, Canu coll., syntype	2	24.64	27.57	.9256	.5474	.0345	.0076						
21A	*Diplodidymia ratoniensis* (Waters, 1887)	Recent, Seria, Brunei, beach sand. (Cheetham, 1968b)	5l	22.10	24.31	.9130	.5549	.0823	.0076	.4000	.6481	.0063	.0283	.0374	.0063
			3f	18.61	21.37	.9266	.5772	.0947	.0078	.4715	.6848	.0054	.0090	.0240	.0047
21B*			3f	18.94	21.62	.9235	.5895	.0986	.0162	.7951	.7108	.0044	.0137	.0458	.0182
22	*Ogivalina eximipora* Canu & Bassler, 1917	Eocene, Jacksonian, Castle Hayne Ls., Wilmington, N.C. USNM 62875, holotype	5	52.21	56.74	.9043	.5209	.0797	.0218	4.0596	5.4102	.0100	.0164	.0387	.0118
23	*Coscinopleura* sp.: Cheetham & Håkansson, 1972	Paleocene, *Globigerina triloculinoides-Discoaster multiradiatus* Zone, DSDP Site 117, Rockall Plateau. USNM 172422	5	29.38	33.43	.9294	.5498	.0620	.0100	1.3115	2.1471	.0105	.0382	.0412	.0114
24	*Houzeauina parallela* (Reuss, 1869a)	Eocene, Priabonian, Val di Lonte, Italy. NHM Wien, 1870.XIII.101, syntype	5	27.67	34.33	.9468	.5134	.0983	.0186	.9165	.9695	.0045	.0179	.0346	.0122
25	*Metrarabdotos micropora* (Gabb & Horn, 1862)	?Oligocene, Alabama. ANS Philadelphia, 31285, syntype	2	33.69	40.90	.9353	.5340	.1122	.0280						
26	*Diplodidymia complicata* Reuss, 1869b	Oligocene, Rupelian, Gaas (Tartas), France. topotype	4	19.29	22.91	.9409	.5722	.0888	.0125	1.4213	1.4594	.0045	.0234	.0200	.0071
27	*Tretosina arcifera* Canu & Bassler, 1927	Miocene, Balcombian, Muddy Creek, Victoria, Australia. USNM 85902, syntype	5	34.15	40.17	.9457	.5777	.0505	.0061	1.2410	2.1260	.0134	.0234	.0283	.0045
28	*Pyripora texana* Thomas & Larwood, 1956	Cretaceous, Albian, Georgetown Ls., Loeblich loc. HTL-96, sample 397, Smith Branch, east of Georgetown, Williamson Co., Texas. USNM 206926	4	28.57	34.41	.9379	.5478	.1131	.0103	1.6912	2.5807	.0148	.0352	.0812	.0084
29A*	*Coscinopleura angusta* Berthelsen, 1948	Paleocene, Danian, Mound II-N₁, sample 14, Limhamn, Sweden. (Cheetham, 1971) USNM 169529	5	25.74	28.92	.9203	.5433	.0672	.0111	.3606	1.4142	.0184	.0373	.0374	.0077
29B*		Paleocene, Danian, Mound II-N₁, sample 17, Limhamn, Sweden. (Cheetham, 1971) USNM 206927	5	30.40	34.66	.9298	.5699	.0527	.0081	.6324	.7937	.0071	.0176	.0374	.0071
29C*		USNM 206928	5	31.10	35.64	.9316	.5693	.0593	.0089	.4359	.7348	.0063	.0243	.0264	.0045
29D		USNM 169528	5	33.29	38.76	.9365	.5634	.1274	.0239	2.1748	2.4799	.0055	.0281	.0300	.0064
29E*		USNM 206929	5	32.25	36.67	.9249	.5331	.0459	.0075	1.7234	.9434	.0173	.0451	.0283	.0055
29F*		USNM 169530	5	34.21	37.93	.9196	.5347	.0613	.0148	1.5969	.5744	.0161	.0348	.0374	.0095
30A*	*Wilbertopora mutabilis* Cheetham, 1954	Cretaceous, Albian, Ft. Worth Ls., Krum, Denton Co., Texas. LSU 4600, holotype	8	24.90	27.73	.9154	.4962	.0750	.0182	1.0116	1.0173	.0113	.0289	.0761	.0166
30B		USNM 186569	5	33.42	39.19	.9444	.5534	.1843	.0412	1.2728	1.0817	.0126	.0261	.0640	.0259
31	*Poricellaria alata* d'Orbigny, 1854	Eocene, Lutetian, Damery (Marne), France. MNHN Paris, d'Orbigny coll. 9656, holotype	3	23.81	29.32	.9620	.6314	.1487	.0224	2.3281	2.7946	.0045	.0342	.0173	.0055

* included in neither PCA nor total anova
+ included in PCA but not in total anova

n = number of zooecia
a = a-zooecia
b = b-zooecia
f = frontal zooecia
l = lateral zooecia

Literature Cited

Abbott, M. B.
1973. Intra- and Intercolony Variation in Populations of *Hippoporina* Neviani (Bryozoa-Cheilostomata). Pages 223–245 *in* R. S. Boardman, A. H. Cheetham, and W. A. Oliver, Jr., editors, *Animal Colonies: Development and Function Through Time.* 11 figures. Stroudsburg, Pennsylvania: Dowden, Hutchinson, and Ross.

Anstey, R. L., and D. A. Delmet
1972. Genetic Meaning of Zooecial Chamber Shapes in Fossil Bryozoans: Fourier Analysis. *Science,* 177: 1000–1002, 2 figures.
1973. Fourier Analysis of Zooecial Shapes in Fossil Tubular Bryozoans. *Geological Society of America Bulletin,* 84:1753–1764, 11 figures.

Banta, W. C.
1969. The Body Wall of Cheilostome Bryozoa, II: Interzoidal Communication Organs. *Journal of Morphology,* 129:149–170, 26 figures, 1 plate.
1972. The Body Wall of Cheilostome Bryozoa, V: Frontal Budding in *Schizoporella unicornis floridana. Marine Biology,* 14:63–71, 3 figures.

Batschelet, E.
1965. Statistical Methods for the Analysis of Problems in Animal Orientation and Certain Biological Rhythms. *American Institute of Biological Sciences Monograph,* 57 pages.

Berthelsen, O.
1948. Studies on the Bryozoan Species *Coscinopleura elegans* and *C. angusta* n. sp. from the Senonian and Danian Deposits of Denmark. *Danmarks geologiske Undersøgelse,* 3(3):1–15, 4 figures.

Boardman, R. S., A. H. Cheetham, and P. L. Cook
1970. Intracolony Variation and the Genus Concept in Bryozoa. Pages 294–320 *in* Part C *in* The Genus: A Basic Concept in Paleontology. *Proceedings of the North American Paleontological Convention.* 12 figures. Lawrence, Kansas: Allen Press.

Busk, G.
1854. *Catalogue of Marine Polyzoa in the Collection of the British Museum,* Part II: *Cheilostomata* (part). Pages i–viii + 55–120, plates 69–124. London: British Museum.

Canu, F.
1907. Les Bryozoaires des terrains tertiaires des environs de Paris. *Annales de Paléontologie,* 2:57–88, plates 1–4.
1908. Les Bryozoaires des terrains tertiaires des environs de Paris. *Annales de Paléontologie,* 3:61–104, plates 9, 10.
1914. Contributions à l'étude des Bryozoaires fossiles, XIV: Bryozoaires du Stampien. *Bulletin de la Société géologique de France,* series 4, 14:147–152, plate 4.

Canu, F., and R. S. Bassler
1917. A Synopsis of American Early Tertiary Cheilostome Bryozoa. *United States National Museum Bulletin,* 96: 87 pages, 6 plates.
1919. Fossil Bryozoa from the West Indies. *In* T. W. Vaughan, editor, Contributions to the Geology and Paleontology of the West Indies. *Carnegie Institution of Washington Publications,* 291:73–102, plates 1–7.
1920. North American Early Tertiary Bryozoa. *United States National Museum Bulletin,* 106: 879 pages, 279 figures, 162 plates.
1927. Classification of the Cheilostomatous Bryozoa. *Proceedings of the United States National Museum,* 69(14):1–42, 1 plate.
1928a. Fossil and Recent Bryozoa of the Gulf of Mexico Region. *Proceedings of the United States National Museum,* 72(14):199 pages, 35 figures, 34 plates.
1928b. Bryozoaires du Bresil. *Bulletin de la Société des Sciences de Sein-et-Oise,* series 2, 9(5):58–110, 9 plates.
1929. Bryozoaires éocènes de la Belgique conservés au Musée royal d'Histoire naturelle de Belgique. *Mémoires du Musée royal d'Histoire naturelle de Belgique,* number 39, 69 pages, 5 plates.

Cheetham, A. H.
1954. A New Early Cretaceous Cheilostome Bryozoan from Texas. *Journal of Paleontology,* 28:177–184, 5 figures, plate 20.
1968a. Morphology and Systematics of the Bryozoan Genus *Metrarabdotos. Smithsonian Miscellaneous Collections,* 153(1): vii+121 pages, 24 figures, 18 plates.
1968b. Evolution of Zooecial Asymmetry and Origin of Poricellariid Cheilostomes. *In* E. Annoscia, editor, Proceedings of the First International Conference on Bryozoa. *Atti della Societa Italiana di Scienze Naturali e del Museo Civico di Storia Naturale di Milano,* 108:185–194.
1971. Functional Morphology and Biofacies Distribution of Cheilostome Bryozoa in the Danian Stage (Paleocene) of Southern Scandinavia. *Smithsonian Contributions to Paleobiology,* 6: 87 pages, 29 figures, 17 plates.
1972. Cheilostome Bryozoa of Late Eocene Age from Eua, Tonga. *U. S. Geological Survey Professional Paper,* 640-E: 26 pages, 7 figures, 7 plates.
1973. Study of Cheilostome Polymorphism Using Principal Components Analysis. Chapter 38 (pages 385–

409) *in* G. P. Larwood, editor, *Living and Fossil Bryozoa: Recent Advances in Research*. 10 figures, 1 plate. London: Academic Press.

Cheetham, A. H., and E. Håkansson
1972. Preliminary Report on Bryozoa (Site 117). Volume 12 (pages 432–441) *in* A. S. Laughton, W. A. Berggren, et al., *Initial Reports of the Deep Sea Drilling Project*. 1 figure, plates 13–28.

Cook, P. L.
1964. Polyzoa from West Africa, I: Notes on the Steganoporellidae, Thalamoporellidae, and Onychocellidae (Anasca, Coilostega). *In* Résultats scientifiques des campagnes de la *Calypso*: Iles du Cap Vert. *Annales de l'Institut océanographique* (Monaco), 41:43–78, 13 figures, 1 plate.

Defrance, J. P. M.
1829. Vinculaire (Foss.). *Dictionnaire des Sciences Naturelles*, 58:214.

D'Orbigny, A.
1839. Bryozoaires. Pages 1–16 in Zoophytes, part 4 *of* volume 5 in *Voyage dans l'Amerique meridionale*.
1851. Bryozoaires. Volume 5 *in* Terrain crétacé in *Paléontologie française: Description des animaux invertébrés*. Pages 1–188. Paris: Masson.
1852. Bryozoaires. Volume 5 *in* Terrain crétacé in *Paléontologie française: Description des animaux invertébrés*. Pages 185–472. Paris: Masson.
1853. Bryozoaires. Volume 5 *in* Terrain crétacé in *Paléontologie française: Description des animaux invertébrés*. Pages 473–984. Paris: Masson.
1854. Bryozoaires. Volume 5 *in* Terrain crétacé in *Paléontologie française: Description des animaux invertébrés*. Pages 985–1192, plates 600–800. Paris: Masson.

Ehrlich, R., and B. Weinberg
1970. An Exact Method for Characterization of Grain Shape. *Journal of Sedimentary Petrology*, 40:205–212, 5 figures.

Farmer, J. D., and A. J. Rowell
1973. Variation in the Bryozoan *Fistulipora decora* (Moore and Dudley) from the Beil Limestone of Kansas. Pages 377–394 *in* R. S. Boardman, A. H. Cheetham, and W. A. Oliver, Jr., editors, *Animal Colonies: Development and Function Through Time*. 8 figures. Stroudsburg, Pennsylvania: Dowden, Hutchinson, and Ross.

Gabb, W. M., and G. H. Horn
1862. Monograph of the Fossil Polyzoa of the Secondary and Tertiary Formations of North America. *Journal of the Academy of Natural Sciences of Philadelphia*, 5(2):111–178, plates 19–21.

Gordon, D. P.
1971. Zooidal Budding in the Cheilostomatous Bryozoan *Fenestrulina malusii* var. *thyreophora*. *New Zealand Journal of Marine and Freshwater Research*, 5:453–460, 5 figures.

Håkansson, E.
1973. Mode of Growth of the Cupuladriidae (Bryozoa, Cheilostomata). Chapter 27 (pages 287–298) *in*

G. P. Larwood, editor, *Living and Fossil Bryozoa: Recent Advances in Research*. 2 figures, 2 plates. London: Academic Press.

Harmer, S. F.
1900. A Revision of the Genus *Steganoporella*. *Quarterly Journal of Microscopical Science*, new series, 43:225–298, plates 12, 13.
1957. The Polyzoa of the Siboga Expedition, Part IV: Cheilostomata Ascophora II. Pages 641–1147 *in* volume 28 in *Siboga Expeditie*. Figures 49–118, plates 42–74.

Lutaud, G.
1961. Contribution à l'étude du bourgeonnement et de la croissance des colonies chez *Membranipora membranacea* (Linné), bryozoaire chilostome. *Annales de la Société royale zoologique de Belgique*, 91:157–300, 28 figures, 8 plates.

Malmgren, B.
1970. Morphometric Analysis of Two Species of *Floridina* (Cheilostomata, Bryozoa). *Acta Universitatis Stockholmiensis-Stockholm Contributions in Geology*, 23:73–89, 7 figures, 1 plate.

Mayr, E., E. G. Linsley, and R. L. Usinger
1953. *Methods and Principles of Systematic Zoology*. ix + 336 pages, 45 figures. New York: McGraw-Hill.

Osburn, R. C.
1952. Bryozoa of the Pacific Coast of America, Part 2: Cheilostomata-Ascophora. *Allan Hancock Pacific Expeditions*, 14:271–611, plates 30–64.

Pohowsky, R. A.
1973. A Jurassic Cheilostome from England. Chapter 44 (pages 447–461) *in* G. P. Larwood, editor, *Living and Fossil Bryozoa: Recent Advances in Research*. 3 figures, 1 plate. London: Academic Press.

Reuss, A. E.
1848. Die fossilen Polyparien des Wiener Tertiärbeckens. *Haidingers naturwissenschaftliche Abhandlungen* (Wien), 2:1–109, 11 plates.
1869a. Paläontologische Studien über die älteren Tertiärschichten der Alpen, II Abtheilung: Die fossilen Anthozoen und Bryozoen der Schichtengruppe von Crosara. *Denkschriften der matematisch-naturwissenschaftlichen Classe der kaiserlichen Akademie der Wissenschaften in Wien*, 30:215–298, plates 17–36.
1869b. Zur fossilen Fauna der Oligocänschichten von Gaas. *Sitzungsberichte der matematisch-naturwissenschaftlichen Classe der kaiserlichen Akademie der Wissenschaften in Wien*, 59:446–488, plates 1–6.

Roger, J., and E. Buge
1947. Les Bryozoaires du Redonien. *Bulletin de la Société géologique de France*, series 5, 16:217–230, 4 figures.

Rohlf, F. J.
1972. An Empirical Comparison of Three Ordination Techniques in Numerical Taxonomy. *Systematic Zoology*, 21:271–280, 5 figures.

Silén, L.

1944a. The Anatomy of *Labiostomella gisleni* Silén (Bryozoa Protocheilostomata) with Special Regard to the Embryo Chambers of the Different Groups of Bryozoa and to the Origin and Development of the Bryozoan Zoarium. *Kungl. Svenska Vetenskapsakademiens Handlingar*, series 3, 21:1–111, 85 figures, 5 plates.

1944b. On the Formation of the Interzoidal Communications of the Bryozoa. *Zoologiska Bidrag från Uppsala*, 22:433–488, 59 figures, 1 plate.

Sneath, P. H. A.

1967. Trend-surface Analysis of Transformation Grids. *Journal of Zoology*, 151:65–122, 20 figures.

Sneath, P. H. A., and R. R. Sokal

1973. *Numerical Taxonomy: The Principles and Practice of Numerical Classification*. xv + 573 pages. San Francisco: W. H. Freeman.

Sokal, R. R., and F. J. Rohlf

1969. *Biometry: The Principles and Practice of Statistics in Biological Research*. xxi + 776 pages. San Francisco: W. H. Freeman.

Stach, L. W.

1935. Growth Variation in Bryozoa Cheilostomata. *Annals and Magazine of Natural History*, series 10, 16:645–647.

Thomas, H. D., and G. P. Larwood

1956. Some "Uniserial" Membraniporine Polyzoan Genera and a New American Albian Species. *Geological Magazine*, 93:369–376, 3 figures.

1960. The Cretaceous Species of *Pyripora* d'Orbigny and *Rhammatopora* Lang. *Palaeontology*, 3:370–386, 4 figures, plates 60–62.

Thompson, D'A. W.

1942. *On Growth and Form*. 2nd edition, 1116 pages, 554 figures. Cambridge: University Press and New York: MacMillan Company.

Van Valen, L.

1962. A Study of Fluctuating Asymmetry. *Evolution*, 16:125–142, 1 figure.

Waters, A. W.

1887. Bryozoa from New South Wales, North Australia, etc., Part II. *Annals and Magazine of Natural History*, series 5, 20:181–203, plates 5, 6.